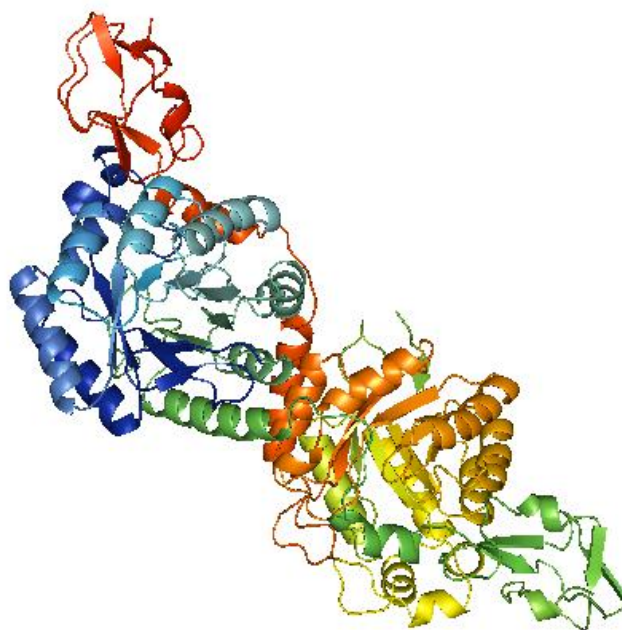


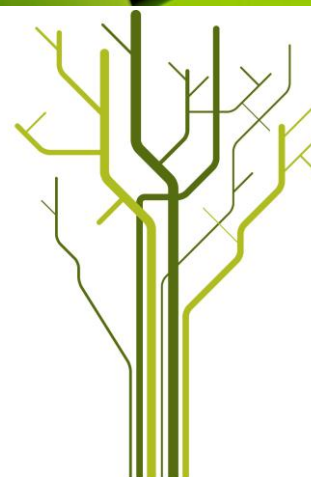
Characterization of a Neuraminic acid Synthase from the psychrophilic organism *Moritella viscosa*



Tor Olav Berg

KJE-3900 Master's Thesis in Chemistry

May 2013



Abstract

Sialic acids are family of nine carbon α -keto acids found to have important roles mammals and bacteria. They are negatively charged sugars which have found to play critical roles in the cognitive development, as well as being a part of the innate immune system and being targets for pathogens. Mammalian cells express sialic acids to confer self to the immune system, a trait being exploited by some pathogens that use sialic acid on their cell surface to hide themselves from the hosts immune system. *Moritella viscosa* is a psychrophilic bacteria found to a causative agent for winter ulcer in salmon. This bacteria have been found to have the genes necessary to synthesise sialic acids. The neuraminic acid synthase responsible for the reaction that synthesises neuraminic acid from ManNAc and PEP have been successfully cloned and expressed in two constructs NHis and CHis which coded for a TEV cleavable His-tag and a non-cleavable His-tag. The constructs were successfully expressed in two different expression strains and purified based on affinity chromatography. The activity was tested with the TBA assay and both NHis and CHis were found to be active. Both were expressed and purified in large scale and a purification table was made to analyse the process. The NHis construct was found to precipitate during purification preparations and only a low amount of the protein was obtained. CHis was found to give high amounts of protein. The NeuB1 enzyme was characterized in regards to pH, temperature, metals and stability. It was found that the optimum pH was 8.0. The optimum temperature was 30°C and cobalt was found to bind strongly at low concentrations. The stability of NeuB1 was assayed at the three temperatures 25°C , 37°C and 45°C and it was found the residual activity after 2 hours, 1 hour and 30 minutes was 70, 20 and 5% respectively. K_m and k_{cat} was found for ManNAc and PEP. K_m was 18.1254 ± 5.2537 and k_{cat} was 222.997 for ManNAc and K_m was 0.7646 ± 0.1674 and k_{cat} was 225.438 for PEP. Crystallization conditions were found for NeuB1 to be PEG 3350 and sodium citrate, no crystals were obtained. Using HPLC-MSMS to detect sialic acids in *Moritella viscosa* gave positive results for several compounds.

Keywords

Sialic acids, Neuraminic acid, neuraminic acid synthase, *Moritella viscosa*, cloning, purification, kinetics, crystallization, HPLC-MSMS, temperature optimum, stability, pH optimum

Contents

1. Introduction	4
1.1 Sialic acids.....	5
1.2 The functions of Sialic acids	8
1.2.1 Sialic acids in the Mammalian Brain.....	8
1.2.2 Sialic acids and Pathogens.....	9
1.3 Sialic acid Metabolism	11
1.4 Neuraminin acid synthases mechanism.....	12
1.4 Cold Adapted Enzymes	13
1.5 <i>Moritella viscosa</i>	15
2. Aims	16
3. Background	17
4. Materials.....	18
5. Method	25
5.1 Bioinformatics	25
5.2 Gene amplification	26
5.3 Cloning	29
5.4 Pilot Protein Expression	31
5.5 Pilot Protein Purification	32
5.6 Pilot Activity Assay.....	33
5.7 Large Scale Expression	35
5.9 Purification Table	37
5.10 pH Optimum.....	38
5.11 Temperature Optimum	38
5.12 Metal Dependency.....	39
5.13 Stability Assay.....	39
5.14 Differential Scanning Calorimetry	39
5.15 Kinetics.....	40
5.16 Crystallization	43
5.17 Sialic acid MS	45
6. Results	48
6.1 Bioinformatic Analysis.....	48

6.2 Gene Amplification	55
6.3 Pilot Expression.....	56
6.4 Pilot Protein Purification	57
6.5 Pilot Activity Assay.....	63
6.6 Large Scale Expression and Purification.....	63
6.8 Purification table	71
6.9 pH Optimum.....	73
6.9 Temperature Optimum	73
6.10 Metal Dependency.....	75
6.11 Stability Assay.....	76
6.12 Kinetics.....	77
6.14 Crystallization	80
6.15 Sialic acid Mass Spectrometry	82
7. Discussion	87
7.1 Bioinformatic analysis of NeuB1	87
7.2 Purification of NeuB1	88
7.3 NeuB1 Assay.....	91
7.5 NeuB1 Kinetics	94
7.7 Is NeuB1 Cold Adapted?.....	94
7.8 Crystallization	95
7.9 Sialic acid MS	95
8. Conclusion.....	96
9. Future work	97
11. Litterature	98
Appendix I.....	102
Appendix II	103
Appendix III	105
Appendix IV	106
Appendix V	107
Appendix VI.....	109
Appendix VII.....	110
Appendix VIII	112
Appendix IX.....	113
Appendix X	114

1. Introduction

Carbohydrates, or more commonly known as sugars, are an important class of molecules that serve a variety of roles in the continuity of life for all organisms. They are a source of energy as well as structure and protective elements in the cell wall of plants and bacteria and animal connective tissue. They are important for cell communication, recognition and adhesion and can act as signal molecules when bound to proteins or lipids. They are a diverse group of compounds depending on what kind of functional groups are present in the molecule and this gives a complexity that is termed “the third language of life” where the first is nucleic acids and the second proteins. Carbohydrates in their simplest form follow the empirical formula $(CH_2O)_n$ but can also contain sulphur, phosphorus and nitrogen, and are by chemical name polyhydroxy ketones or aldehydes. Three major classes exist for carbohydrates, monosaccharides, disaccharides (oligosaccharides) and polysaccharides which specify how many sugars are bonded in the molecule. Mono is one, di is two or more and poly is more than 20 sugars.

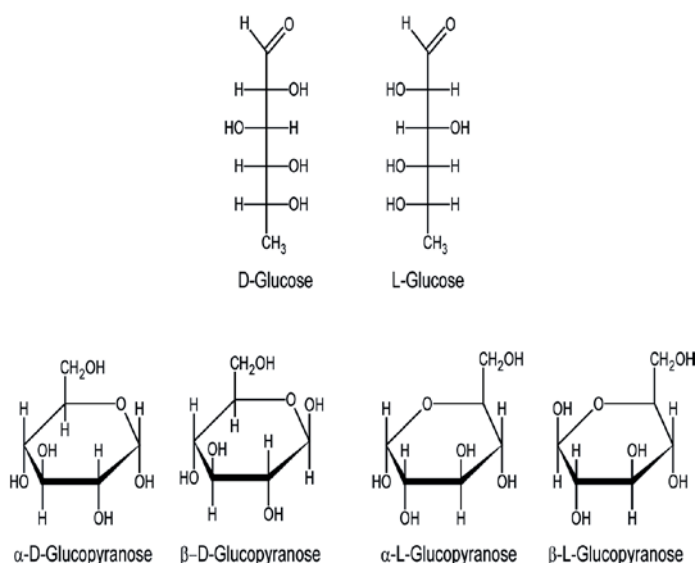


Figure 1.1: Glucose is perhaps the most abundant carbohydrate on earth and is a stereoisomer that is denoted by either L- or D-Glucose. It exists mostly in ring form where a new chiral carbon is introduced and the ring can either be in α or β form

is more than 20 sugars. They can be found in either an open chain or ring depending on if there are more than four carbons in the chain, which tend to give cyclic structures. By looking at the open chain structure one carbon is bound to oxygen with a double bond to form a carbonyl group. If this carbon is placed at the end of the chain the monosaccharide is an aldose, at any other location the monosaccharide is a ketose. All sugars with few exceptions contain one or more asymmetric carbon atoms giving them different optical isomers, or enantiomers that are denoted with either L or D for absolute configuration. When found in ring form the carbonyl group has formed a bond with oxygen in a hydroxyl group along the chain. The reaction between aldehydes or ketones and alcohol gives derivatives called either hemiacetals or hemiketals respectively, and this also introduces a new asymmetric carbon that can exist in two stereoisomeric forms. These forms are denoted as either α or β depending on

whether the newly formed hydroxyl group is on the same side as the hydroxyl group at the farthest chiral center (α) or on opposite sides (β). When two or more monosaccharides bond together, this bond is called a glycosidic bond and an example is the O-glycosidic bond where a hydroxyl group of one sugar reacts with the anomeric carbon of another. These bonds are resistant to base cleavage but are easily hydrolyzed with acid [1].

1.1 Sialic acids

Among the carbohydrates is a class of naturally occurring compounds known as sialic acids (Sia). The discovery of this class has its starting point in 1927 when researchers working with cerebroside fractions from animal kidney, spleen and brain found that a substance in the samples caused a purple colour when tested with Bial's orcinol reagent [2]. This was later found to be caused by a new type of carbohydrate, confirmed by two different research groups working with glycoproteins and glycolipids respectively. The discovery was also supported by work with the influenza virus in the 1940s, where it was observed that a low molecular compound was removed from the surface of red blood cells by the virus, reducing the overall negative charge in the process. This compound was isolated and shown to have the same characteristics as the sugar isolated from previous studies. Compiling these data showed that the sugar discovered in the different experiments belonged to the same group and were derivatives of the same common compound which was named neuraminic acid. The family of compounds was named sialic acids [3].

The sialic acid family today contains more than 50 structurally related molecules that are based on four basic structures, figure 1.2. In the beginning the only known compound was neuraminic acid, NeuNAc (5-amino-3,5-dideoxy-D-glycero-D-galacto-non-2-ulopyranosonic acid) figure 1.2 A, but as more structures were determined this list now also includes KDN (2-keto-3-deoxy-nononic acid), figure 1.2 B, pseudaminic acid (5,7-diamino-3,5,7,9-tetradecy-L-glycero-L-manno-nonulosonic acid), figure 1.2 C and legioaminic acid (5,7-diamino-3,5,7,9-tetradecy-D-glycero-D-galacto-nonulosonic acid), figure 1.2 D [4].

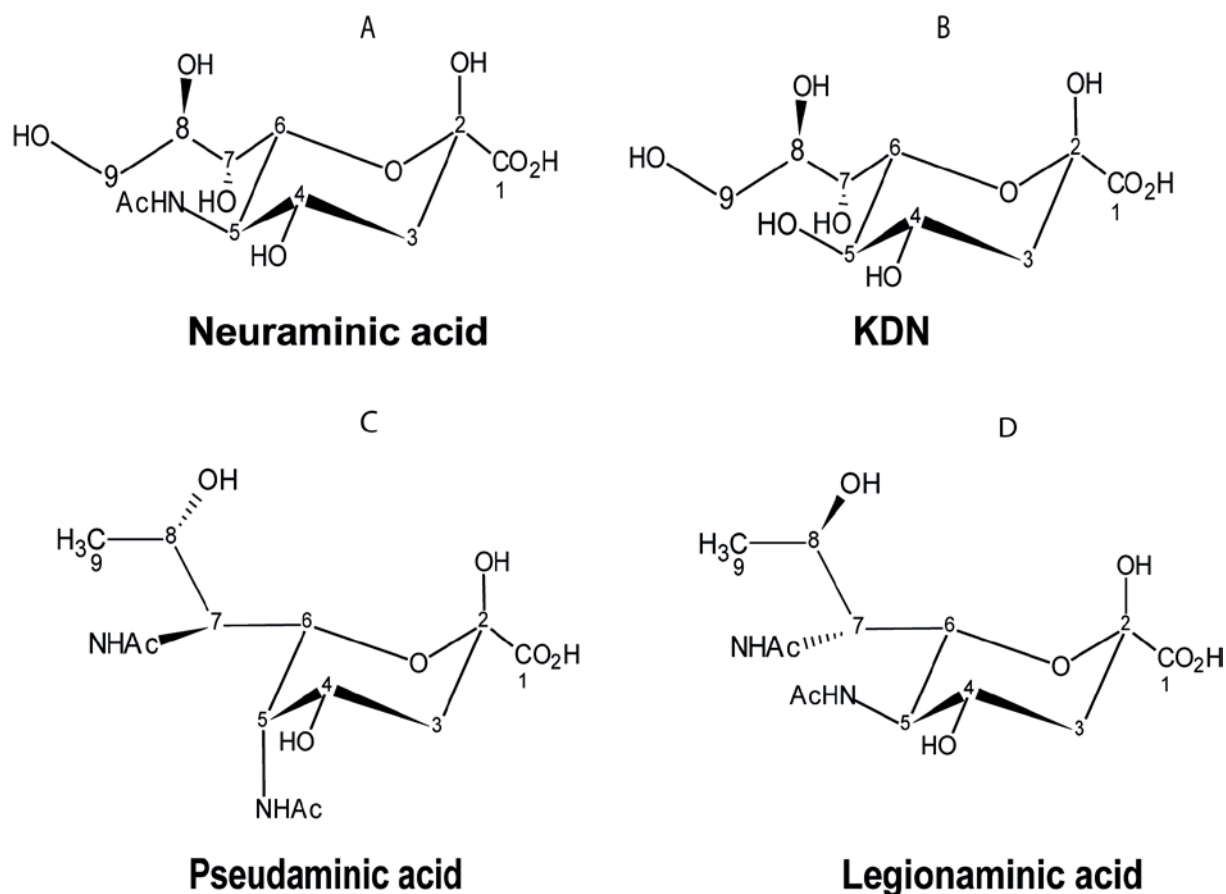


Figure 1.2: The sialic acid family contains four members that are the source of more than 50 compounds. They are Neuraminic acid or NeuNAc (A), KDN (B), Pseudaminic acid (C), Legioaminic acid (D).

Of these four structures there is only NeuNAc that is found in all species that synthesise Sia, while the others are dependent on species. Legioaminic acid was found in the lipopolysaccharide (LPS) of *Legionella pneumophila* and has the same D-glycero-D-galacto configuration as NeuNAc and KDN, while pseudaminic acid was found in the LPS of *Pseudomonas* species and because of its L-glycero-L-manno configuration it is a Sia isomer. Besides configuration they all have in common that they are synthesised by using phosphoenolpyruvate (PEP) [5].

The qualities of Sia that set them apart from other carbohydrates found is that they tend to occupy the ends of glycan chains where they can interact with other molecules and that they possess nine carbons in the backbone as opposed to five and six carbon sugars that are normally found in glycan chains. They are also a diverse group in the sense that they can undergo several modifications in the structure and have several possible ways to form

glycosidic bonds. Looking at NeuNAc, there are several naturally occurring modifications where different functional groups are located at different positions, figure 1.3.

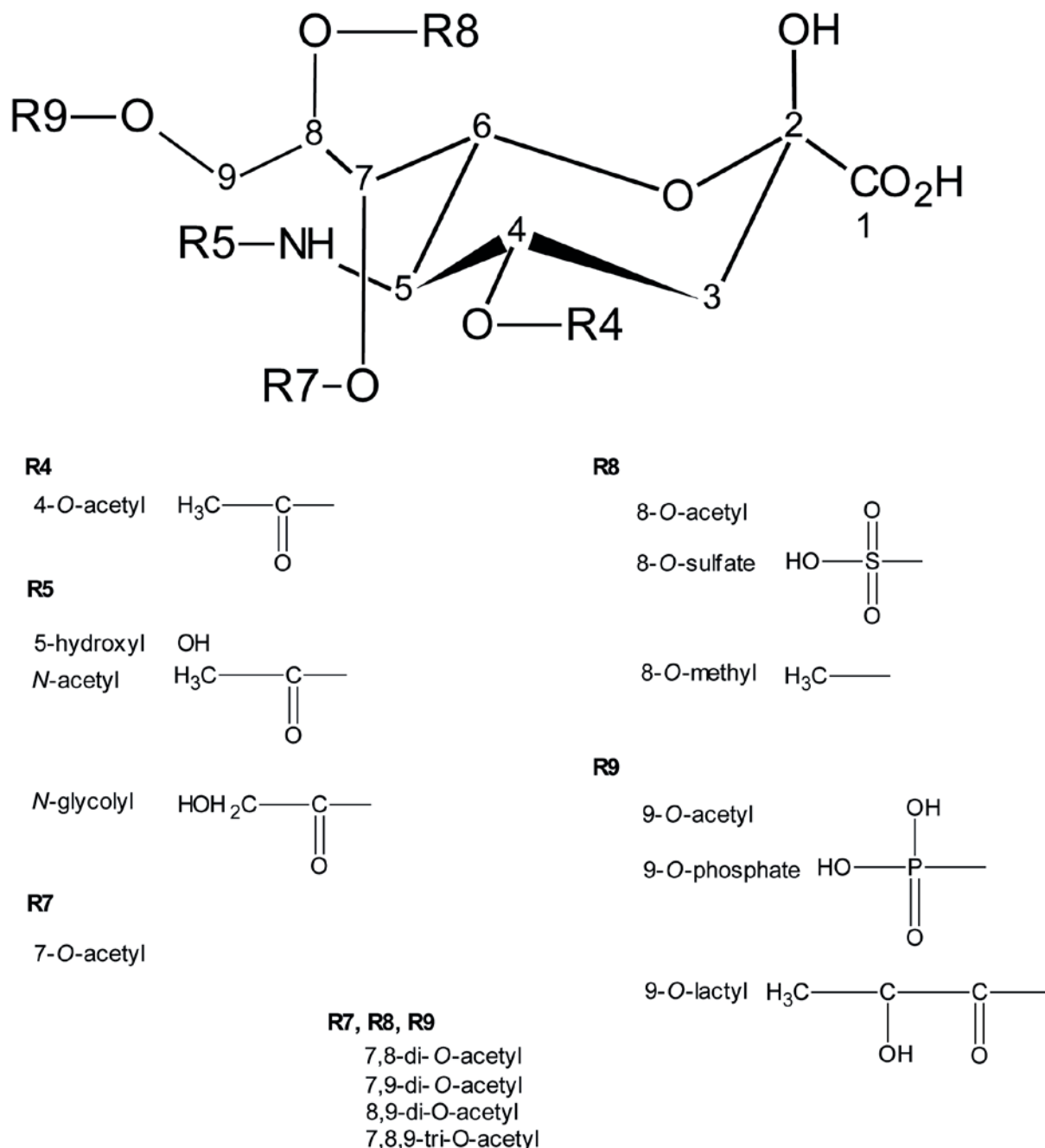


Figure 1.3: Neuraminic acid is the basis for many different sialic acids that occur in nature. The figure above show what positions are modified and with what kind of functional groups

Of these several derivatives, three of them are most common in nature, the *N*-acetyl (NeuNAc), *N*-glycolylneuraminic acid (Neu5Gc) and *N*-acetyl-9-*O*-acetylneuraminic acid (Neu5,9Ac₂). NeuNAc is the most studied Sia, and next is the Neu5Gc which is found frequently in animals but not in healthy human tissue and bacteria. The distribution of Sias seems to depend on type of species, cells and function [6].

1.2 The functions of Sialic acids

The location of Sia on the end of glycan chains is key for a multitude of cellular and intercellular processes, like signalling and adhesion, all important for the organisms synthesising them. The negative charge on Sia are involved in binding and transporting molecules with a positive charge and also repulse molecules and cells [7]. Examples of their function are repulsion between erythrocytes in the bloodstream and giving mucins high viscosity to protect endothelia when part of glycoproteins. The negative charge also contributes to the confirmation of gangliosides and the supramolecular structures in cell membrane components. The diversity of Sias also gives them different physio-chemical properties, as when the functional group sulphate is present and the acidity of the Sias is increased [8]. The effect of having Sia present works also as a masking or shield on receptors like galactose or antigenic sites. When these are desialylated the receptors are able to bind and carry out the designated process, as when erythrocytes are desialylated and the galactose is exposed, which enables the cells to bind to phagocytes and be degraded [9].

1.2.1 Sialic acids in the Mammalian Brain

In humans the importance of Sias is still a subject for study, but there is evidence that the Sias are important for the growth of the brain and cognitive development. When it comes to newborn infants they have a huge dependency on precursors and nutrients important for their development. Especially the brain during its fast growth after birth needs a lot of components to develop correctly, and the amount of Sias is shown to be an important factor to this. One of the most vital sources for nutrients for infants is breastmilk, which contains Sias to varying degrees. During the development of the cells in an unborn infant the polySia is expressed in abundance in the nervous tissue, then to be downregulated after birth and only be expressed in developing parts of the adult brain [10]. The enzyme responsible for the first step in the Sia pathway in mammals is the UDP-N-acetylglucosamine-2-epimerase/N-acetylmannosamine kinase [11], and it is shown that the expression of the complimentary gene is low after birth when there is no supplementary Sia compared to when Sia is added to the diet. Then the mRNA expression of UDP-N-acetylglucosamine-2-epimerase/N-acetylmannosamine kinase is increased significantly in brain hippocampus and liver, giving more sialylated glycoconjugates for the increased demand for neural development [12]. The Sia that is found on neural cells are polymerized into a linear homopolymer with negatively charged α 2-8-linked NeuNAc residues. The length of these chains vary from below 7 to over 400 residues and they are important for the posttranslational modification and dynamic

regulation of the function of neural cell adhesion molecules (NCAM) during central nervous system (CNS) development [13]. The NCAMs are adhesion molecules that are members of the immunoglobulin superfamily and are expressed on the surface of cells in the CNS. Carrying polySia regulates cell migration, neurite outgrowth, axon elongation and synaptic formation and plasticity in vertebrate cells [14]. The basic role of polySia in the neural cells depends on the negative charge in the molecule that promotes changes in the structure of the nervous system from child to adult. NCAM with covalently bonded Sia gives the adhesion molecules properties that affect the cellular binding through homophilic and heterophilic bonding and cells that are highly sialylated are more nonadherent than cells that have lower amounts [15]. The reason for this is thought to be from the negative charge and steric hindrance in Sia chains [16]. When signals are transmitted through the synapse, the cell sending the signal may express NCAM and the receiving cell may or may not express NCAM, when these are the options the cells will make more connections if both are expressing NCAM [17]. If these are sialylated the steric and physiochemical hindrance will affect the pathway of the signal. The degree of sialylation in neural cells decreases over time and in turn affects the brain plasticity or the morphology and functional parameters [18]. Taking this into account when looking at memory and learning the adding of new knowledge means changing the synapse plasticity and this is achieved by polySia that modulates the adhesive properties of NCAM [19]. It is also shown that Sia incorporated into the neural tissue increases with learning [20].

1.2.2 Sialic acids and Pathogens

Sia does not only play an important role in the development of neural cells, but are also considered a part of the immune system. Because of their physio-chemical properties they can function as masks for receptor molecules on the cell, and regulate cell-cell communication. Antigenic determinants are sometimes carbohydrates, but in most cases they work as shields for antigenic sites on the cell, as can Sia. This makes Sia an indicator for the immune system that this cell is “self”. When the cells are desialylated the antigenic site is exposed and makes the cell vulnerable for the immune system. This method of using Sia makes them a part of the innate immune system [21]. Pathogens have developed ways to make use of this to facilitate their spreading by either using carbohydrate binding proteins known as lectins, or by decorating their own cell surface with Sia to avoid the immune system of the host. The best known example of binding to Sia is the influenza virus A, as mentioned above was part of the discovery of Sia. The binding to Sia is mediated by a lectin called

hemagglutinin followed by the release of Sia by an enzyme originally called “receptor-destroying enzyme” which today is known as neuraminidase or sialidase. The infection mechanism starts with the virus binding to the Sia-rich mucins in the respiratory tract, and then penetration of the cell, when inside the replication of the virus starts followed by exocytosis [22]. This knowledge made it possible to make an inhibitor for the sialidase known as 2,3-didehydro-2,4-dideoxy-4-guanidiny-*N*-acetylneuraminic acid [23]. Other viruses also use this type of mechanism to attach to cells and infect, examples are corona, adenoma and rota viruses, HIV uses sialylated glycans that are both on the virus and the cell receptors [7]. Bacteria uses adhesins that are specific for carbohydrates to colonize by deploying them to their fimbria or pili. Examples of bacteria using this is strains of *E.coli*, *Streptococci* and *Helicobacter pylori* [24]. The knowledge about this usage of adhesins enables more specific treatments of the diseases and minimizes the use of antibiotics. Returning to the levels of Sia in newborns, it is thought that the use of sialylated oligosaccharides as soluble ligands may regulate and prevent the attachments of pathogene bacterias and viruses in the intestines and allow specific non pathogens to colonize instead [25].

The other mentioned method of pathogens to use Sia to infect is by decorating their cells by either synthesising themselves or scavenge from the host. A number of Sia synthesising bacteria is found that include *E.coli K1*, *Neisseria meningitides* and *C.jejuni* [26]. The others that scavenge may utilize sialidases to remove Sia from the host [27], but there are examples that some pathogens like *H. influenza* do not possess the genes but are still dependent on Sia from the host [28]. It is believed that these bacteria either use free Sia that is released by sialidases from other bacteria in the same niche [29] or that they depend on the host to use their own sialidases that is released during inflammation [30] [31]. When the pathogens have access to free Sia the next step is to transport it into the cell to be utilized. For this they use transporter proteins with Sia affinity. Not surprisingly it seems that there are several paths to capture Sia among the bacteria which underlines the importance of this process.. The captured Sia is incorporated into capsules of the bacteria to form polysialylated or sialylated lipopolysaccharides capsules, where the Sia can undergo further modifications with regards to acetylation or deacetylation before they are deployed to the bacterial surface [26] [32]. Some sialylated bacterias are shown to give a poor immunogenic response by hosts, most likely because they now have structurally identical polysialylated chains as the host. The mechanism for how this helps evade the immune system is not clear, but for some bacteria it may hinder the insertion of the complement membrane attack complex (MAC) in

the bacterial membrane, in others it inhibits the system for marking the pathogen to be destroyed [33].

1.3 Sialic acid Metabolism

As mentioned some bacteria are able to synthesise Sia themselves, but genes encoding Sia pathways is not found in all organisms. Life is organized into three domains of cellular organisms; Eukarya, Bacteria and Archea. Among the Eukarya is the deuterostome branch, which includes vertebrates, where Sia is found regularly. In the other domains, like the bacteria Sias are expressed in some strains of some species, and most of these are pathogens. In the Archea, there is no direct evidence of Sia, but similar genes have been found that may give production of Sia or related molecules [4]. The pathways of Sia biosynthesis were elucidated in the 1960s by the Roseman [34] [35] and Warren [36] [37] groups for both vertebrates and bacteria. A stepwise scheme of the biosynthesis pathways is shown in figure 1.4. The first step in NeuNAc synthesis, similar for both vertebrates and bacteria was suggested to be the epimerisation of UDP-acetylglucosamine (UDP-GlcNAc) to ManNAc.

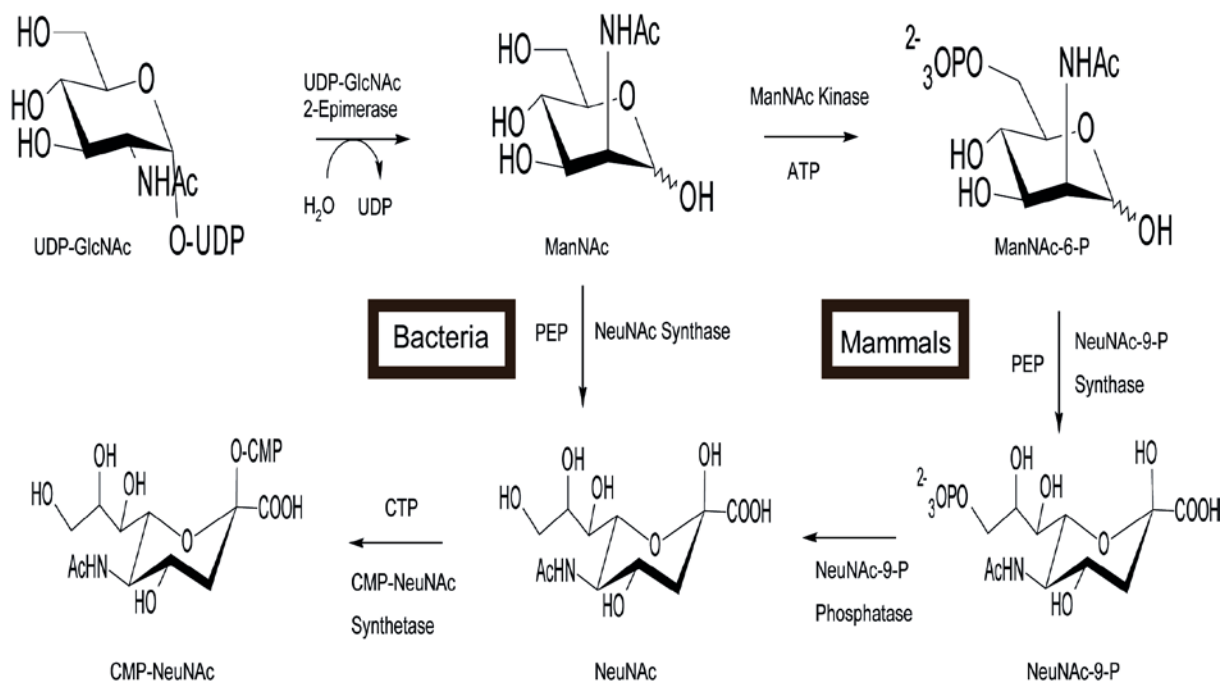


Figure 1.4: The Sia synthesizing pathway in mammals and bacteria. The mammalian pathway contains three additional reactions to produce NeuNAc

In vertebrates this first step is catalysed by the enzyme UDP-*N*-acetylglucosamine 2-epimerase / ManNAc kinase which is a bifunctional enzyme that inverts the stereochemistry of C-2 in the UDP-GlcNAc, hydrolyses the glucosidic phosphate bond and phosphorylates the

C-6 position [38] [11] [39] shown in the figure 1.4 as the first two reaction steps. The bacterial version of the enzyme only catalyses the first step shown in the figure, and lack the kinase activity [40] [41] . The following step is the formation of NeuNAc by NeuNAc synthase or NeuNAc-9-P synthase with the incorporation of phosphoenolpyruvate (PEP). In the vertebrates the phosphate is removed by a phosphatase [42] [4]. To be able to utilize the NeuNAc it must be converted to the active form by using cytidine -5-triphosphate (CTP) which is catalysed by CMP-Neu5AC synthetase. This is the final step before the product is transferred to the Golgi apparatus for modifications by several sialyltransferases and deployment in vertebrates. In bacteria, which lack this kind of organelle there is no need for transport and the sialyltransferases work directly on the product [4].

The degradation of Sia is carried out by sialidases that hydrolyse the sugar either intracellular or extracellular, and there exist a large family of these to carry out the reaction [43]. The released Sia can then be either transported into the cell where it will be reactivated and recycled or they are decomposed into pyruvate and acylmannosamine by sialate pyruvate lyase [44].

1.4 Neuraminin acid synthases mechanism

The synthesis of NeuNAc occurs in the cytoplasm of bacteria with the substrates ManNAc and PEP. The mechanism for this reaction has been studied and two potential mechanisms were considered. For one mechanism the the C-3 of PEP attacks the carbonyl group of ManNAc which would give an oxocarbenium ion that would readily be attacked by water to give a tetrahedral intermediate. The intermediate would then lose the phosphate and bring about the open chain keto form of NeuNAc, shown in figure 1.5A. The second alternative for a mechanism is where the initial attack is made by water at the phosphorus of PEP. This reaction leads to the release of free phosphate and the enolate of pyruvate. This enolate could attack the ManNAc carbonyl in an aldol-like fashion giving the open chain form of NeuNAc, figure 1.5 B [45] [46]. The difference between these two mechanisms is that the first one cleaves a C-O bond in order to synthesise NeuNAc while the other cleaves a P-O bond. In order to investigate the mechanism an isotope labelled oxygen was used on PEP, which would undergo the reaction. The hypothesis was that if the label retains in the substrate the mechanism would be a C-O bond cleavage, on the other hand if the labelled atom ended up in the product the mechanism would happen by P-O bond cleavage. It was eventually confirmed that the mechanism would go by a C-O cleavage [47].

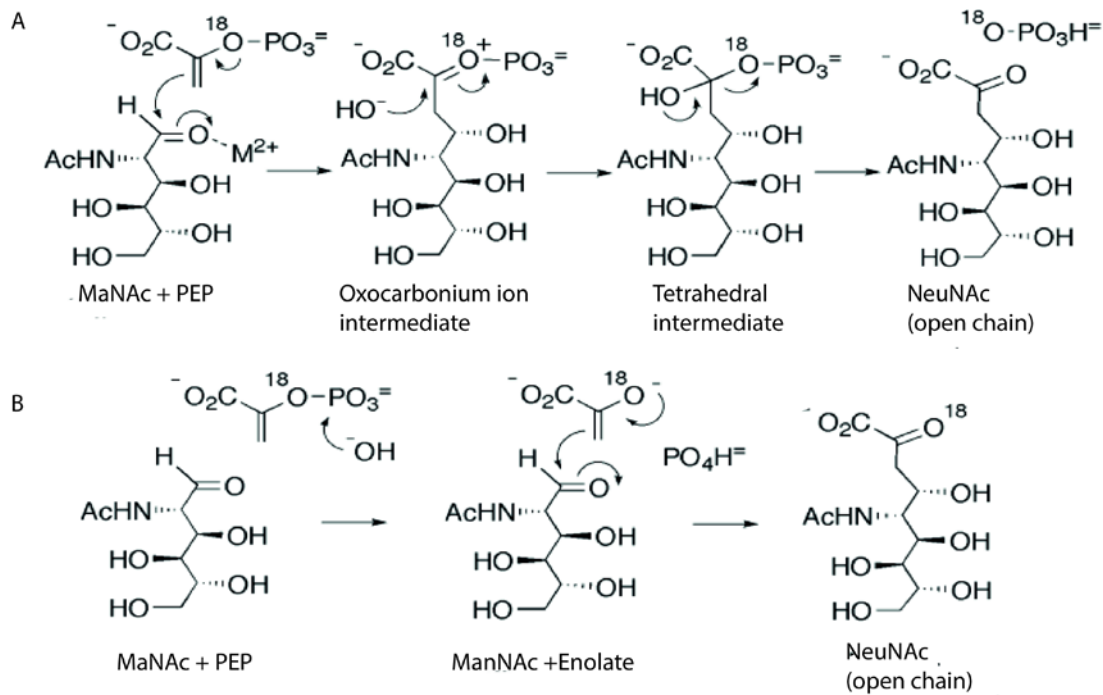


Figure 1.2: Two potential mechanisms for the formation of NeuNAc by neuraminic acid was hypothesised. A) where the reaction proceeds by breaking a C-O bond or B) where the reaction proceeds by breaking a P-O bond.

1.4 Cold Adapted Enzymes

The complexity and adaptivity of life is remarkable and is perhaps best shown in how some organisms have evolved to thrive in environments that is deadly or harmful to humans. These organisms are named extremophiles and are mostly bacterial species that have evolved to proliferate in extreme conditions found on Earth, this could be pH, pressure, salinity and temperature. The biomass that is generated on Earth comes mostly from the microorganisms in the sea that produce this at cold temperatures, below $5^\circ C$ [48], and it is known that chemical reactions slow down with decreased temperature, so these organisms must have adapted their cellular machinery to be able to work under these conditions. Organisms capable of metabolization at low temperatures are termed psychrophilic, or cold loving. Enzyme reaction rate can be described using the Arrhenius equation (equation 1.1)

$$k_{cat} = A\kappa e^{-E_a/RT} \quad 1.1$$

k_{cat} is the enzyme reaction rate, which increases with an increase in absolute temperature (T) and decrease of activation energy (E_a). A is the preexponential factor, κ is the dynamic transmission coefficient and R is the universal gas constant ($8,314 J mol^{-1} K^{-1}$). When the

temperature is below 4°C there is not enough kinetic energy in the system to get over the reaction barriers, so psychrophilic organisms have devised strategies to overcome this effect at cold temperatures, like increasing the enzyme concentration [49], expressing isoenzymes at specific periods [50] express proteins that have evolved to become temperature independent and be controlled by diffusion or shift the optimum temperature (T_{opt}) with a decrease in stability [51]. This last strategy also seems to give the enzymes a higher reaction rate than their mesophilic counterparts, by decreasing the activation free energy (ΔG^\ddagger) between the ground state and transition state of the substrate. The equation for free energy is composed of two parts (equation 1.2)

$$\Delta G^\ddagger = \Delta H^\ddagger - T\Delta S^\ddagger \quad 1.2$$

ΔH^\ddagger is the change in activation enthalpy, ΔS^\ddagger is the change in activation entropy and T is the absolute temperature [52]. The following equation (equation 1.3) is given when using transition state theory (TST) where k_{cat} is related to temperature and thermodynamic activation parameters.

$$k_{cat} = \left(\frac{k_B T}{h}\right) e^{-\Delta G^\ddagger / RT} \quad 1.3$$

k_B is the Boltzman constant (1.38×10^{-23} J K⁻¹) and h is the Planck constant (6.63×10^{-34} J s) [52] [53] [54] [55] [56]. Using equation 1.2 with the value of ΔG^\ddagger inserted into equation 1.3 gives equation 1.4 which is used to consider the effect of ΔH^\ddagger and ΔS^\ddagger on k_{cat}

$$k_{cat} = \left(\frac{k_B T}{h}\right) e^{-\{(\Delta H^\ddagger / RT) + (\Delta S^\ddagger / R)\}} \quad 1.4$$

To increase the k_{cat} at low temperatures, following equation 1.4 either ΔH^\ddagger must decrease or ΔS^\ddagger must increase. Looking at cold adapted enzymes known (table 1; [57]) almost all have a low ΔH^\ddagger which results in less temperature dependent reaction rates and at low temperatures a high reaction rate (k_{cat}) is maintained [53] [55]. To accomplish the reduction in ΔH^\ddagger , the structure of the enzyme contains a reduced number of enthalpy interactions that need to be broken when the transition state is formed. This is probably to give the active site more flexibility and the ground state enzyme substrate will as a consequence have a wider distribution of conformational states compared to the activated enzyme-transition state complex. Comparing the sequences of cold adapted enzymes and their mesophilic counterparts show that the catalytically important amino acids are conserved and so the increased flexibility is therefore caused by other parts in the structure [58] [59]. The protein is

held together by several types of interactions that vary from protein to protein, in cold adapted proteins the major factors that give rise to higher flexibility of the structure are the nature and magnitude of interactions between hydrophobic residues and solvent water and between hydrophobic residues themselves. For the latter these hydrophobic residues are located within the structure and it is observed that the amino acids tend to be less hydrophobic and smaller. The type of interaction governing hydrophobicity is van der Waals forces which are sensitive to distance and weak. This will in the case of cold adapted proteins give reduced van der Waals interactions and destabilize the structure [60] [61] [62]. The hydrophobic residues on the surface are in contact with water and there is a tendency to be more of these in cold adapted enzymes. The reasoning is that these will destabilize the structure because of water molecules decreasing in entropy, but at lower temperatures this gain in entropy is reduced since water loses mobility [63] [64] [61] [65]. In contrast to the hydrophobicity there is also contribution from charged and hydrophilic residues on the surface, where particularly negative charges has been described for cold adapted enzymes [66]. These residues interact with water that has a high dielectric constant at low temperatures which makes it energetically costly to disrupt hydrogen bonds and ensure solvation and maintain flexibility [67]. The charges could also contribute to charge repulsion and destabilize the structure [57].

1.5 *Moritella viscosa*

Winter ulcer is a fish disease that affects cultured salmonid fish at temperatures below 8° C. It manifests itself as external skin and muscle lesions but also have internal effects that causes blood loss and cell death [68]. The mortality of the disease over time is estimated to be up to 10 % and represent a challenge in animal welfare and food production [69]. One of the causative agents for this disease is the bacteria *Moritella viscosa*, formerly known as *Vibrio viscosus*. *M. viscosa* is a gram negative psychrophilic facultative anaerob bacteria found outside the coast of Norway, Iceland and Scotland. The bacteria cells are motile non spore forming pleomorphic rods containing a single polar flagellum. The name is derived from the viscous adherent threads that it form [70]. The method of infection and virulence of *M. viscosa* is poorly understood but it is generally accepted that the pathogen has to penetrate the primary barriers and gain entry through mucosal surfaces of skin, gastrointestinal tract and gills [71] [72] [73] [74]. Treatment of *M. viscosa* infections is standard antibiotics but there is a need for more effective vaccines to combat the disease [75] [76].

2. Aims

The aim of the project was to clone and express the *neuB1* gene from *Moritella viscosa* 06/09/139 and purify the enzyme in order to characterize the enzyme with aspect to pH, temperature, kinetics and stability. Also included was to investigate if it might be cold adapted and set up crystallization trials with the enzyme to allow structure determination. Using HPLC-MSMS the presence of sialic acids in *Moritella viscosa* was to be investigated.

3. Background

Sugar modifying enzymes are of great interest as they facilitate a number of reactions and synthesis of molecules that could be of interest in industry and medicine. Sugars have a vast part in life as they are part of communications between cells, a mode of entry for pathogens and also as a part of the immune system, and they are found in many forms that could be the template for a new medicine or biochemical reaction. The local bacterial genome projects are a source for genes which may have new and interesting functions that could be used for further research and commercialization. Among the sequenced genomes are that of *Moritella viscosa* 06/09/139 which is a causative agent for winter ulcer in salmon. The bacterium was found to have genes that encode for neuraminic acids and pseudaminic acid, sugars that are interesting in both research and for commercial purposes. The main focus of this work will be on neuraminic acid, more specific the neuraminic acid synthase. The genes for the neuraminic acid pathway have identified, shown in figure 3.1, and a more detailed study is needed to find out if and how the bacteria utilizes these sugars, along with the characterization of the enzymes involved in the biosynthetic pathways.

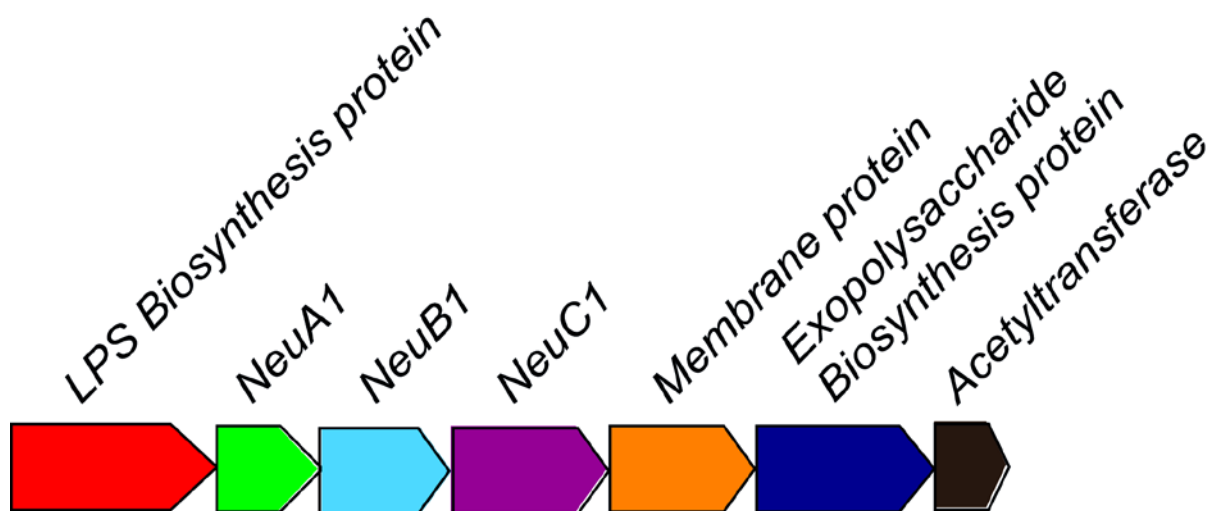


Figure 3.3: The genes responsible for the biosynthetic pathway of neuraminic acid in *Moritella viscosa* have not yet been characterized and their function is unknown.

4. Materials

Table 4.1: Materials used for bioinformatics analysis.

Server/Program	Link	Reference
BioEdit	http://www.mbio.ncsu.edu/bioedit/bioedit.html	x
ExPASy Compute pI/Mw Tool	http://web.expasy.org/compute_pi/	[77] [78]
Pfam	http://pfam.sanger.ac.uk/	x
EMBL-EBI T-coffee	http://www.ebi.ac.uk/Tools/msa/tcoffee/	[79]
PSIPRED	http://bioinf.cs.ucl.ac.uk/psipred/	[80]
ExPASy SWISS-MODEL		[81] [82]
Workspace	http://swissmodel.expasy.org/workspace/	[83]
ESPrpt 2.2	http://esprpt.ibcp.fr/ESPrpt/ESPrpt/	x
		[84] [85]
PyMol	http://www.pymol.org/	[86]
Ramachandran 2.0	http://dicsoft1.physics.iisc.ernet.in/rp/	[87]

X= no reference included

Table 4.2: Buffers used for running electrophoresis gels.

Buffer	Composition	Remarks
TAE-Buffer	40 mM Tris-HCl 20 mM Acetic acid 1 mM EDTA dH ₂ O	Stored at room temperature
Tris-Glycine Buffer	Running 25 mM Tris-HCl 192 mM Glycine 0,1% SDS dH ₂ O	Stored at room temperature

Table 4.3: Media used for cultivation of *E.coli* strains

Media	Composition	Remarks
LB-media	1% (w/v) Tryptone 0.5% (w/v) Yeast Extract 1% (w/v) NaCl dH2O	Autoclaved and stored at 4 C
Selective plates	1% (w/v) Tryptone 0.5% (w/v) Yeast Extract 1% (w/v) NaCl 1% (w/v) Agar dH2O	Autoclaved and cooled to 60 before adding antibiotics and poured on plates stored at 4C
S.O.C- media	2% (w/v) Tryptone 0.5% (w/v) Yeast Extract 10 mM NaCl 2.5 mM KCl 10 mM MgCl ₂ 10 mM MgSO ₄ 20 mM Glucose	Stored at 4C

Table 4.5: Buffers used for purification of NeuB1

Buffer	Composition	Comments
Lysis Buffer	50 mM Tris-HCl 250 mM NaCl 5 mM β -ME 10 % Glycerol dH ₂ O pH 7,5	Stored at 4°C
HisTrap Buffer A	50 mM Tris-HCl 500 mM NaCl 5 mM β -ME 10 mM Imidazole 10 % Glycerol dH ₂ O pH 7,5	Degassed and stored at 4°C
HisTrap Buffer B	50 mM Tris-HCl 500 mM NaCl 5 mM β -ME 500 mM Imidazole 10 % Glycerol dH ₂ O pH 7,5	Degassed and stored at 4°C
Gel Filtration Buffer	50 mM Tris-HCl 150 mM NaCl 5 mM β -ME 10 % Glycerol dH ₂ O pH 7,5	Degassed and stored at 4°C

Table 4.6: Assay Buffer used to prepare TBA assay

Buffer	Components	Comments
Assay Buffer	50 mM Tris-HCl 250 mM NaCl 5 mM β -ME 5 mM MnCl ₂ dH ₂ O pH 7,5	Stored at 4°C

Table 4.7: Buffers used for TEV cleavage of NeuB1 NHis construct

Buffer	Components	Comments
TEV Buffer	10 mM Tris-HCl 100 mM NaCl 1 mM β -ME 1 mM EDTA 5 % Glycerol dH ₂ O pH 7,5	Stored at 4°C
HisTrap Buffer A	50 mM Tris-HCl 500 mM NaCl 5 mM β -ME 10 mM Imidazole 10 % Glycerol dH ₂ O pH 7,5	Stored at 4°C

Table 4.8: Buffers used for dialysis of NeuB1 for DSC experiment

Buffer	Components	Comments
DSC Buffer 1	50 mM HEPES 250 mM NaCl dH ₂ O pH 8,0	Stored at 4°C
DSC Buffer 2	50 mM HEPES 250 mM NaCl 1 mM MnCl ₂ dH ₂ O pH 8,0	Stored at 4°C
DSC Buffer 3	50 mM HEPES 250 mM NaCl 1 mM MnCl ₂ 10 % Glycerol dH ₂ O pH 8,0	Stored at 4°C
DSC Buffer 4	50 mM HEPES 500 mM NaCl 1 mM MnCl ₂ 10 % Glycerol dH ₂ O pH 8,0	Stored at 4°C

Table 4.9: Buffers used for Metal Titration Assay

Buffer	Components	Comments
EDTA Buffer	50 mM Tris-HCl 250 mM NaCl 5 mM β -ME 10 mM EDTA 10 % Glycerol	Stored at 4°C
Metal Assay Buffer	50 mM Tris-HCl 250 mM NaCl 5 mM β -ME	Stored at 4°C

5. Method

5.1 Bioinformatics

The sequencing of DNA has led to a massive amount of information about genes, proteins and their functions in organisms and has given rise to the field of bioinformatics. Using informatics tools to comprise and extract data from sequences and structures, this can be used to predict features about new genes and proteins. The tools used for the bioinformatical procedures are shown in table 4.1. Default settings were used if not specified otherwise.

To calculate physical data based on the protein sequence of NeuB1 from *Moritella viscosa* for the constructs CHis, NHis and NHis TEV cleaved, the ProtParam tool from ExPASy was used.

A multiple sequence alignment of NeuB1 sequence homologues was calculated using the T-coffee server. The list of organisms is based on the alignment done with regards to *N.meningitides* [47] with available sequences and includes *M. viscosa* and *A. salmonicida* [88]. The other sequences were from the following organisms with TrEMBL accession codes; *Aeromonas punctata* (Q9R9S2), *Escherichia coli* (Q46675), *Pseudomonas aeruginosa* (Q8KH52), *Prochlorococcus marinus* (Q7V953) and *Neisseria meningitides* (Q7DDU0). The output is presented graphically using the ESPRIPT 2.2 server. Included is also the secondary structure of *N. meningitides* (1XUZ) and *M. viscosa*. The latter secondary structure was predicted using the PSIPRED server.

To investigate the structure of NeuB1 the protein sequence from *M. viscosa* was analysed using Pfam to obtain information about domains present.

The sequence identity between the NeuB1 sequence of *M. viscosa* compared to NeuB1 from the different organisms mentioned above were determined using the Pairwise Alignment and Calculate Identity/Similarity for two sequences in BioEdit.

A homology model of *M.visocsa* NeuB1 was made using automated mode in SWISS-MODEL Workspace based on the *N. meningitides* structure (1XUZ) as template. The output file contains in addition to structure, assessment of the structure given with QMEAN Z-factor. In order to confirm the validity of the the NeuB1 homology model, the file was uploaded into Ramachandran Plot 2.0 to make a Ramachandran plot to investigate if there are any amino acids in conformations that can give steric hindrance. The homology model was uploaded in

PyMol together with the template (1XUZ) and the monomers were superimposed to a smallest possible root mean square distance (RMSD) for the atom locations. Using the colour by B-factor in PyMol the homology model could be assessed in terms of how much information was transferred from the template

Using PyMol with the structures side by side were made to give a qualitative output.

The two ligands reduced ManNAc and PEP contained in the template file was used to identify the active site of the model. In addition electrostatic maps were made of the monomers of both model and template in order to compare the surface charges around the active site

The genes encoding sialic acid biosynthesis pathway was identified in *M.viscosa* and an overview figure was made using Adobe Illustrator.

5.2 Gene amplification

5.2.1 Polymerase Chain Reaction

To amplify the neuB1 gene a technique called Polymerase Chain Reaction (PCR) was used. This is a technique developed in the 1983 by Kary Mullis [89], and was based on previous research in the 1970s [90]. PCR has had a huge impact on the advances of molecular biology and related fields and is a relatively simple approach to amplify large amounts of DNA from a very little starting point. Only a few materials are needed to do an amplification; a template DNA from where the sequence to be amplified is located, short pieces of DNA that flank the sequence in both reverse and forward direction called primers, nucleotides, a DNA polymerase and a thermocycler to change the temperature. The DNA polymerase was previously added after each cycle since the temperatures required to separate the DNA strands is high and the polymerase would therefore be denatured. A short time after the introduction of PCR a heat resistant DNA polymerase, previously discovered [91], was applied to the process [92]. There are three basic steps in a PCR cycle; denaturation, annealing and elongation. When the starting material is added the temperature is raised to around 90°C for the DNA template strands to separate. The temperature is then lowered to around 50° to allow the primers to anneal to the template and then raised to around 70°C for the DNA polymerase to start synthesising and elongating the DNA strands. After a certain amount of time the temperature is again raised to around 90°C to denature the original and the newly synthesised strand and the cycle is repeated.

The primers (table 4.4) were designed to allow cloning with the Gateway system (Invitrogen) by inserting attb1 and attb2 sites at the ends of the gene and additionally a N-terminal cleavable His-tag for one insert (NHis) and an uncleavable C-terminal His-tag (CHis) for another insert. The NHis forward primer contains a TEV protease specific cleavage site to remove the His-tag after protein purification. The vectors being used is also taken into account and for the CHis insert a Shine-Dalgarno sequence is inserted to facilitate ribosomal binding and initiation of protein synthesis. For construction of the NHis construct the Shine-Dalgarno sequence is provided through the vector pDEST 17. This is not present in the vector pDEST 14 used for construction of the CHis construct. A graphic view of the constructs is shown in figure 5.1.

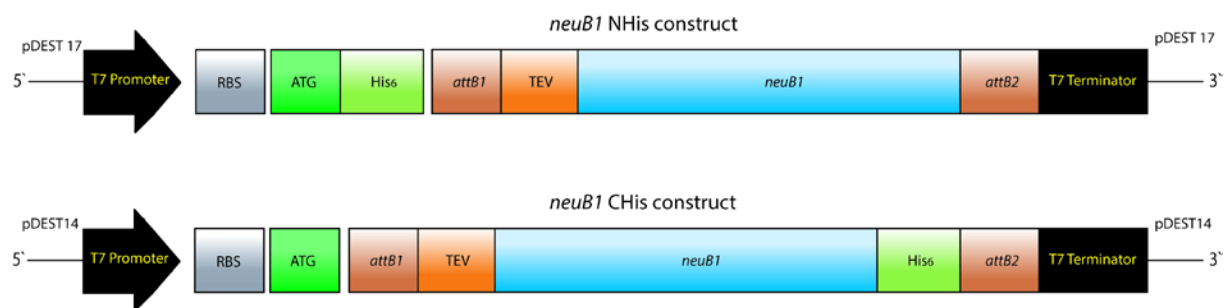


Figure 5.4: The *neuB1* from *M. viscosa* was amplified using designed primers to give two inserts NHis and CHis. NHis contains a N-terminal six residue histidine tag (His) from the pDEST 17 vector, followed by a TEV protease specific cleavage site from the insert to remove the tag after purification. The CHis construct contain a C-terminal His-tag which cannot be cleaved in addition to a Shine-Dalgarno sequence in the N-terminal end, both is introduced through the insert. The attB sites in both ends are required for the Gateway-cloning.

The amplification procedure is done in two PCR steps with intermediate purification. The designed primers were dissolved according to manufacturers' orders and diluted to a final concentration of 10 μ M. The first PCR step was done with the following reaction mix and concentrations; 1x Phusion HF Buffer (Thermo Science), 300 μ M dNTP mix (Thermo Science), 0.3 μ M forward and reverse primer, table , approximately 132 ng of *M. viscosa* genomic DNA, 0.02 U/ μ L Phusion polymerase (Thermo Science) and nuclease free water to a total volume of 50 μ L. The following program was used for the reaction; incubation at 98°C for 2 min for initial denaturing, then 35 cycles of denaturation at 98°C for 20 seconds, incubating at 50°C for 20 seconds for primer binding and incubating at 72°C for 20 seconds for DNA synthesis before the cycle is repeated. After 35 cycles the reaction mix is left for incubation at 4°C. The program was run on a DNA Engine Dyad® (BioRad).

5.2.2 DNA Gel Electrophoresis

The PCR products were thereafter analysed with agarose gel electrophoresis to confirm that the gene had been amplified. This was done by preparing 50 mL 1% liquid agarose gel by dissolving agarose powder in TAE-buffer (table 4.2) and heated until it dissolved and kept at 60°C until use. Before use, 2.5 µL RedSafe nucleic acid staining solution (ChemBio) was added to the agar solution. The gel was cast by pouring it into a gel casting tray and left to cool down. A comb was set in the tray to give wells that the sample could be loaded into when the gel had been solidified and comb removed. The solidified gel was removed from the tray and transferred to the electrophoresis chamber. The following prepared samples were added to the wells, 1 µL DNA ladder mixed with 5 µL 6x Blue Dye and 30 µL of the PCR products CHis and NHis was added 5 µL 6x Blue Stain respectively. The gel was covered with TAE buffer and run at 90 V for 60 min and then removed from the chamber and placed under an UV source (BioRad GelDoc) to visualize and cut out the bands containing the PCR-products.

5.2.3 Extraction of DNA from agarose gel

Bands containing the PCR products were cut from the gel, and DNA extracted by using the QIAquick Gel Extraction Kit (250) according to protocol for microcentrifuge tube.

5.2.4 2nd PCR

The extracted DNA containing the amplified PCR-products was used in a second PCR round with attB specific primers (table 4.4) to obtain the gene with the attB sites for cloning. The setup for the second round is identical to the previous one except the use of primers and template. For creation of the NHis insert the forward primer and reverse primer used is; NHis-F2 and NHis-R2 respectively. For creation of the CHis insert the forward and reverse primer used is CHis-F2 and CHis-R2 respectively. The concentration of each primer in the reaction mix was 0.3 µM. The PCR products were run on an agarose gel and extracted according to previously described method, section 5.2.1.

5.2.5 Determining DNA Concentration

The concentration of the DNA was determined using a NanoDrop 2000c spectrophotometer.

5.3 Cloning

In order to produce significant amounts of the vector containing the insert, usually called cloning, the vector is inserted into a bacterial host, typically *E.coli* in order to replicate the vector. This will give more amounts of the vector that can be used.. The vector can then be inserted into the bacteria by heat shock treatment, a type of transformation. This is done by mixing the bacteria and vector and for a short amount of time expose the bacteria for high temperatures that will open the pores of the bacteria and let the vector be taken up into the bacterial cell. The bacteria is then incubated and let multiply. This can be done several times to produce enough vector material to clone the host that will be expressing the gene.

5.3.1 Preparation of Gateway constructs

The NHis and CHis constructs were made according to the Gateway cloning protocol “One Tube Protocol” (Life Technologies). The first step was to insert the PCR-products into the donor vector pDONR221 for each construct using the BP Clonase II reaction [93] . For this reaction 100 ng of each DNA inserts, CHis and NHis, was mixed with 225 ng of pDONR221, 2 μ L BP Clonase II enzyme and TE buffer to a total volume of 15 μ L. The reaction was left at room temperature for 20 hours. The reaction was terminated by adding 1 μ L proteinase K and incubated at 37°C for 10 minutes.

In the next step the entry clones are inserted into their intended destination vectors. The NHis entry clone was transferred into a pDEST 17 vector and the CHis into a pDEST 14 vector using the LR reaction. For each reaction 10 μ L of their respective BP mix added with 2 μ L LR Clonase II and 1,5 μ L TE buffer. For NHis 225 ng of pDest14 was added, while for CHis 112,5 ng was added. The reactions were left at room temperature for 6 hours and then terminated with the addition of 1 μ L proteinase K with incubation at 37°C for 10 minutes. The leftover BP reaction mix and the LR reaction mix were stored at -20°C until transformation.

5.3.2 Transformation

The prepared constructs with the NHis and CHis inserts were cloned into pDEST14 and pDEST 17 (Invitrogen, Life Technologies) destination vectors respectively, and was transformed into One Shot TOP 10 competent cells according to the protocol from Life

Technologies. Four tubes of competent cells were incubated with 3 μL each of the destination vectors on ice for 30 minutes. The cells were then heat shocked by emerging in 42°C water for 42 seconds before being placed back on the ice for 2 minutes. The cells were then added 250 μL of room temperate S.O.C. Media (table 4.3) and shaken for 60 minutes at 37°C at 225 rpm.

5.3.3 Cultivating

The transformed cells containing the NHis and CHis constructs were spread on Lysogeny Broth (LB) agar plates (table 4.3) containing 50 $\mu\text{g}/\text{mL}$ Kanamycin and 100 $\mu\text{g}/\text{mL}$ ampicillin. Different volumes were spread on the plates, 50 μL and 150 μL giving a total of 8 plates. The plates were incubated overnight at 37°C.

Six tubes with 4.5 mL of room temperate LB media (table 4.3) were prepared each containing 100 $\mu\text{g}/\text{mL}$ ampicillin. Three colonies from each plate (150 μL) containing the NHis and CHis construct were added to each tube separately. The tubes were incubated at 37°C at 230 rpm overnight. The cultures were then transferred to centrifuge tubes and centrifuged at 2300 g for 20 min. Before centrifugation 800 μL of the cultures were transferred to cryotubes and added 800 μL 40% glycerol for storage as freeze stocks in -80°C freezer. The supernatant from the centrifugation was discarded and plasmid were extracted and purified using ZR Plasmid Miniprep Classic protocol (Zymo Research).

5.3.4 Sequence Verification

To verify that the constructs contained the correct inserts, PCR sequencing reactions were set up for Sanger sequencing. Two reactions containing forward and reverse primer separately for each colony of the two constructs were sequenced using 2 μL of the vector, 1 μL T7 forward primer or pDEST 14 reverse primer, 2 μL Big Dye 3.1, 1.5 mM MgSO_4 and water to a total volume of 20 μL . The PCR cycles used were as mentioned . The sequencing products were sent to the University Hospital of Northern Norway (UNN) for sequencing. The resulting sequences were analysed using BioEdit for confirmation.

5.3.5 Transformation of Expression Strains

The confirmed constructs NHis and CHis were transformed into expression strains. Both constructs were transformed into the strains *E.coli* Rosetta 2 (DE3) plysS and *E.coli* BL21* pRare 2 plysS (Novagen) using the previous mentioned method, section 5.3.2. After adding

the S.O.C. media the tubes were incubated at 37°C and 200 rpm for 1 hour and then plated on LB agar plates containing 100 µg/mL ampicillin and 34 µg/mL chloramphenicol. Each of the plates were plated with 25 µL cell culture and 25 µL S.O.C. media and 50 µL cell culture giving a total of eight plates that were incubated overnight at 37°C.

5.4 Pilot Protein Expression

To analyse the protein expression in the strains, 12 tubes with 4,5 mL LB media with 100 µg/mL ampicillin and 34 µg/mL chloramphenicol were prepared and for each tube a separate colony (x2) and a mix (scoop) of colonies were selected and added respectively. The cultures were incubated at 30°C at 220 rpm for 16 hours.

The cultures were transferred to prepared 250 mL flasks containing 50 mL LB media + 100 µg/mL ampicillin and 34 µg/mL chloramphenicol and incubated at 37°C at 220 rpm. Freeze stocks were prepared before transfer by mixing 800 µL culture with 800 µL 40 % glycerol and storing at -80°C.

The OD of the cultures was checked every hour by taking out 1 mL and measuring absorbance at 600 nm until the value was approximately 0,6 and the temperature was lowered to 20°C. The cultures were then induced with 0,5 mM isopropyl-β-D-1-thiogalactopyranoside (IPTG) and incubated at 20 °C at 220 rpm overnight. Before inducing, 3 hours after and next morning samples were taken out to analyse the expression. 50 µL samples were centrifuged at 13 000 rpm for 2 min and the supernatant discarded. The pellets were stored at -20°C until they could be run on SDS-PAGE. The induced cultures were transferred to centrifugal tubes and centrifuged at 4000 rpm for 12 min at 4°C. The supernatant were discarded and the pellets stored at -20°C.

5.4.1 SDS-PAGE

Sodium Dodecyl Sulfate Polyacrylamide gel electrophoresis (SDS-PAGE) is a technique that separates proteins based on their size in a gel. The protein samples are denatured with sodium dodecyl sulfate that denatures the proteins and binds to give a negative charge relative to the size.

Preparing the cell pellets for SDS-PAGE included adding 83 mM DTT and 10 µL 4x SDS-PAGE NuPage Buffer (Invitrogen, Life Technologies). The sample were then incubated at 95°C for 5 minutes and spinned down. The total volumes of the samples were added in the gel

wells along with 12 μ L Mark12TM Unstained Standard (Invitrogen) as molecular weight marker. The samples were run on a Mini-PROTEAN® TGXTM precast gel (BioRad) with Tris-Glycine running buffer (table 4.2) for 40 min at 200 V and 12,5 W. After the run the gel was washed with water and boiled for 1 min three times with change of water between before being stained with Simply BlueTM SafeStain (Invitrogen, Life Technologies) for 20 min. The stain was then washed off and the gel left in water until analysis (BioRad GelDoc)

5.4.2 Preparing MS samples

To confirm that the expressed protein was the correct one, samples were run on SDS-PAGE as described, section 5.4.1, and cut out of the gel and transferred to an Eppendorf tube. The samples were sent for MS analysis at Tromsø University Proteomics Platform (TUPP).

5.5 Pilot Protein Purification

In order to study the protein of interest it is vital that the sample is pure enough, meaning that there is no other molecules in the sample that could affect the experiments to be carried out. In order to purify protein samples, several methods are available in the domain of chromatography, because proteins inherent properties like charge, size, hydrophobicity and affinity. A method often used is the affinity chromatography where the proteins affinity for a certain compound is used to separate it from other proteins in the sample, like histidines affinity for nickel. This is done by inserting a sequence in either terminal end of the gene encoding the protein coding for histidine. Usually six histidines are included in the sequence which will give a strong affinity for nickel and give a better purification. The proteins can also be separated by size exclusion chromatography which separates in terms of size of the protein. A column with a porous material is used which allows large molecules to flow through the column faster than the smaller ones that will spend time going inside the pores and be retarded.

5.5.1 Sonication

Each of the pellets from the pilot expression experiments were mixed and resuspended in Lysis Buffer (table 4.5) to a total volume of 35 mL and added a Proteinase Cocktail Complete EDTA-free (Roche) and DNase I (Roche) and sonicated with 9,9 seconds on and 9,9 seconds off, 25% amplitude, temperature limit 20°C for 30 min with a VibraCellTM (Sonics). The sonicated solution was then centrifuged at 9000 g for 30 min at 4°C and the supernatant was transferred to a new tube, the pellet was discarded. The solution was filtered using a syringe

with 0.2 μm Amicon® 25 mm syringe filter (Pall Corporation). Sample of 50 μL were taken out after sonication to be run on SDS-PAGE.

5.5.2 HisTrap Purification

The HisTrap ff Crude column 1mL (GE Healthcare) was prepared by running through 5 mL 20% ethanol, water and equilibrated with HisTrap Buffer A (table 4.5) with pressure limit 0.5 MPa and flow 1 mL/min at 4°C. The system used was Äktaprime plus (GE Healthcare) and the program Unicorn 5.0 The sample was injected through pump A and when baseline was re-established 5 % HisTrap Buffer B (table 4.5) was washed through before setting a HisTrap Buffer B gradient from 5 to 100 % over 10 mL. Fractions were collected when gradient was initiated. Flowthrough and 5% wash were collected separately and samples were taken out along with the fractions for SDS-PAGE.

The SDS-PAGE for protein in solution was carried out as described, section 5.4.1, but with differences in the preparations of the denaturation of protein. 21 mM DTT, 8 μL 4x SDS-PAGE NuPage Buffer and 15 μL of protein sample was mixed and heated to 95°C before being spinned down. The gel was set up as previously and 15 μL of the prepared samples was added to the wells along with the Mark12 marker.

5.5.3 Determining Protein Concentration

The protein concentration was determined using the Nanodrop 2000c spectrophotometer determining protein concentration at 280 nm using calculated molecular weight and average extinction coefficient for the protein. The blanks used was the current buffer the protein was stored in.

5.6 Pilot Activity Assay

The activity of the enzyme was determined using the Thiobarbituric acid assay developed for Sia [94] [95] [96] [97]. The assay measures the amount of NeuNAc after the reaction by addition of sodium periodate (NaIO_4) in acidic solution (H_2SO_4). The high acidity stops the enzymatic reaction and also contributes in the formation of the chromogen. The stepwise reaction shown below in figure 5.2 starts with the addition of periodate that oxidised the NeuNAc and gives 4-deoxyhexos-5-uluronic acid as a prechromogen by incubating at 37°C for 15 minutes and shaking at 220 rpm. Sodium arsenite is then added to neutralize the sodium periodate and 2-thiobarbituric acid is added which hydrolyses the 4-deoxyhexos-5-

uronic acid into β -formylpyruvic acid and N-(2-Oxoethyl)acetamide. This step is performed by heating in a boiling water for 7,5 minutes. The chromogen β -formylpyruvic acid condenses with the 2-thiobarbituric acid and gives the red/pink chromophore which is extracted with acidic 1-butanol under vigorous shaking for 10 minutes. The absorbance is measured using a wavelength of 549 nm.

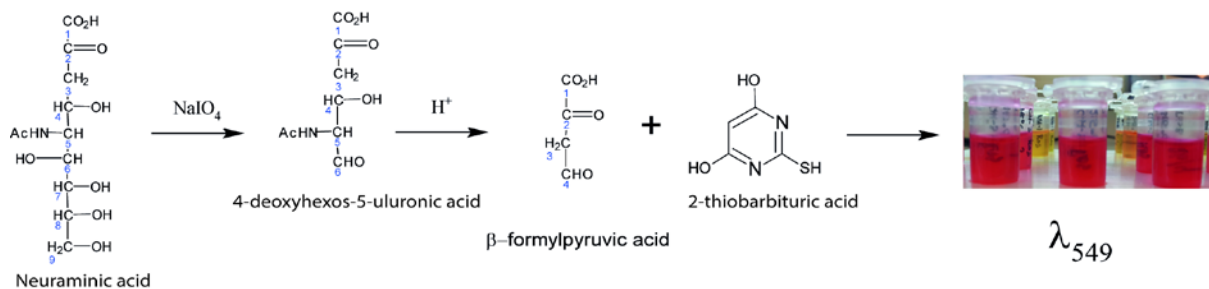


Figure 5.5: The thiobarbituric acid assay (TBA) is used to determine the amount of neuraminic acid produced in the assays. This is done by preparing β -formylpyruvic acid that will react with 2-thiobarbituric acid and give absorbance at 549 nm. The preparations are done by adding sodium periodate that will oxidise the open form of the sugar and give 4-deoxyhexos-5-uluronic acid. The sodium periodate is then neutralized by addition of sodium arsenite followed by the addition of 2-thiobarbituric acid that hydrolyses the 4-deoxyhexos-5-uluronic acid and gives β -formylpyruvic acid that again reacts with the 2-thiobarbituric acid to give the chromophore.

5.6.1 TBA Assay Preparations

In order to measure the production of Sia the enzyme sample needed to be dialysed in Assay Buffer (table 4.5) in order to remove glycerol which interferes with the TBA assay and can give a false negative. The dialysis preparations before all endpoint assays were done as described unless otherwise specified. The protein sample was transferred to a Slide-A-Lyzer® Dialysis Cassette (Thermo Scientific) with a molecular weight cut off (MWCO) of 3500 and maximum volume of 3 mL. The cassette was submerged in the assay buffer and dialysis was performed at 4°C with stirring for 18 hours and one buffer exchange. The sample was then recovered and protein concentration was determined with Nanodrop 2000c as described 5.5.3, before performing assay.

5.6.2 TBA Assay

After the reaction was complete, the mixture is prepared for analysis by adding 127 μL 2.5 mg/mL sodium periodate (NaIO_4) in 57 mM H_2SO_4 . The solution is then incubated at 37°C for 15 minutes with shaking 220 rpm. Then 50 μL of 2,5 mg/mL sodium arsenite (NaAsO_2) in 0.5 M HCl. The tube is shaken by hand until the solution is clear and 100 μL of 25 mg/mL 2-thiobarbituric acid pH 9 is added. The solution is then heated in a boiling water bath for 7.5 minutes and kept on ice for 5 minutes before being kept in room temperature until 1 mL of 1-butanol with 2% HCl can be added. The tubes are then shaken for 10 minutes in a vertical position at 230 rpm followed by centrifugation at 13 000 rpm for 7 minutes and they are ready for absorbance reading.

5.6.3 TBA Assay Measurement

The extracted chromophore solution was transferred to a Falcon Microtest™ 96 well plate (Becton Dickinson Labware) for absorbance reading with 200 μL volume of each sample. The absorbance was measured using SpectraMax M2^e with the program Softmax Pro 5,2 (Molecular Devices) at wavelength 549 nm, and 5 seconds premixing. When needed the samples were diluted with 1-butanol in order to get exact measurements. Dilution factors are given for those samples.

5.6.4 Pilot Assay

To test if the purified protein was active 1,5 mL of each construct expressed in the Rosetta strain was transferred to a Slide-A-Lyzer® Dialysis Cassette (Thermo Scientific) with a molecular weight cut off (MWCO) of 3500 and maximum volume of 3 mL. The sample was dialysed in Assay Buffer over night at 4°C with one buffer exchange. The solutions were removed from the cassette and kept on ice until the reaction mix was ready. Reaction mix was prepared with 10 mM ManNAc, 10 mM PEP, 120 mM Tris-HCl pH 8 and 5 mM MnCl_2 , 62 ng CHis and 3,14 ng NHis and water to a total volume of 50 μL . The reaction was carried out at room temperature for one hour and the reaction was terminated using 137 μL sodium periodate and assayed as described, section 5.6.2 and 5.6.3.

5.7 Large Scale Expression

The precultures were set up by adding sample from freeze stock to 10 mL LB media with 100 $\mu\text{g}/\text{mL}$ ampicillin and 34 $\mu\text{g}/\text{mL}$ chloramphenicol and incubated for 16 hours at 37°C at 220

rpm. The precultures were added to 1 L LB media containing 100 µg/mL ampicillin and 34 µg/mL chloramphenicol and incubated at 37°C at 220 rpm until OD was 0,6 when the temperature was lowered to 20 °C. The cultures were then induced with 500 µL 1 M IPTG and incubated at 20°C at 220 rpm overnight. 50 µL samples were taken out before inducing, 3 hours after and the next morning to be run on SDS-PAGE. The cells were harvested by transferring the cultures to centrifugal tubes and centrifuged at 6000 rpm for 30 minutes at 4°C. The supernatant was discarded and the pellet stored at -20°C until purification.

5.8 Large Scale Purification

5.8.1 HisTrap Purification

The frozen pellet was prepared for purification by sonication as described in section 5.5.1. The volume of the sample was measured and 500 µL of the sample was saved for construction of a purification table. The protein was purified using a HisTrap High performance Column 5 mL which was prepared by washing with 25 mL of 20% ethanol, water and equilibrated in HisTrap Buffer A with flow of 2 mL/min and pressure limit 0,5 MPa, until baseline was established. The purification was performed with using Äktaprime plus with Unicorn 5.0 (GE Healthcare). The protein sample was applied through pump A and the flowthrough was collected. When the baseline was re-established the column was washed with 5% HisTrap Buffer B until the baseline was re-established again, both flowthrough and 5% wash was collected separately. The protein was eluted with a gradient of HisTrap Buffer B from 5 to 100% over 50 mL. Fractions of 1.5 mL was collected as gradient was started. The collected flowthrough, 5% wash and fractions were stored and run on SDS-PAGE as described above, section 5.4.1. The fractions containing the protein were pooled and 500 µL was taken out for Purification table.

5.8.2 TEV Cleaving

To be able to cut of the His-tag on the NHis construct the insert contained a TEV protease cleavage site. The protease recognizes the sequence ENLYFQ(G/S) and cuts between Q and G/S. The cleaving was carried out by dialysing the protein solution in TEV-buffer (table 4.7) over night at 4°C with one buffer exchange. The TEV protease (2.7 mg/mL, Labstock) was added in two rounds, 1.5 mL. First at the beginning of the dialysis and when buffer exchange was performed. This was done to maximise the cleaving efficiency as the activity is lost over time. To remove the TEV-protease and His-tag from the protein solution the solution was

dialysed against HisTrap Buffer A (table 4.7) with two buffer exchanges to remove the EDTA that could bind the nickel in the HisTrap column. The solution was purified on a 5 mL HisTrap High Performance column (GE Healthcare) prepared as before. The sample was injected through pump A and fractions were collected at the beginning. The column was washed with 5% HisTrap Buffer B and following gradient as previously. The fractions, 5% wash and gradient was collected and run on SDS-PAGE. The fractions containing the protein were pooled and 500 μ L sample was taken out for the purification table.

5.8.3 Gel Filtration

The column Superdex 200TM prep grade 26/600 (GE Healthcare) was prepared by washing through with 230 mL 20% ethanol, water and Gel Filtration Buffer (table 4.5) with a flow of 1,5 mL/min and pressure limit 0,5 MPa. The system used was Äktaprime plus (GE Healthcare) with Unicorn 5.0. The protein sample was injected through pump A. Fractionation was started when an increase in the baseline was observed. Fractions belonging to peaks were run on SDS-PAGE. The fractions containing the protein were pooled and 500 μ L sample was taken out for Purification table.

5.9 Purification Table

To analyse the effectiveness of the protein purification a purification table was made. The table require the volume of the injected samples, concentration and activity of the protein. The volume of the samples injected was measured using a volumetric cylinder. For the activity and concentration measurements the endpoint assay and a Bradford assay was used respectively.

5.9.1 Bradford Assay

The Bradford Assay was performed as described in the protocol for Standard procedure for Microtiter plates (BioRad). The standards used to measure the protein concentration was prepared by serial dilution of Bovine Serum Albumin (BSA) to concentrations 0.05, 0.1, 0.15, 0.25 and 0.5 mg/mL. Water was used for dilution. For the unknown samples dilutions were prepared for the lysate, HisTrap and Gel filtration purified protein. Lysate was diluted with a dilution factor of 10 and 100, HisTrap and Gel filtration purified samples were diluted with a dilution factor of 10. The dye used was Protein Assay Dye Reagent Concentrate (BioRad) that was prepared by diluting 5 mL dye with 20 mL water in a ratio 1:4 and by filtration using a 24 cm filter paper (Whatman). 10 μ L of the standards

and unknown samples, in three parallels, were added to a Falcon Microtest™ 96 well plate (Becton Dickinson Labware) and added 200 µL dye using a multichannel pipette and let stand in room temperature for 5 min before reading absorbance at 595 nm using SpectraMax M2^e (Molecular Devices). The data was analysed using SoftMax Pro 5.2.

5.9.2 Activity Assay

200 µL of the samples from the purification steps were dialyzed as described, but with a Slide-A-Lyzer® Dialysis Cassette (Thermo Scientific) with a molecular weight cut off (MWCO) of 3500 and maximum volume of 0.5 mL To analyse the activity of the samples reaction mix containing 10 mM ManNAc, 10 mM PEP, 5 mM MnCl₂, 120 mM Tris-HCl pH 8, 20 µL of each sample and water to a final volume of 50 µL. The assay was performed with three parallels of each sample and blank using Assay Buffer. The reaction was carried out at room temperature for 1 hour and stopped and analysed as described.

5.10 pH Optimum

To find the pH where the enzyme has its optimum activity an assay was carried out by first preparing 2 M solutions of HEPES and Tris-HCl. 5 mL of each was transferred to 5 tubes to a total of 10 tubes and pH was adjusted using either 5 M NaOH or 37% HCl. Water was added to give a total concentration of 1 M of each Tris-HCl and HEPES pH-buffer. The pH used in the assay was for HEPES 6.0, 6.5, 7.0, 7.5 and 8.0 while for Tris-HCl it was pH 8.0, 8.5, 9.0, 9.5 and 10. The protein was prepared by dialysis as described. The experiment was carried out with three parallels and one blank for each pH. The reaction mixture was composed of 120 mM Buffer, 10 mM ManNAc, 10 mM PEP, 5 mM MnCl₂, 5 µg NeuB1 CHis and water to a final volume of 50 µL. The reaction was carried out at room temperature for 1 hour and terminated as described followed by analysis.

5.11 Temperature Optimum

To investigate the temperature optimum for the enzyme, the enzyme was prepared by dialysis in Assay Buffer. To vary the temperature a PCR machine (MJ Mini Thermal Cycler, BioRad) was used. The temperature range that was investigated was 5, 15, 25, 30, 32, 34, 36, 38, 40, 45 and 55°C. The reaction mixture was prepared with 10 mM ManNAc, 10 mM PEP, 5 mM MnCl₂ and 120 mM HEPES pH 8 and water that with the addition of the protein gave a total volume of 50 µL. The reaction mixture and protein sample was incubated at the respective temperature separately for 5 min before the protein was added to the reaction mixture and let run for 30 min. The experiment was carried out with three parallels and one blank for each

temperature. Assay buffer was used as blank solution for enzyme. The reactions were stopped by adding 2 μL conc. sulphuric acid (H_2SO_4) and let stand in room temperature until activity could be measured as described in section 5.6.2 and 5.6.3.

5.12 Metal Dependency

To investigate the dependency of metal present in the enzyme and effect of other metals, apoenzyme was prepared by dialysing protein sample in EDTA Buffer (table 4.9) to bind and remove any metal in the sample. The sample was dialysed at 4°C with three buffer exchanges over 24 hours and then dialysed again against Metal Assay Buffer (table 4.9) without MnCl_2 to remove the EDTA (4°C , overnight and two buffer exchanges). The reaction mixtures were prepared by using three different divalent cations, Mn^{2+} , Mg^{2+} and Co^{2+} with varying concentration. The titration was carried out with the following concentrations of each metal, 0.1, 0.5, 1.0, 3.0, 5.0 and 7.0. In addition the reaction mixture contained 10 mM ManNAc, 10 mM PEP, 120 mM Tris-HCl pH8, 5 μg NeuB1 CHis and water to a final volume of 50 μL . The assay was performed with three parallels and blanks for each metal concentration. The reaction was carried out at room temperature for 1 hour and terminated and analysed as described.

5.13 Stability Assay

To investigate the stability of the enzyme over time at different temperatures protein sample was prepared as described. The experiment was carried out with three parallels for each time point and three samples were kept on ice as reference. The three temperatures analysed was 25°C , 37°C and 45°C . Samples were taken out after five minutes for all the temperatures, then every 15 minutes starting from zero for 25°C until two hours, every 10 minutes starting from 5 minutes for 37°C until one hour and every five minutes for 45°C until 30 minutes. 20 μL of protein sample was incubated at each temperature, taken out at the specific time and kept on ice until assay could be carried out. The reaction mixture contained of 10 mM ManNAc, 10 mM PEP, 120 mM Tris-HCl, 5 mM MnCl_2 and 5 μg of the NeuB1 CHis and water to a total volume of 50 μL . Three blank were prepared as well with assay buffer as solution. The reaction was carried out at room temperature for one hour and the activity analysed as described.

5.14 Differential Scanning Calorimetry

To prepare the sample for DSC the protein was dialysed in DSC-Buffer (table 4.8) overnight at 4°C and one buffer exchange. The sample was then transferred to a falcon tube by filtering

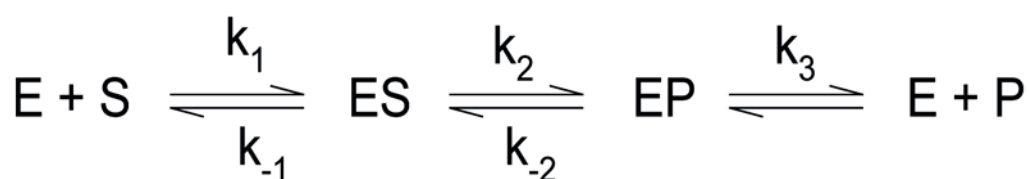
with syringe through a 0.2 μm Acrodisc® 25 mm syringe filter (Pall Corporation) and degassed for 10 min. The DSC was prepared by washing with 50% degassed and filtered acetic acid in a temperature range of 25 to 80°C with an increase of 1°C/min in the cell. The cells was then washed with 1L of water and filled with degassed and filtered water and scanned overnight from 4 to 80°C with a temperature increase of 1°C/min. The experiment was started with scanning filtered and degassed DSC-buffer in both cells from 4 to 80°C with a temperature increase of 1°C/min. The sample was added by filling the sample cell after reducing the pressure during the cooling period at temperature 10°C. The sample was then heated from 4 to 80°C

5.15 Kinetics

Living organisms depend on enzymes to carry out chemical reactions that otherwise would take too much time. The enzymatic production of compounds is tightly regulated by the organism and is influenced by many factors like temperature, pH substrate amount and inhibitors. The rate of which the products are made can be studied using enzyme kinetics and the mathematical fomula for this is the Michaelis-Menten equation

$$v_0 = \frac{V_{max}[S]}{K_m + [S]}$$

The emzyamtic reaction rate is here related to the concentration of substrate, following the equation the V_{max} is the maximum rate that the system can achieve and K_m is the half of the maximum rate and is also used as an indication of the enzymes substrate affinity.



Considering the equation which describes an enzymatic reaction the steps involved in the formation of the product are all described with rate constant, and in this case the release of substrate from the enzyme-substrate complex is the rate limiting step. In order to compare the rate of product formation between enzymes a general rate constant k_{cat} is used. This constant can describe only a single rate limiting step in the process or be a complex of several rate limiting steps. In the Michaelis-Menten equation k_{cat} is defined as;

$$k_{cat} = \frac{v_{max}}{[E_t]}$$

where $[E_t]$ is the total enzyme concentration. This gives a Michaelis-Menten equation as;

$$v_0 = \frac{k_{cat}[E_t][S]}{K_m + [S]}$$

In order to measure the production of NeuNAc formed by NeuB1 a coupled assay was used which takes advantage of the phosphate released from PEP during catalysis. Purine nucleoside phosphorylase (PNP) is an enzyme that catalyzes the reaction of cleaving 2-amino-6-mercapto-7-methylpurine ribonucleoside (MESG) which is an analogue of guanosine, into ribose phosphate and 2-amino-6-mercapto-7-methylpurine with the addition of phosphate, figure 5.3. The formation of one molecule of neuraminic acid leads to one molecule of 2-amino-6-mercapto-7-methylpurine, which has an absorbance maximum at 360 nm. The change of absorbency is utilized for activity measurements.

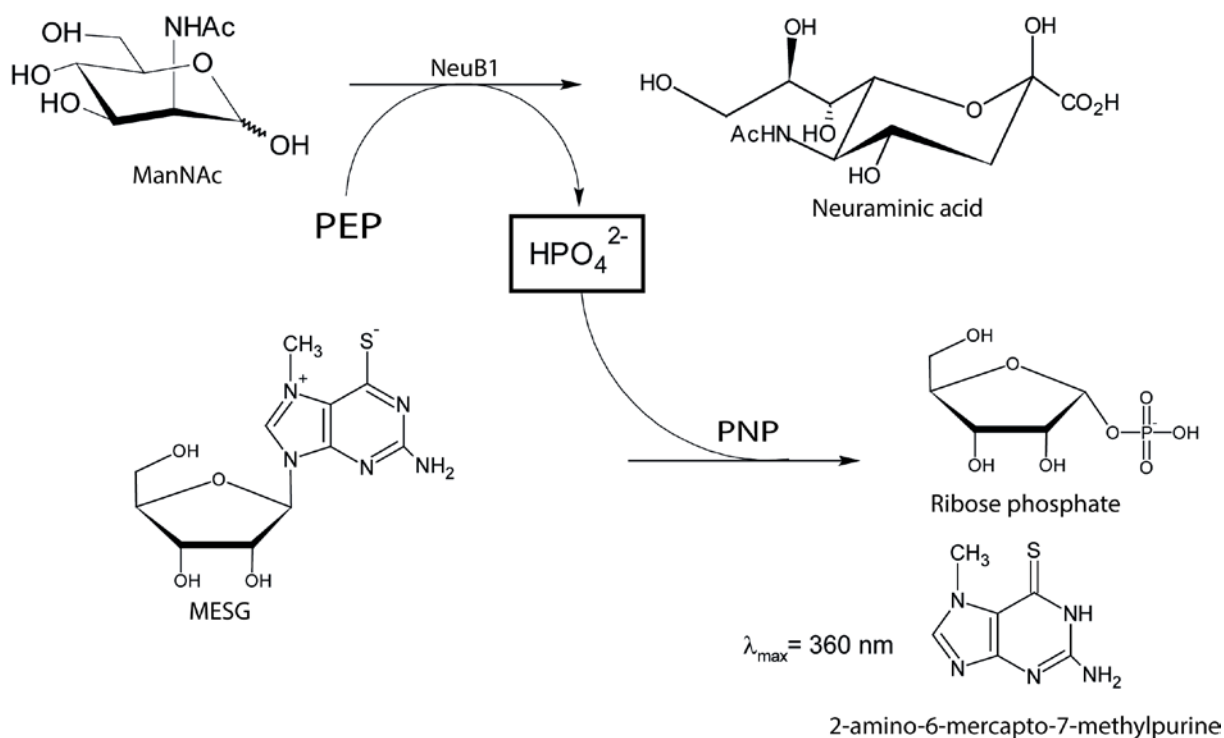


Figure 5.6: To follow the reaction of NeuB1 in the formation of NeuNAc a coupled assay was used to determine the kinetic constants. PNP that utilises the released phosphate group from the NeuB1 reaction to phosphorylate the 2-amino-6-mercapto-7-methylpurine ribonucleoside to give ribose phosphate and 2-amino-6-mercapto-7-methylpurine. The latter has an absorption maximum of 360 nm that is measured as the reaction progresses.

5.15.1 Pilot Experiments

The NeuB1 CHis used for the kinetics assay was dialyzed in Assay Buffer as described before the experiments were carried out.

In order to measure kinetic parameters of NeuB1 at 25°C in the coupled assay, a test was set up to analyse the activity of the PNP (Sigma) at 25°C and 37°C. For each temperature a mix of 0.2 U/ μ L PNP, 0.2 mM MESG, 100 mM Tris-HCl pH 8, 5 mM ManNAc and 5 mM PEP was used. The amount of NeuB1 CHis used was varied and 5, 10 and 20 μ g was added along with water to a total reaction volume of 200 μ L. The reaction mix and NeuB1 CHis was incubated at the respective temperature for 5 minutes before NeuB1 CHis was added and the absorption read. The reaction was measured using SpectraMax M2^o Kinetics measurement (Molecular Devices) with absorbance 360 nm and 5 seconds mixing before reading.

To find the optimal amount of NeuB1 CHis to use in the kinetic assay a test were set up with varying concentrations. The reaction mix was set up and contained 0.2 U/ μ L PNP, 0.2 mM MESG, 100 mM Tris-HCl pH 8, 5 mM ManNAc and 5 mM PEP. The amount of NeuB1 CHis was varied from 0.25, 0.5, 1.0, 2.0, 3.0, 4.0, 5.0 and 10.0 mM. Water was added to give a total reaction volume of 200 μ L. The reaction mix and enzyme was incubated separately for 5 minutes at 25° before the enzyme was added and the absorption read as described.

5.15.2 Protein Concentration

In order to determine the exact concentration of the enzyme for calculations the concentration was determined using both Bradford and Nandrop as described above.

5.15.3 ManNAc

To determine the K_m value for ManNAc the reaction was set up with varying concentrations of ManNAc, 0.1, 0.5, 2.0, 5.0, 10.0, 20.0, 40.0 and 60.0 mM. The reaction mix was set up with 0.2 U/ μ L PNP, 0.2 mM MESG, 100 mM Tris-HCl pH 8, 5 mM PEP, 0.5 μ g NeuB1 CHis and water to a total volume of 200 μ L. The experiment was carried out with three parallels and blank. Each of the parallels and blank were carried out one by one, but for all the reaction mix and NeuB1 CHis was incubated at 25°C before mixing and reading absorbance at 25°C as described above. Calculations were performed in SigmaPlot.

5.15.4 PEP

To determine the K_m value for PEP the reaction was set up with varying concentrations of PEP, 0.05, 0.1, 0.25, 0.5, 1.0, 3.0, 5.0 and 10.0 mM. The reaction mix was set up with 0.2 U/ μ L PNP, 0.2 mM MESG, 100 mM Tris-HCl pH 8, 10 mM ManNAc, 5 mM $MnCl_2$, 0.95 μ g NeuB1 CHis and water to a total volume of 200 μ L. The experiment was carried out with three parallels and blank. Each of the parallels and blank were carried out one by one, but for all the reaction mix and enzyme was incubated at 25°C before mixing and reading absorbance at 25°C as described above. Calculations were performed in SigmaPlot.

5.15.5 Phosphate Standard Curve

The phosphate released in the assay which is used in the production of 2-amino-6-mercapto-7-methylpurine correlates to the amount of neuraminic acid and to determine the amount of Neuraminic acid produced in the kinetic assay a phosphate standard curve was made. A standard curve was made by setting up a reaction using different concentrations of phosphate, 1.75, 3.5, 10.5, 17.5, 35.0, 70.0, 105.0, 140.0 and 175.0 μ M. The reaction mixture was set up with three parallels of each phosphate concentration and blank. The reaction mix contained 0.2 mM MESG, 10 μ L reaction buffer (1 M Tris-HCl pH 7.5 + 20 mM $MgCl_2$). The reaction was initiated by addition of PNP (0.2U/ μ L) and the reaction was carried out at room temperature for 30 minutes before reading the plate. The plate was read using SpectraMax M2^e (Molecular Devices) with absorbance 360 nm and 5 seconds mixing before reading. The absorbancy values was used to make a standard curve in SigmaPlot.

5.16 Crystallization

To determine the structure of a protein there are two mainly used methods, NMR and X-ray crystallography. They are considered complimentary methods and have their advantages and drawbacks. The major drawback with NMR is the size of the molecules it is able to structurally determine because of more noisy spectra. In order to try to determine the structure of NeuB1 x-ray crystallography is the method of choice. To use this technique the protein must be in crystalline which is considered as a real bottleneck. To find the conditions for a protein to crystallize, screenings of i.e different compounds and temperatures and pH values is required. In order to save time and protein amounts, robots have been developed that use minimal with protein in screening with many different conditions. When a condition has been found that may be optimized to give crystals, the next step is to set up larger volume screens that vary around the conditions found.

In order to crystallize NeuB1 an initial screening with robot was set up using Phoenix DT crystallization robot (Rikagu) with sitting drops. Five different screens were used in order to find conditions that may give crystals, this includes two inhouse made screens, KCSG and Stockpegs16 (made by Kenneth Johnson, UiT/NorStruct) and three commercial screens, The Cations suit (Nextal), The Anions Suit (Nextal) and Crystal Screen 1+2 (Hampton).

A promising condition found in the initial robot screen was investigated by setting up hanging drops and vary the precipitant concentration and buffer pH. The hanging drop screens were set up with PEG 3350 precipitant and sodium citrate ($\text{Na}_3\text{C}_6\text{H}_5\text{O}_7$) pH 8,5 as buffer. PEG 3350 was screened with the concentrations 10, 15, 20, 25, 30 and 35 %, and sodium citrate was screened with concentrations, 0.1, 0.15, 0.2 and 0.25 M to a total volume of 500 μL with water. The screens were set up with a protein concentration of 7,3 mg/mL, by mixing 2 μL protein and 2 μL reservoirs solution. The crystallization plate was stored at room temperature.

A screen was set up using PEG 3350 concentrations 14, 15, 16, 17, 18 and 19%, with sodium citrate concentrations 0.1, 0.15, 0.2 and 0.25 M. In addition 10% glycerol as additive. The screen was set up with a total reservoir volume of 500 μL and 2 μL protein drops with a concentration of 3 mg/mL and 2 μL reservoir volume. The plate was set up in the cold room at 4°C and stored there.

A seeding trial was set up by using the same conditions as described first for one plate. An addition plate was set up with PEG 3350 30%(v/v) and 0,15 M sodium citrate with 18 wells and a total well volume of 500 μL . Hanging drops were set up with 2 μL protein with a concentration of 3,2 mg/mL and 2 μL reservoir solution. The seeding was done by several methods from the high protein concentration plate to the low. The first row was seeded by streaking a hair through the high protein drop and then the low protein drop. The next row was seeded by transferring whole needles using a loop, followed by the next row which was set up using 0,2 μL solution from the high protein drop. The plates was stored at room temperature.

A crystalline matter was mounted for x-ray measurement by transferring the crystal to a cryo-solution containing 30%(v/v) PEG 3350, 0,15 M sodium citrate and 40% glycerol. The crystal was washed and flash frozen in liquid nitrogen for storage until testing. The crystal was tested at the synchrotron in Berlin (Bessy) by Ronny Helland and Hanna-Kirsti Schröder Leiros (Department of Chemistry, UiT/NorStruct)

5.17 Sialic acid MS

Mass spectrometry (MS) is a technique used to determine the molecular weight of molecules and gives important data for identification and characterization of compounds. The general scheme of a MS-analysis is ionization, separation and detection. In order to analyse the compound it has to be ionized, this is can be done in several ways were two of the most common is matrix-assisted laser desorption ionization (MALDI) and electrospray ionization (ESI). The ionized sample is then accelerated through an electric field and separated based on their mass (m) to charge (z) ratio m/z and detected on an ion detector. Variants of MS are the MS-MS techniques were three or more quadrupole mass analysers are placed after each other. The first separates the ions within a certain range and they are sent to the next analyser which is filled with inert gas causing the ions to collide and fragment. These fragments are then sent on and analysed in the third analyser. It is also possible to combine with chromatography techniques before injecting the sample, HPLC and gas chromatography is often used to separate a mix of compounds based on specific qualities before being analysed.

In order to perform a MS analysis of Sia expressed by *M. viscosa* a commercial kit for labelling Sia with a fluorescent tag was used (Takara). The Sia from the organism is released by mild acid hydrolysis and tagged with 1,2-diamino-4,5-methyleneoxybenzene (DMB) as shown in figure 5.4.

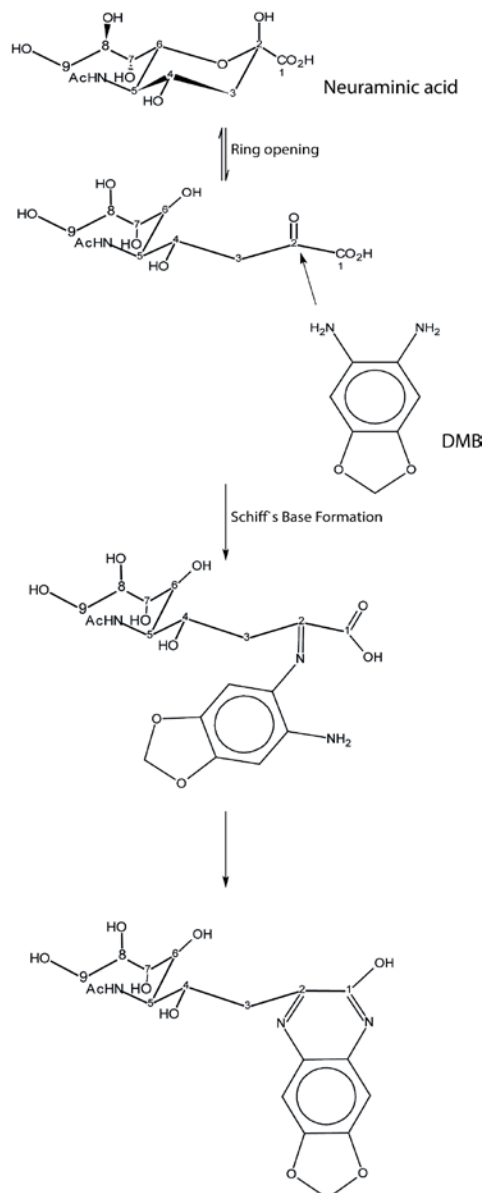


Figure 5.7: Mass spectrometry analysis to determine presence of Sias in *M.viscosa* was done by mild acid hydrolysis of the bacterial samples followed by labeling the Sia with 1,2-diamino-4,5-methyleneoxybenzene (DMB). This two-step process contains the formation of an unstable Schiff's base from the open ring structure of Sia followed by a reduction of the formed imine group that gives the stable labeled Sia.

The labelling of Sia is a two-step process where the open chain form of Sia is attached to the primary amino group of DMB through a nucleophilic attack on the carbonyl carbon of the sugar to form a partially stable Schiff's base. The imine group in the Schiff's base is then reduced to give a stable labelled glycan.

To perform initial investigations to check if sialic acids are expressed in *Moritella viscosa*, the samples were prepared using different growth conditions. Two samples were scraped from the

bacteria grown at 12°C on a LB plate supplemented with 2.5% (w/v) NaCl. Another sample was scraped from the same plate, but inoculated into 3 mL Marine Broth (MB) (Difco™) and grown for two days at 12°C and 200 rpm (LB and MB respectively). Two samples were scraped from blood agar (BA) plates grown at 12°C and containing agar base no. 2 (Oxoid), 7% human blood and 2.5% (w/v) NaCl, where one sample was inoculated to 3 mL liquid LB media supplemented with 2.5% NaCl (BA and BALB respectively) and further grown for two days at 12°C and 200 rpm. The bacteria scraped off from plates were frozen until analysis. The cells grown in liquid media were spun down and pellets used for analysis. All samples were added 200 µL 2 M acetic acid and 3 mL of 1% butylated hydroxytoluene (BHT) to release Sias. All samples were incubated at 80°C for 3 hours. Diethyl-*p*-nitro-phenyl-phosphate was added to a total concentration of 1 mM in each sample to prevent de-*O*-acetylation of Sias. The samples were then centrifuged at 13 000 rpm for 3 min and the pellet discarded. The solution was purified by centrifugation in Amicon Ultra-spin columns with a 10 000 MWCO (Millipore) to remove high molecular compounds. The samples were then lyophilized and stored at -20°C until DMB-labeling and MS analysis.

The dried samples LB, MB, BA and BALB were dissolved in 10 µL water. A solution mix containing Reagent 1 (DMB), Reagent 2 (coupling solution) and water was prepared in the in a ratio of 1:5:4 respectively to a total volume of 1200 µL. 200 µL of the solution mix was added to each sample and mixed briefly. The tubes were wrapped in aluminium foil to avoid light and incubated at 50°C for 2,5 hours. The reaction is then stopped by incubating on ice for 5 minutes.

A standard panel of Neu5Ac and a standard panel of different Sias, Neu5Gc, NeuNAc, Neu5,7Ac₂, Neu5Gc9Ac, Neu5,9Ac₂ og Neu5, (7/8),9Ac₃, (ProZyme) were prepared by preparing 20 µL of each solution to give 1 nmol after labelling with DMB. The labelling was performed as described above. The labelled solutions were then serial diluted by first diluting 500 µL of each sample with 500 µL water to give a new concentration of 0,5 nmol. These are then serial diluted with water to give the amounts 0.25, 0.125, 0.0625, 0.03125, 0.015625, 0.007813 and 0.003906 nmol. The unknown samples and standards were then stored on ice without light until analysis.

The HPCL-MS/MS analysis of the prepared unknowns and standards were performed by senior engineer Jostein A. Johansen at the Department of Chemistry at UiT with specifications given [88].

6. Results

6.1 Bioinformatic Analysis

In order to determine basic physical data about the protein the ProtParam tool from ExPASy was used. The information extracted is shown in table 6.1. The molecular weight and the average extinction coefficient are used to convert Nanodrop A280 nm measurements into protein concentration.

Table 6.10: Molecular weight, average extinction coefficient and pI of the different NeuB1 variants

	Molecular weight (Da)	Average extinction coefficient	Extinction pI
<i>M.viscosa</i> NeuB1	38111,7	20 587,50	5,35
<i>M.viscosa</i> NeuB1-NHis	41656,6	26 547,50	5,75
<i>M.viscosa</i> NeuB1-NHis cleaved	38168,7	20 587,50	5,35
<i>M.viscosa</i> NeuB1-CHis	38934,5	20 587,50	5,74

A multiple alignment was constructed and is shown in figure 6.1. Included is also the secondary structure of *N. meningitides* (1XUZ) and *M.viscosa*. The latter secondary structure was predicted using the PSIPRED server..

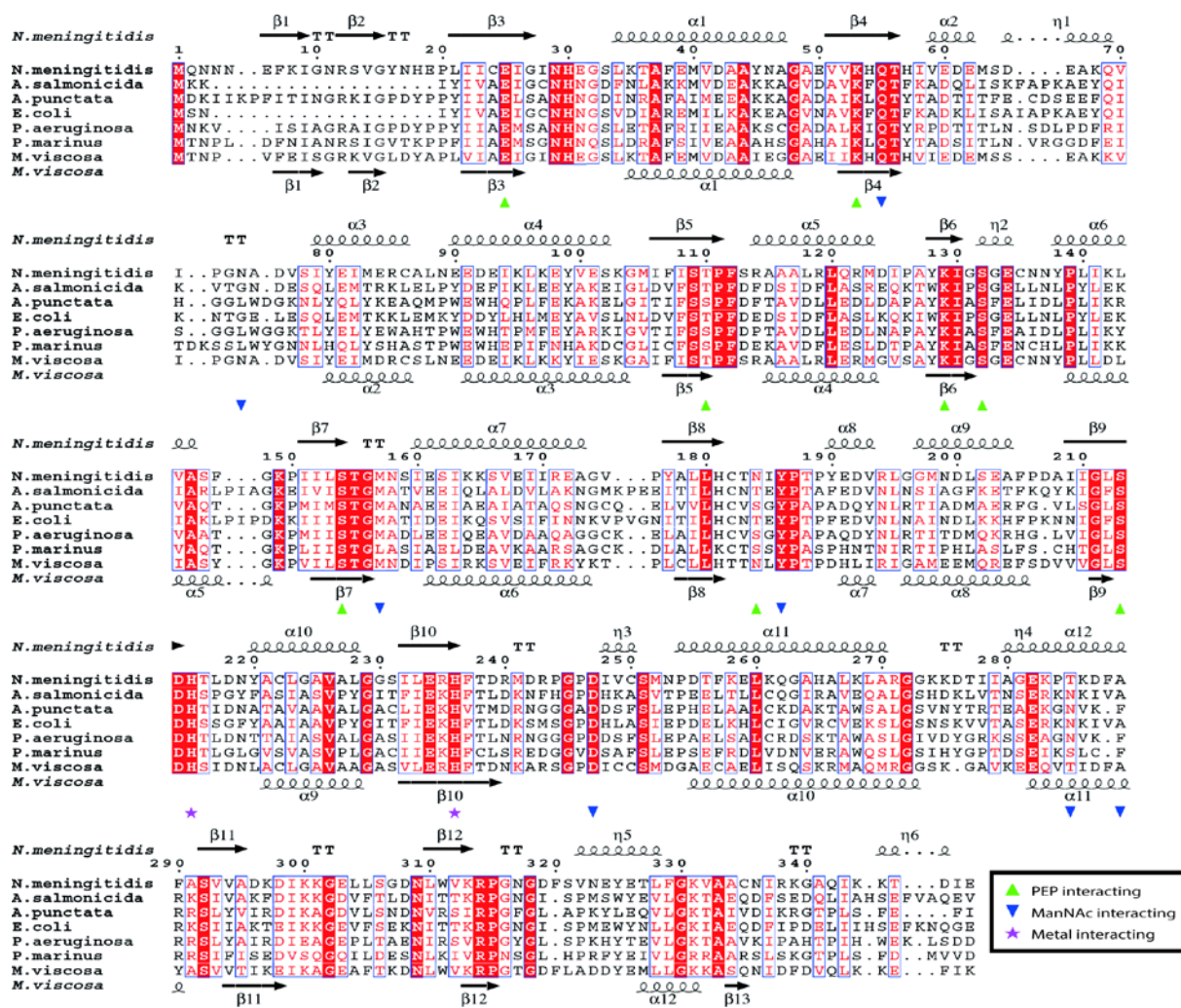


Figure 6.8: Structural sequence alignment of NeuB variants from the bacterial species (with TrEMBL accession codes): *Aeromonas punctate* (Q9R9S2), *Escherichia coli* (Q46675), *Pseudomonas aeruginosa* (QSKH52), *Prochlorococcus marinus* (Q7V953) and *Neisseria meningitidis* (Q7DDU0). Secondary structure elements are shown over and below for *N. meningitidis* and *M. viscosa* respectively. The conserved residues are marked in white letters with red background and residues with properties that are similar are shown as red letters in blue boxes. Substrate interacting residues are shown with coloured symbols explained in the box.

Pfam is a tool to analyse sequences in order to find conserved domains. NeuB1 from *Moritella viscosa* was analysed using Pfam and two domains was recognized. Residues 39-275 was found to belong to the NeuB1 family while residues 288-339 was designated as a SAF domain, which according to EMBL-EBI for neuraminic acid synthases is in this case an anti-freeze protein like domain (AFP).

The sequence identity between the *M. viscosa* NeuB1 and the other sequences in the alignment was determined using an option for this in BioEdit. The results is shown in table 6.2

Table 11: sSequence identity between mvNeuB1 and other bacterial NeuB sequences.

	Sequence Identity with <i>mvNeuB1</i> (%)
<i>N.meningitides</i>	63.04
<i>A.salmonicida</i>	27.62
<i>A.punctata</i>	30.34
<i>E.coli</i>	29.56
<i>P.aeruginosa</i>	32.39
<i>P.marinus</i>	28.01

A homology model of *mvNeuB1* was made using automated mode in SWISS-MODEL Workspace based on the *N. meningitides* structure (1XUZ) as template. The model is assessed by the workspace using the QMEAN Z-value which is a scoring function for both the estimation of the global quality as well as the local. For the NeuB1 model the Z-value given was -0.93.

In order to assess the quality of the the NeuB1 homology model, the file was uploaded into Ramachandran Plot 2.0 to make a Ramachandran plot to investigate if there are any amino acids in conformations that can give steric hindrance. The plot is shown in figure 6.2. Two residues were outside the allowed regions and are marked with black boxes and residue name and number.

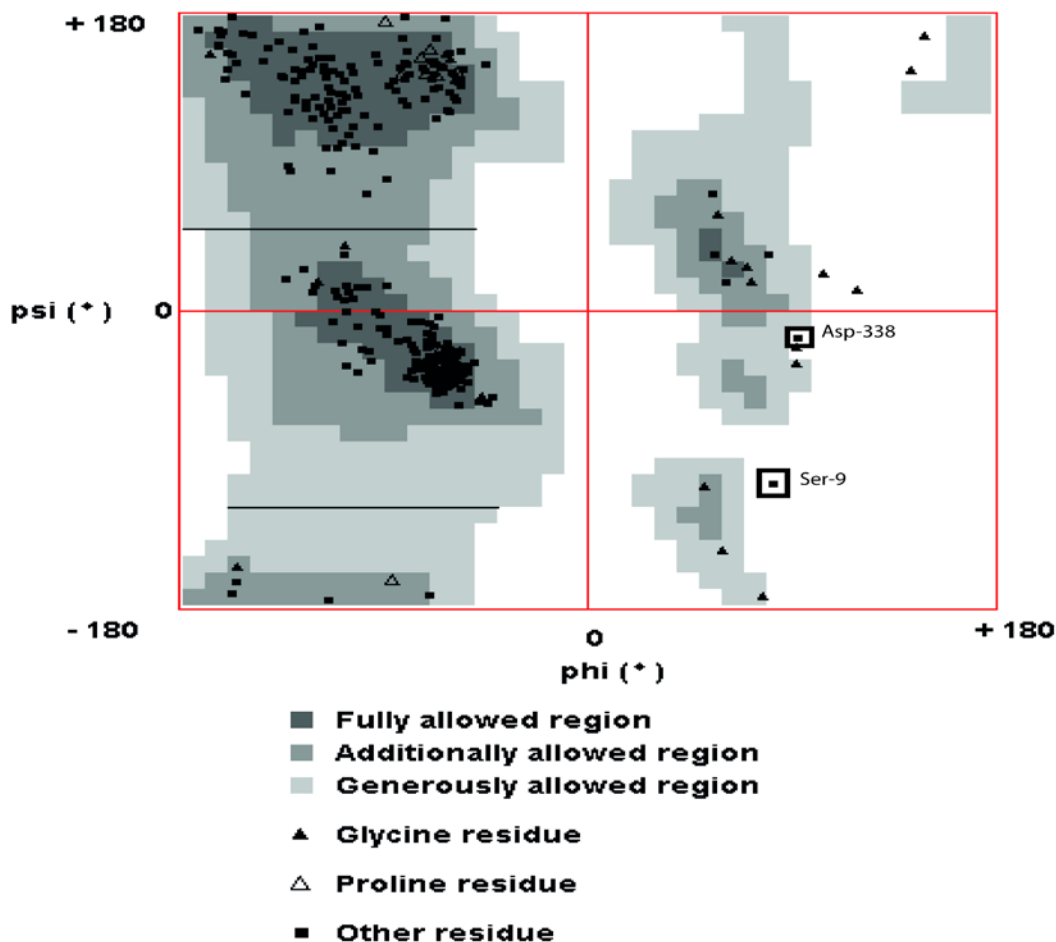


Figure 6.9: To investigate if the homology model contains any residues in unfavourable conformations, the model was used to create a Ramachandran plot. The figure shows four regions according to shades of grey. The dark grey region is the fully allowed region where there are no constraints. The middle grey shows the additionally allowed region and the generously allowed region is indicated with light shading. The white area describes the conformations that are not allowed and will give steric hindrance in the protein. Two residues fall within this region and are marked with black boxes and residue name and number

The monomers of the NeuB1 homology model and template were uploaded into PyMol and aligned to give the Root mean square deviation (RMSD) using the Align command. The score given was 0.056 Å (Ångström). The model was also coloured by B-factor in PyMol which shows how much of the information from the template was used to generate the model (figure 6.3).

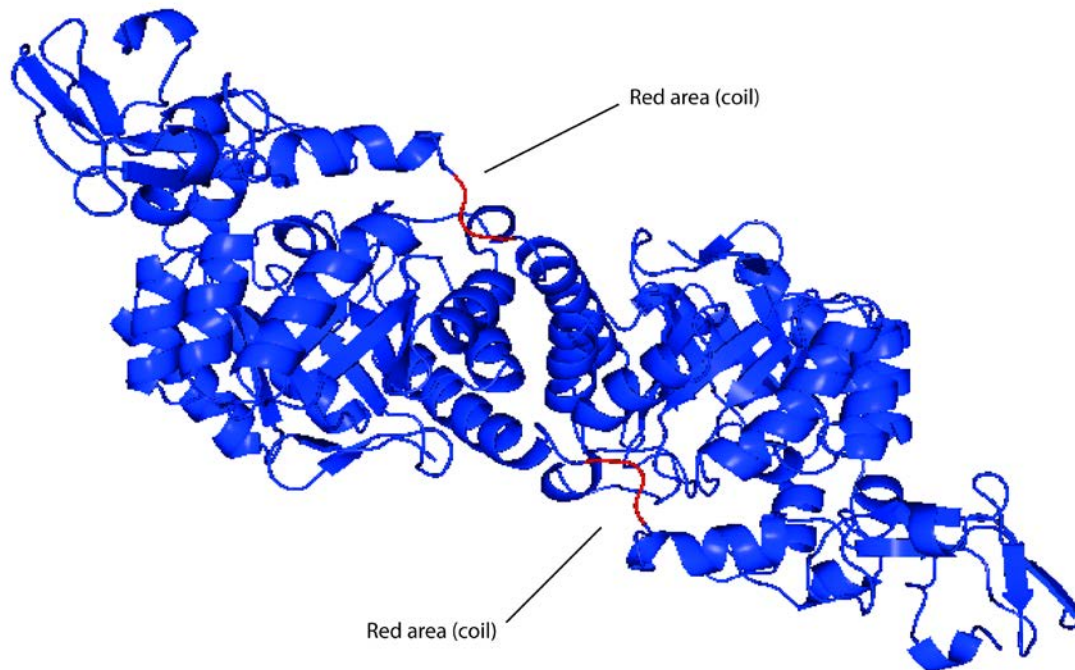


Figure 6.10: The homology model of NeuB1 coloured by B-factor. This colours the model to indicate where the information from the template was sufficient to model the structure (blue) and where the information was insufficient (red)

A comparison of the model and the template is shown in figure 6.4. The model and template was analysed using the vacuum electrostatics function in PyMol that generates an electrostatic potential map showing the charged surface areas of the molecule. The negatively charged areas are coloured red, the positively charged areas are coloured blue and the neutral areas are coloured grey (figure 6.5). Using the substrates from the template substrates to overlap the model, a comparison of the electrostatic potential of the active site with bound substrates was made as shown in figure 6.6.

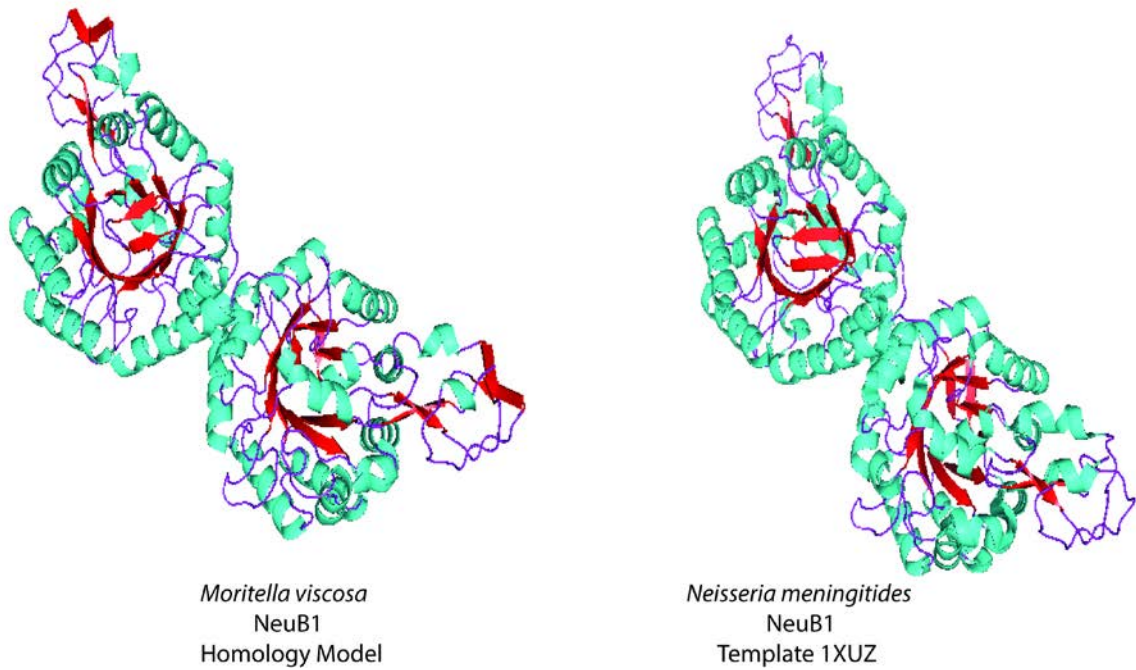


Figure 6.11: Homolgy model of *M. viscosa* NeuB1 (left) based on the *N.meningitides* NeuB1 structure (1XUZ) (right. Secondary structure elements is coloured as follows; α -helices are shown in green, β -sheats are shown in red and coils are shown in purple.

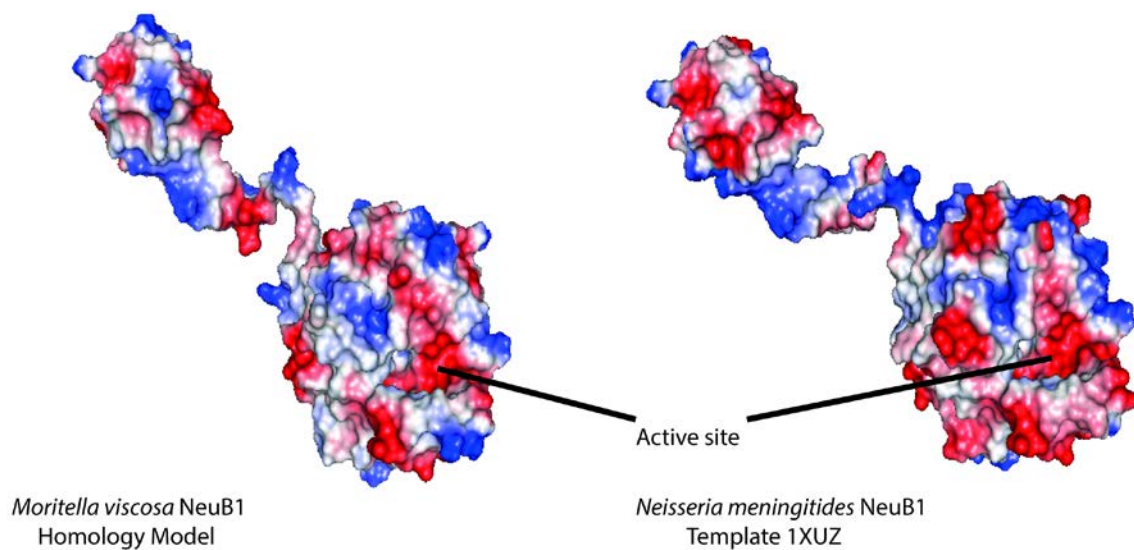
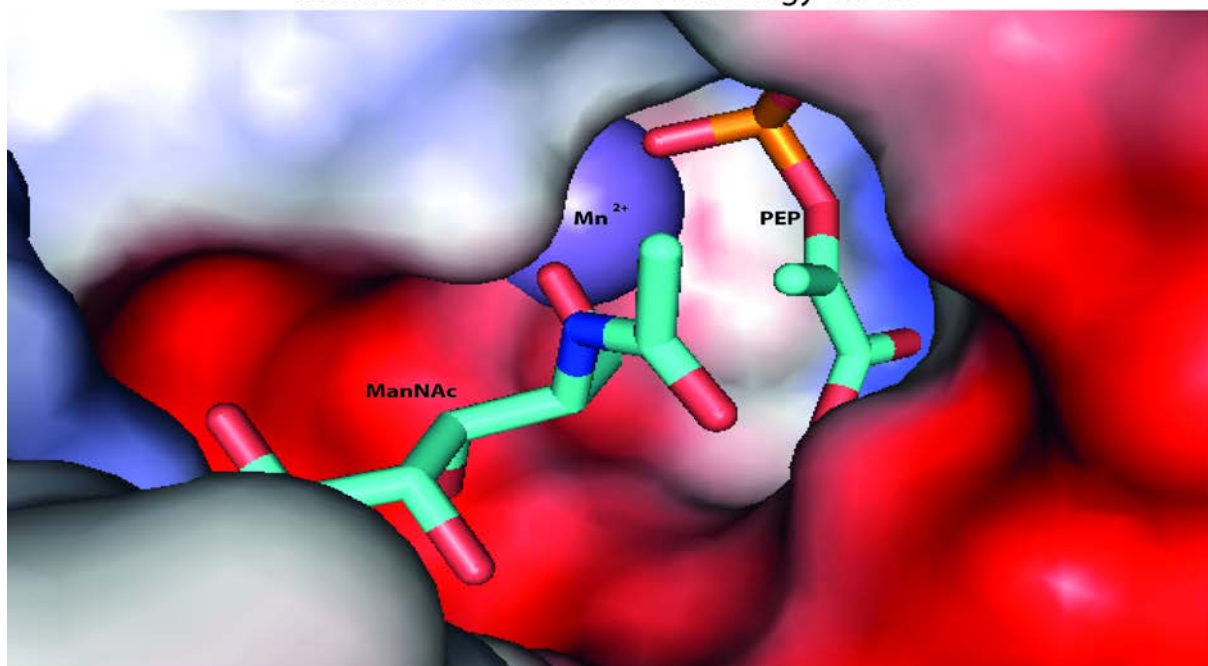


Figure 6.5: Surface representation of the mvNeuB1 model and the 1XUZ template structure from *N.meningitides* (monomer) coloured by electrostatic potential. Blue colour indicates positively charged areas, negatively charged areas are in red and grey colour indicate neutral areas. The active site of the enzyme is marked.

Moritella viscosa NeuB1 Homology Model



Neisseria meningitidis NeuB1 Template 1XUZ

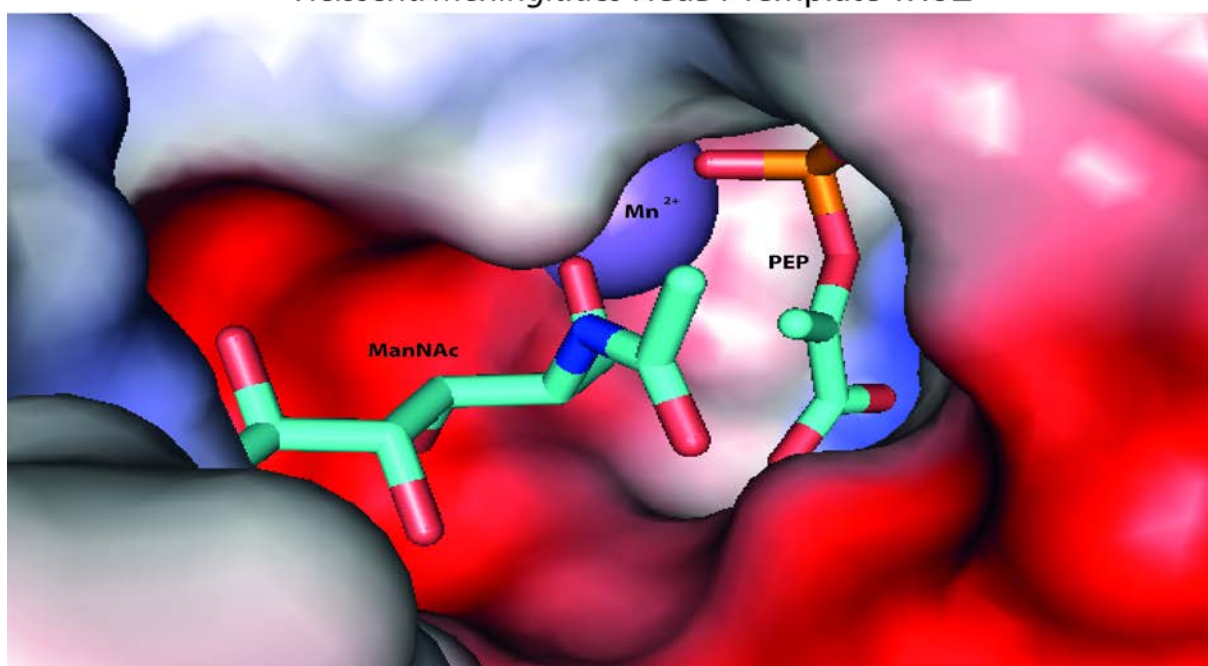


Figure 6.6: Electrostatic surface potential of the active site of mvNeuB1 and nmNeuB. The substrates from *N.meningitidis* template structure were overlapped with the model and the electrostatic surface potential was calculated.. The ligands ManNAc, PEP and Mn^{2+} are marked in the figure. The red surfaces symbolises negatively charged areas, blue positively charged areas while grey shows neutral areas.

6.2 Gene Amplification

The *neuB1* gene from *M.viscosa* was amplified using PCR in two rounds with designed primers to give two, one containing a six residue Histidine tag and a TEV protease specific cleavage site in the N-terminal end of the protein (NHis) and one containing a six residue Histidine tag in the C-terminal end of the protein making the tag uncleavable (CHis). The PCR products from the first PCR round was run on a 1% agarose electrophoresis gel and visualised using UV-light. The bands containing the PCR-products after first PCR are shown in figure 6.6.

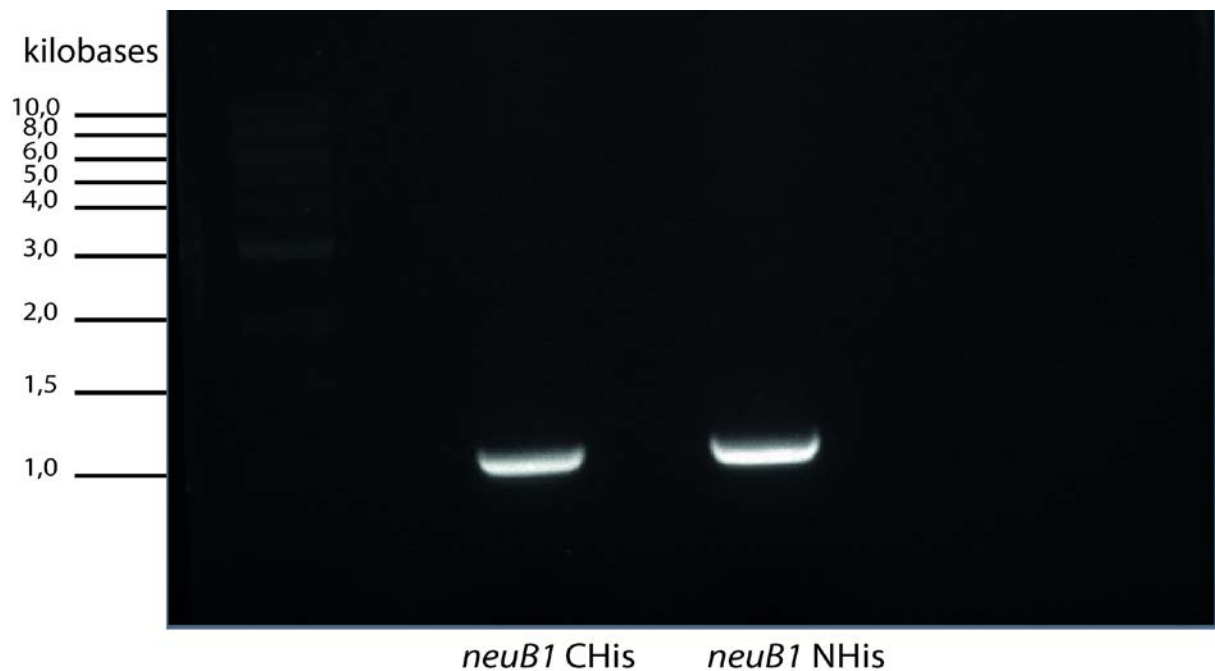


Figure 6.12: The *neuB1* gene from *Moritella viscosa* was amplified using PCR and designed primers to give two inserts CHis and NHis that would be used in constructs to express the NeuB1 protein. The PCR reaction products were run on a 1% agarose gel with 1 kb DNA ladder as marker. The gel shows the amplified products at just above 1 kb.

The PCR-products were cut out and purified using the QIAquick Gel Extraction Kit (250) (Qiagen) and used in the second PCR round. Figure 6.5 shows the bands of the inserts.

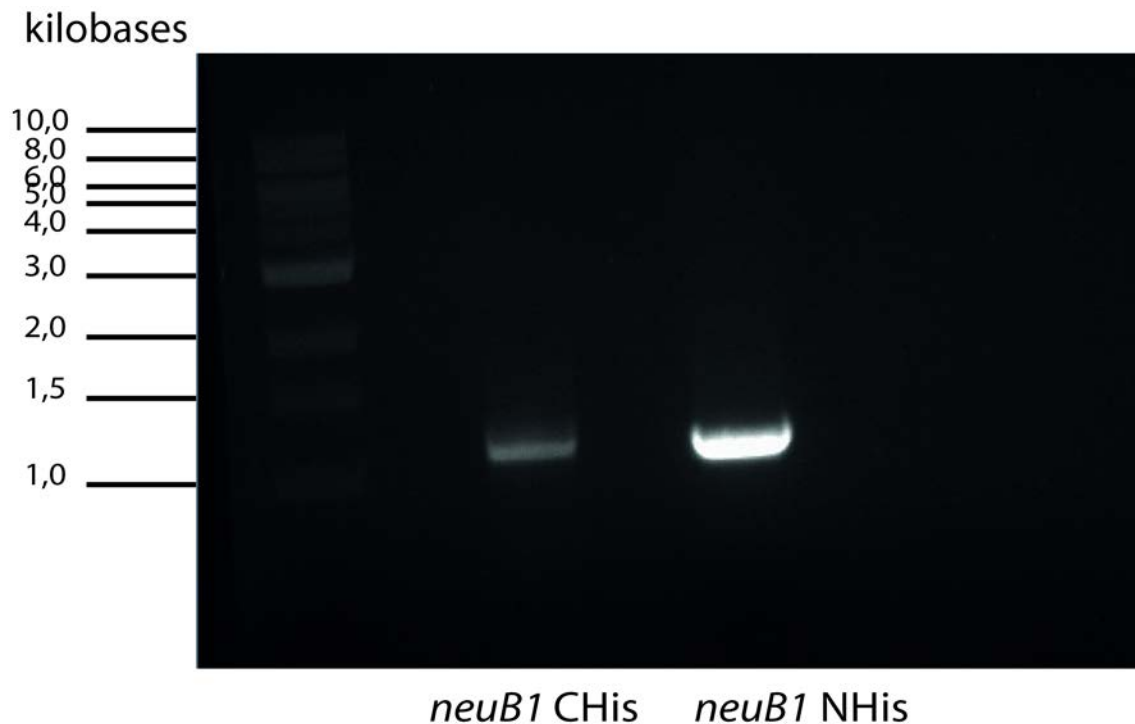


Figure 13: The PCR products from the first round were purified from the gel and run in a second PCR reaction. The PCR products were run on a 1% agarose gel with 1 kb DNA Ladder as marker. The products are shown in the gel just above the 1 kb mark.

The inserts NHis and CHis were cloned into the vectors pDEST 17 and pDEST 14 respectively, and transformed into One Shot TOP 10 competent cells and cultivated. The cells were harvested and plasmid purified. To confirm that the constructs contained the correct sequences they were sequenced and analysed.

6.3 Pilot Expression

The transformed expression colonies containing NHis Ros col 1, NHis Ros col 2, NHis Ros scoop, NHis BL21 col 1, NHis BL21 col 2, NHis BL21 scoop, CHis Ros col 1, CHis Ros col 2, CHis Ros scoop, CHis BL21 col 1, CHis BL21 col 2 and CHis BL21 scoop were tested in pilot expression experiments. They are shown in figure XXX showing Zero samples, samples after 3hour and ON induction respectively. The molecular weight of the protein is around 38 kDa meaning the band representing it should appear around the 36.5 kDa marker. From the gel pictures there is a stronger band around 36.5 kDa showing that the protein is expressed in all the induced samples. To determine if the induced protein is the correct one, the bands belonging to NHis BL21 col 2 3 hr, NHis Ros col 1 ON, CHis BL21 col 1 ON and CHis Ros col 1 was cut out and sent for MS analysis. The results (not included)

showed that the induced protein was NeuB1.

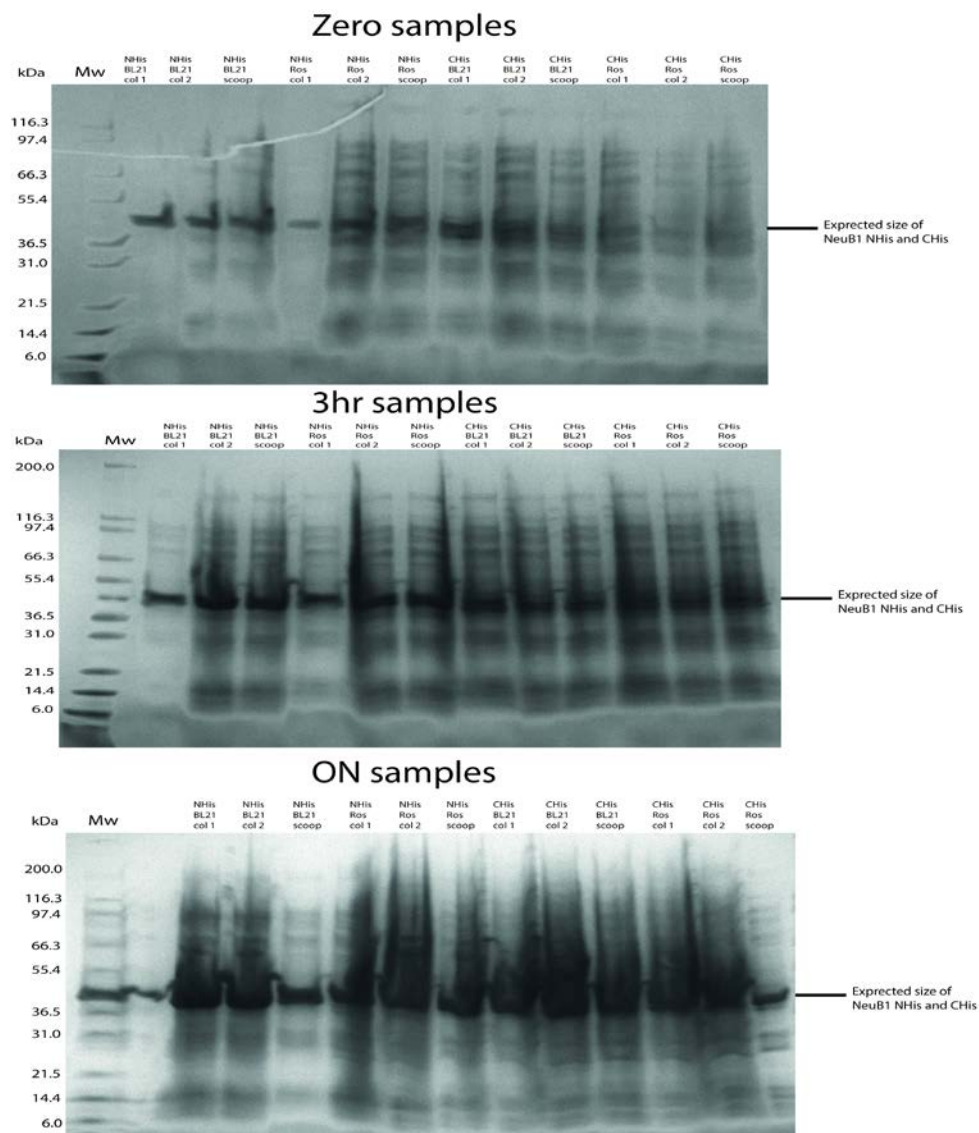


Figure 6.14: The transformed expression strains *E.coli* Rosetta 2 (DE3) plysS and *E.coli* BL21* pRare 2 pLysS containing NHis and CHis each were grown in order to analyse the protein expression. The figure shows the samples NHis Ros col 1, col 2, scoop, NHis BL21 col 1, col 2, scoop, CHis Ros col 1, col 2, scoop, CHis BL21 col 1, col 2 and scoop. The NHis construct has a calculated molecular weight of 41.6 kDa and CHis 38.9 kDa meaning the bands representing the constructs should appear above the 36.5 kDa mark in the gels.

6.4 Pilot Protein Purification

In order to test the activity, the induced protein was purified based on affinity chromatography using the His-tag. The samples colony 1, 2 and scoop of each construct in each strain was pooled by resuspending in Lysis Buffer giving the samples NHis BL21, NHis Ros, CHis

BL21 and CHis Ros for purification. After sonication the lysed cells were centrifuged and the pellet was discarded. What was observed after the centrifugation was that for both expression strains the NeuB1 NHis had precipitated along with the pellet, this was not observed for the CHis construct. The extract was used for purification, and the purification chromatograms for all four samples are shown in figure 6.11-14, included with the flowthrough, 5% HisTrap Buffer B wash and collected fractions that were run on SDS-PAGE.

For NeuB1 NHis Ros the protein was purified and the fractions 2-6 , flowthrough and 5% HisTrap Buffer B wash were collected and run on a SDS-PAGE gel. Even though the precipitation was observed after centrifugation of the lysed sample there is still some of the protein left in the solution. For NeuB1 NHis BL21 the purification was performed as described but the gradient was not used due to wrong settings thereby eluting with 100% HisTrap Buffer B. It was noted that the imidazole used for elution was UV absorbant and could mask relevant peaks. Fractions 1-8 along with flowthrough, 5% HisTrap Buffer B wash was run on gel.

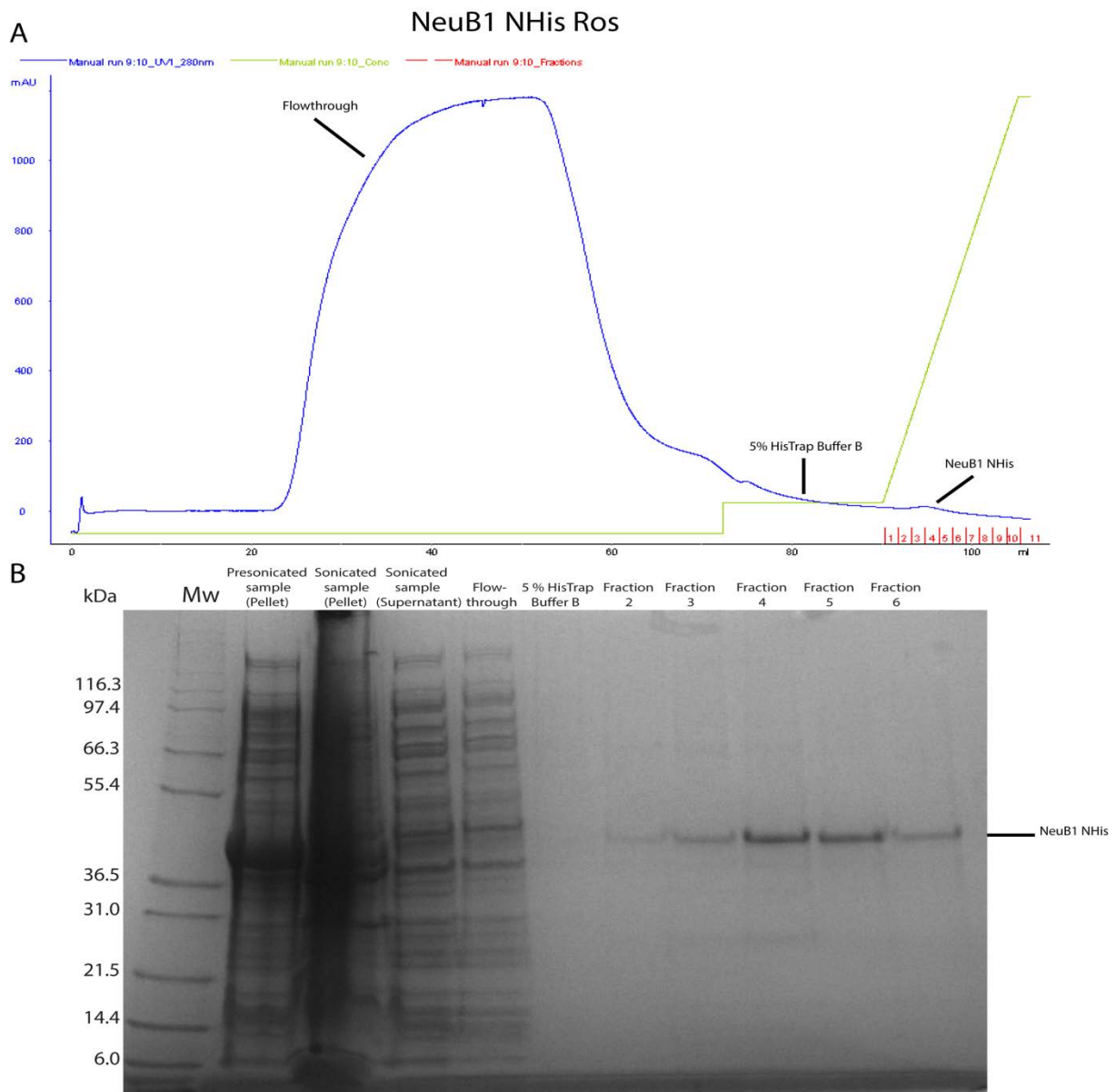


Figure 6.15: Purification of NeuB1 NHis Ros. A) shows the chromatogram from the purification where the blue line is the absorbance at 280 nm, the green line is the % concentration of HisTrap Buffer B and the red lines are fractions. The sample was loaded on the column which was washed with HisTrap Buffer A represented by flowthrough marked in the figure. 5% HisTrap Buffer B was used for washing before a gradient from 5-100% HisTrap Buffer B was used for elution of protein. B) The fractions 2-6 from the purification, pre-sonicated sample pellet, resuspended pellet after sonication, supernatant from after sonication, flowthrough and 5% HisTrap Buffer B wash was analysed on SDS-PAGE gel. The bands corresponding to NeuB1 NHis are indicated in the figure.

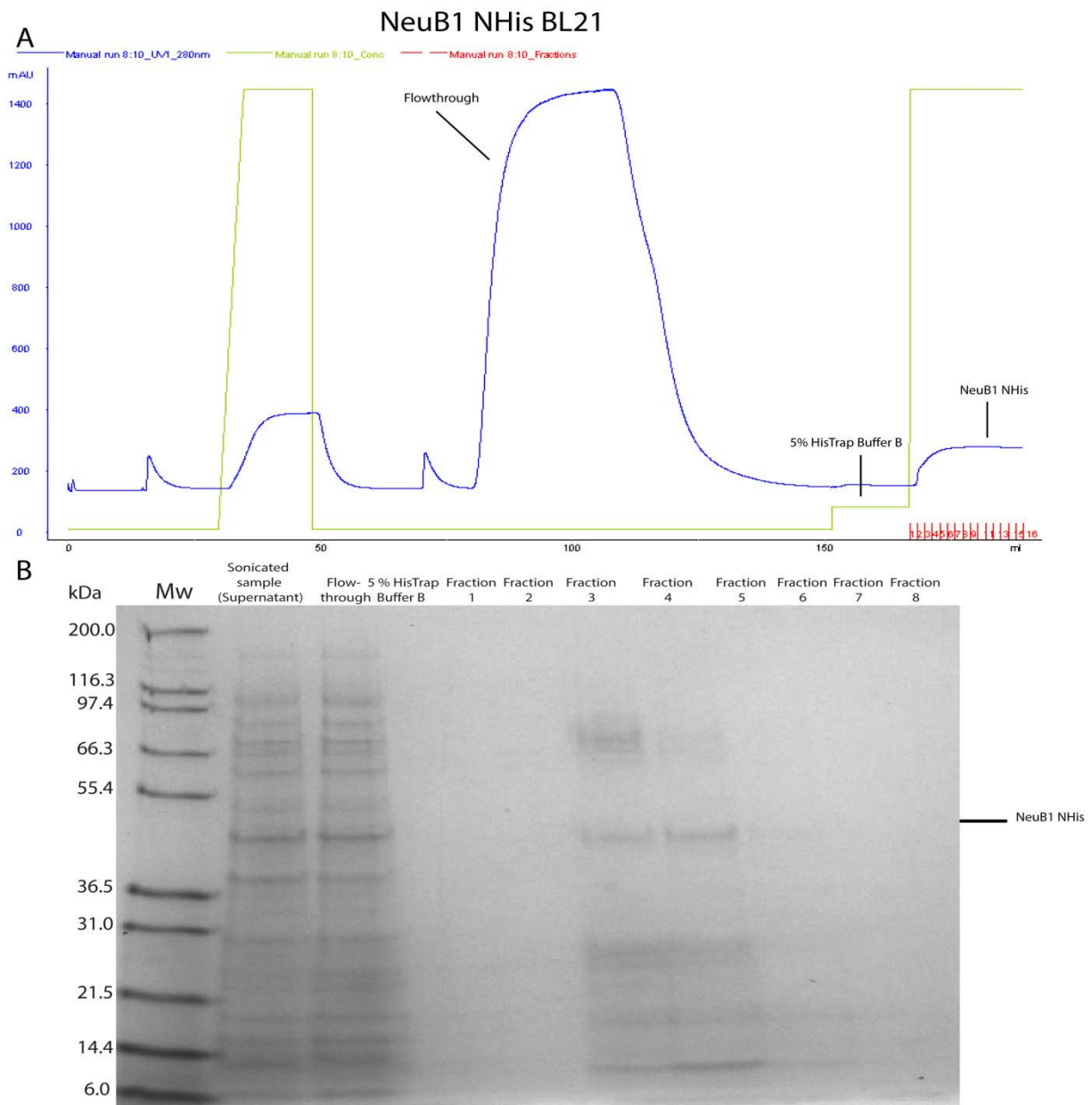


Figure 6.16: Purification of NeuB1 NHis BL21. A) shows the chromatogram from the purification where the blue line is the absorbance at 280 nm, the green line is the % concentration of HisTrap Buffer B and the red lines are fractions. The sample was loaded on the column and washed as described. Gradient was not used in this purification but 100% HisTrap Buffer B. B) Fractions 1-8 from the purification, supernatant after sonication, flowthrough and 5% HisTrap Buffer B wash was run on SDS-PAGE. The bands corresponding to NeuB1 NHis are indicated in the figure.

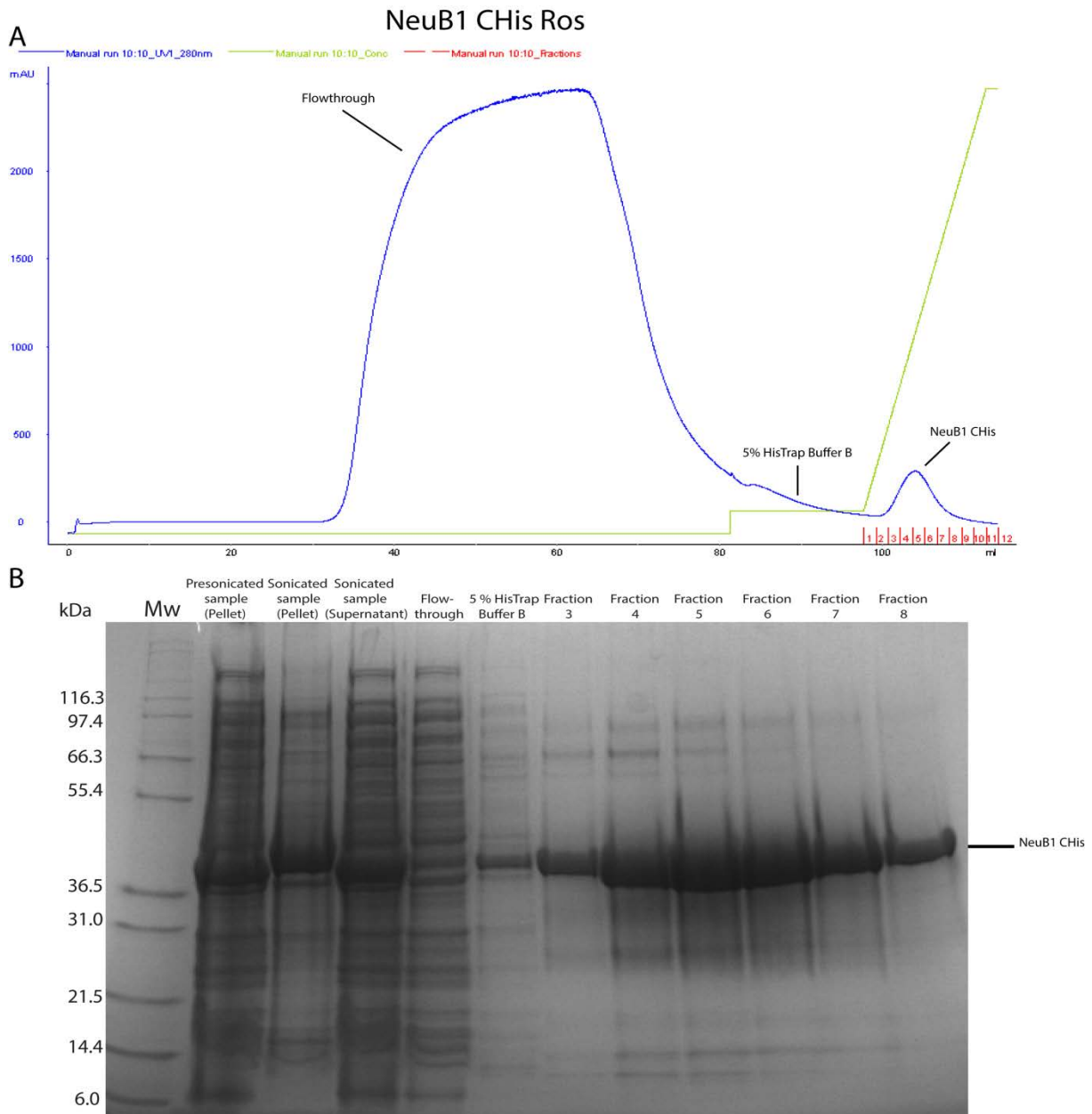


Figure 6.17: Purification of NeuB1 CHis Ros. A) shows the chromatogram from the purification where the blue line is the absorbance at 280 nm, the green line is the % concentration of HisTrap Buffer B and the red lines are fractions. The sample was loaded on the column and washed with HisTrap Buffer A and 5% HisTrap Buffer B before elution of bound protein from 5-100%. B) Fractions 3-8 from the purification, presonicated sample pellet, resuspended pellet after sonication, supernatant after sonication, flowthrough and 5% HisTrap Buffer B wash was run on SDS-PAGE. Bands corresponding to NeuB1 NHis is indicated in the figure.

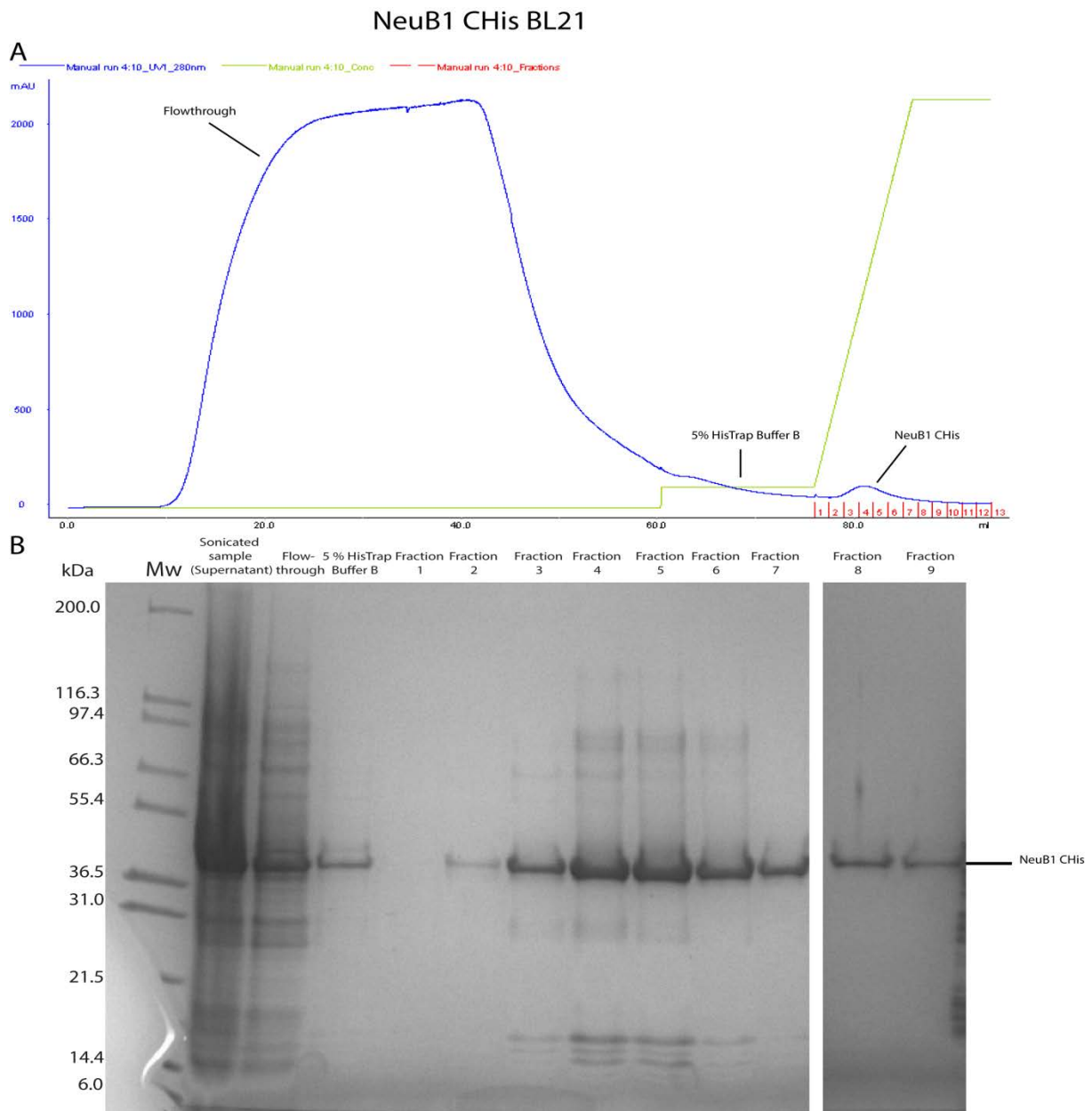


Figure 6.18 Purification of NeuB1 NHis Ros. A) shows the chromatogram from the purification where the blue line is the absorbance at 280 nm, the green line is the % concentration of HisTrap Buffer B and the red lines are fractions. The sample was loaded on the column and washed with HisTrap Buffer A and 5% HisTrap Buffer B before setting a gradient from 5-100% B) Fractions 1-9 from the purification, supernatant after sonication, flowthrough and 5% HisTrap Buffer B wash was run on SDS-PAGE. Bands corresponding to NeuB1 NHis is indicated in the figure.

6.5 Pilot Activity Assay

To see if the purified protein was active samples from the pooled fractions of NeuB1 NHis Ros and NeuB1 CHis Ros were prepared in Assay Buffer. The assay were set up using 10 mM ManNAc, 10 mM PEP, 120 mM Tris-HCl pH 8, 5 mM MnCl₂ and 62 ng of NeuB1 CHis and 3.14 ng NeuB1 NHis to a total volume of 50 μ L. The reaction was carried out at room temperature for one hour before it was stopped and assayed using the TBA assay. Characteristic for the TBA assay is the red colour formed if NeuNAc is present in the sample, as shown in figure 6.15. For the assayed NeuB1 CHis a strong red colour was observed, while for NHis a light pink colour was observed. A blank was used to determine absorbance using Assay Buffer instead of NeuB1 which gave a yellow colour in the TBA assay. The absorbance of the samples were measured at 549 nm giving for OD 3.478 for NeuB1 CHis and OD 1.082 for NeuB1 NHis with blank subtracted.

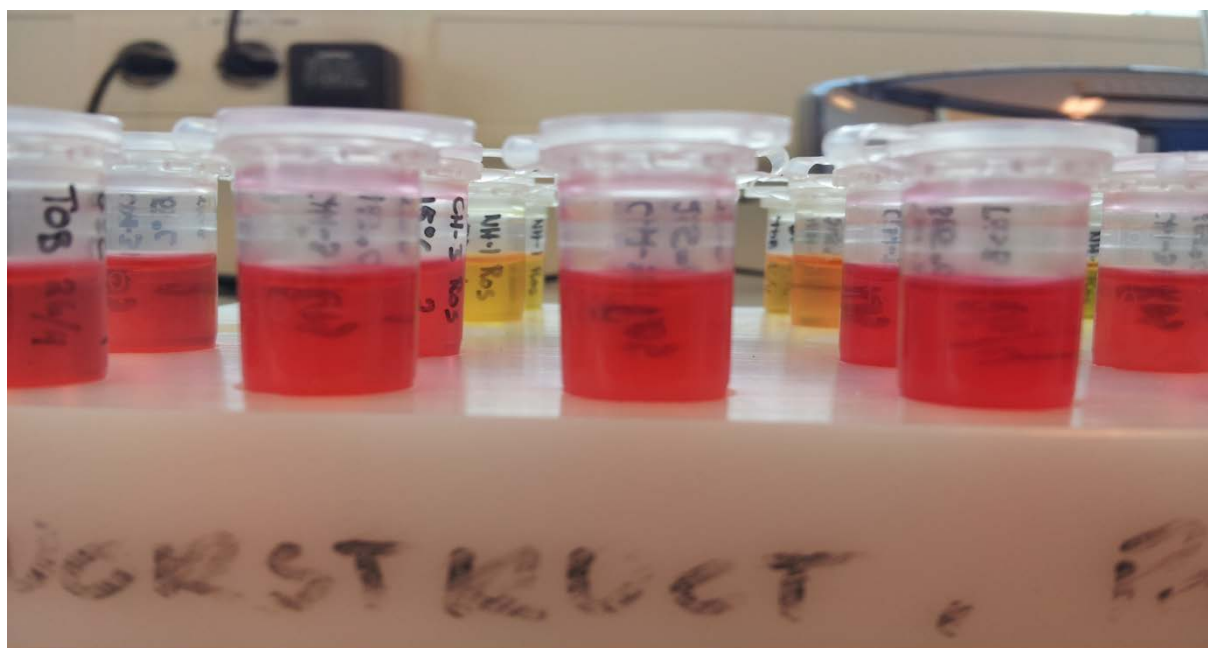


Figure 19: The TBA assay is used to determine the activity of NeuB1 and characteristic for the assay is the red colour formed when NeuNAc is present in the sample. Bsamples and samples without NeuNAc give a yellow colour.

6.6 Large Scale Expression and Purification

In order to characterize and set up crystallization trials for NeuB1 large scale expressions of NeuB1 was performed. Expression of NHis and CHis versions of NeuB1 from the strain *E.coli* Rosetta 2 (DE3) pLysS (Ros) was scaled up.

6.7.1 Purification of NeuB1 NHis

The NeuB1 NHis was purified from 2 L culture in three steps with an intermediate TEV cleaving by dialysis. The first step was affinity chromatography on a HisTrap column as described for small scale purification. The protein was purified on a HisTrap HP 5 mL column using HisTrap Buffer A and HisTrap Buffer B with a flow of 1.5 mL/min and pressure limit 0.5 MPa. The column was equilibrated, the sample applied and the column washed with HisTrap Buffer A, 5% HisTrap Buffer B before eluting bound protein using a gradient of 5-100% HisTrap Buffer B. Air was introduced into the system as the gradient was started, thereby masking the peak of the NeuB1 NHis. Fractions 7-34 were analysed on an SDS-PAGE. The chromatogram and gel is shown in figure 6.16.

Fractions 13-34 was pooled and set up for TEV cleavage. The TEV cleaved sample was purified using HisTrap HP 5 mL column as before. Fractions 8-25 were analysed on SDS-PAGE. Chromatogram and gel is shown in figure 6.17.

Fractions 12-25 from the second HisTrap purification was pooled and purified using gel filtration column Superdex 200 26/600. Fractions 1-18, 65, 66, 75 and 76 from the gelfiltration were analysed on SDS-PAGE. The chromatogram and gel is shown in figure 6.18. The NeuB1 NHis was eluted from the column around 200 mL which according to the manufacturers standards corresponds to a molecular weight of around 75 kDa. Fractions 1-18 was pooled, the protein was up-concentrated using centrifugal tubes with a 3500 MWCO to a final volume of 1.7 mL.

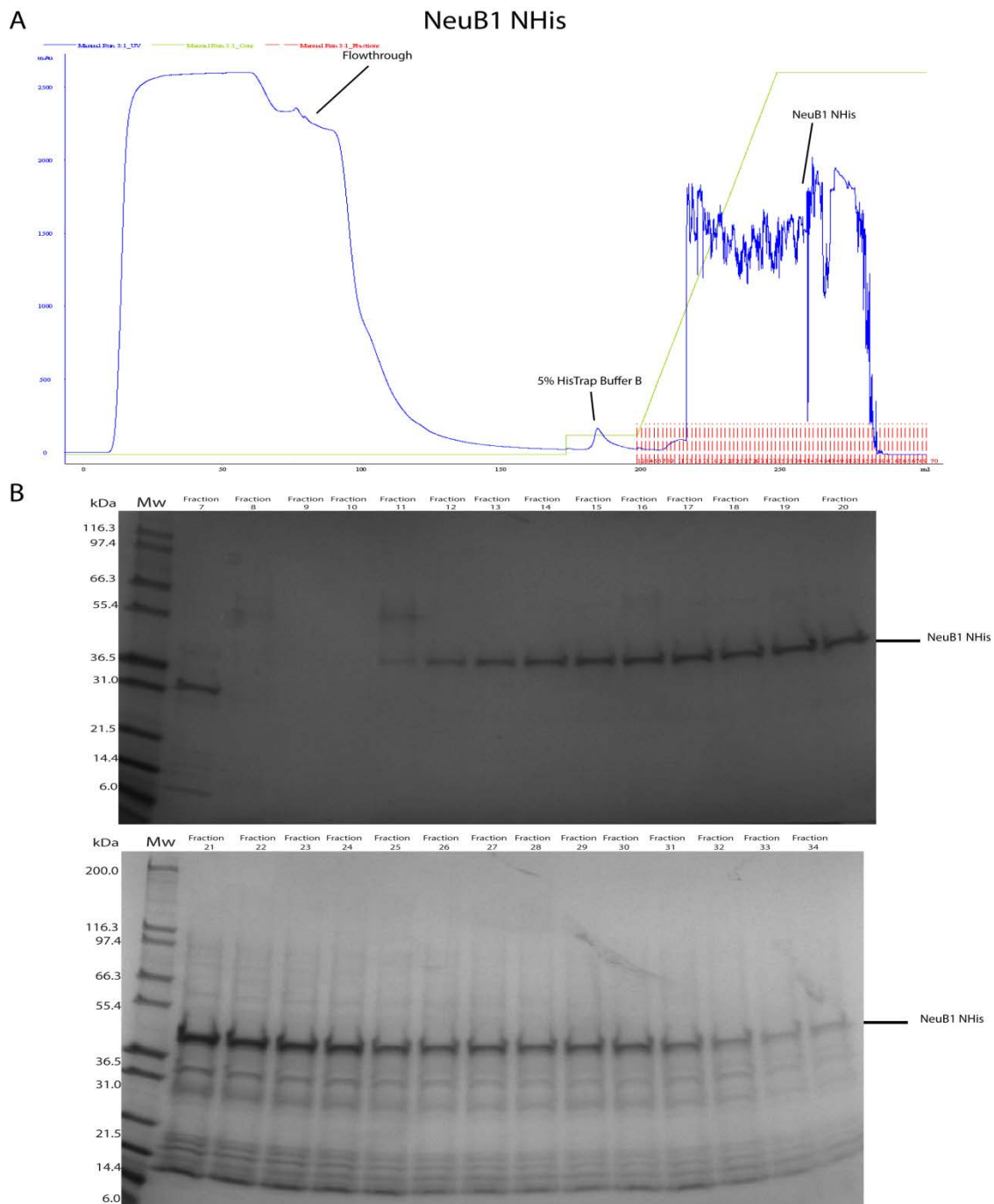
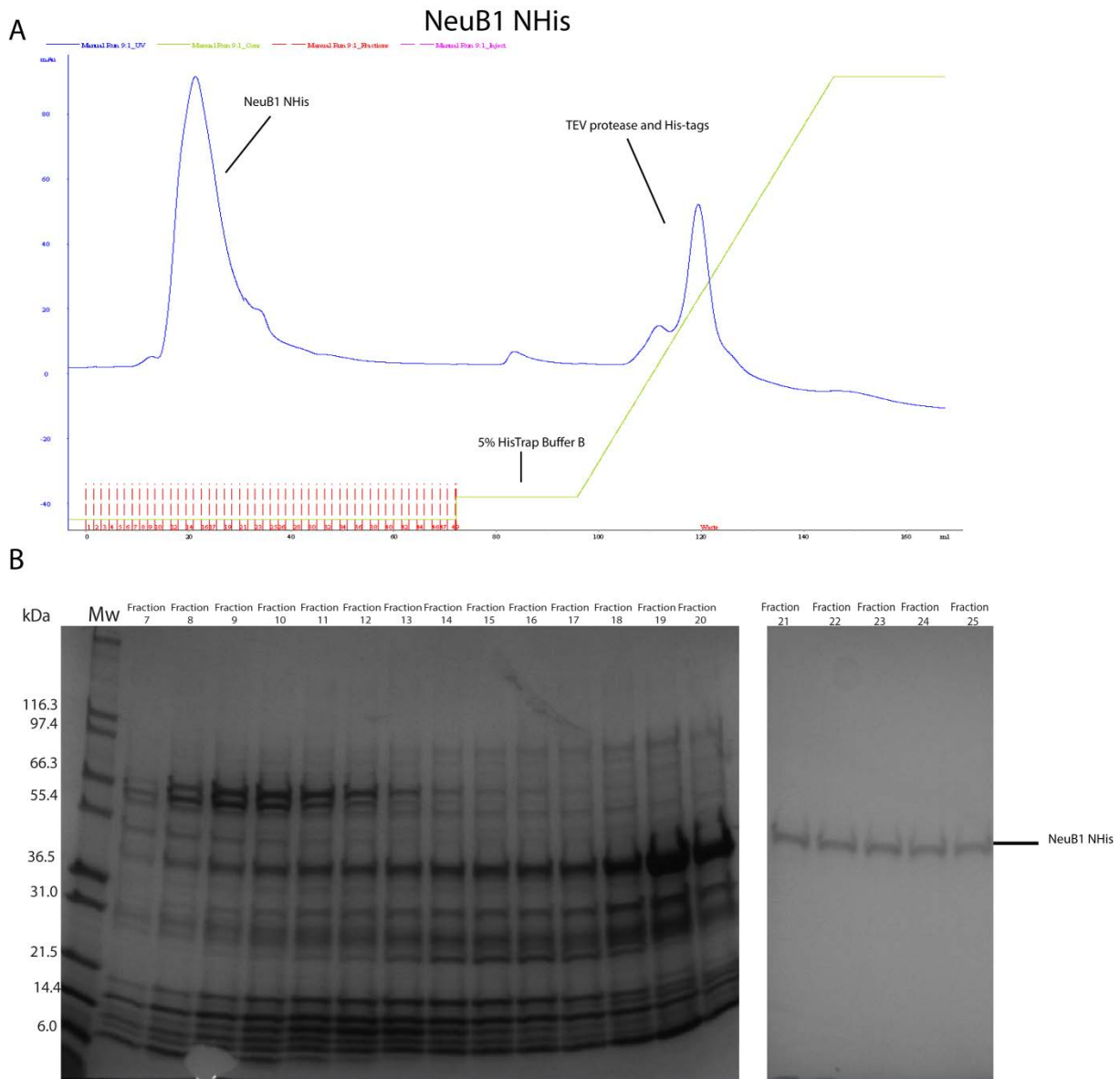


Figure 6.20: NeuB1 NHis large scale .A) shows the chromatogram from the purification where the blue line is the absorbance at 280 nm, the green line is the % concentration of HisTrap Buffer B and the red lines are fractions. The sample was loaded on the column and washed with HisTrap Buffer A, 5% HisTrap Buffer B before bound protein was eluted using 5-100% HisTrap Buffer B. **B)** Fractions 7-34 from the purification were analysed on SDS-PAGE. Bands corresponding to NeuB1 NHis are indicated in the figure.



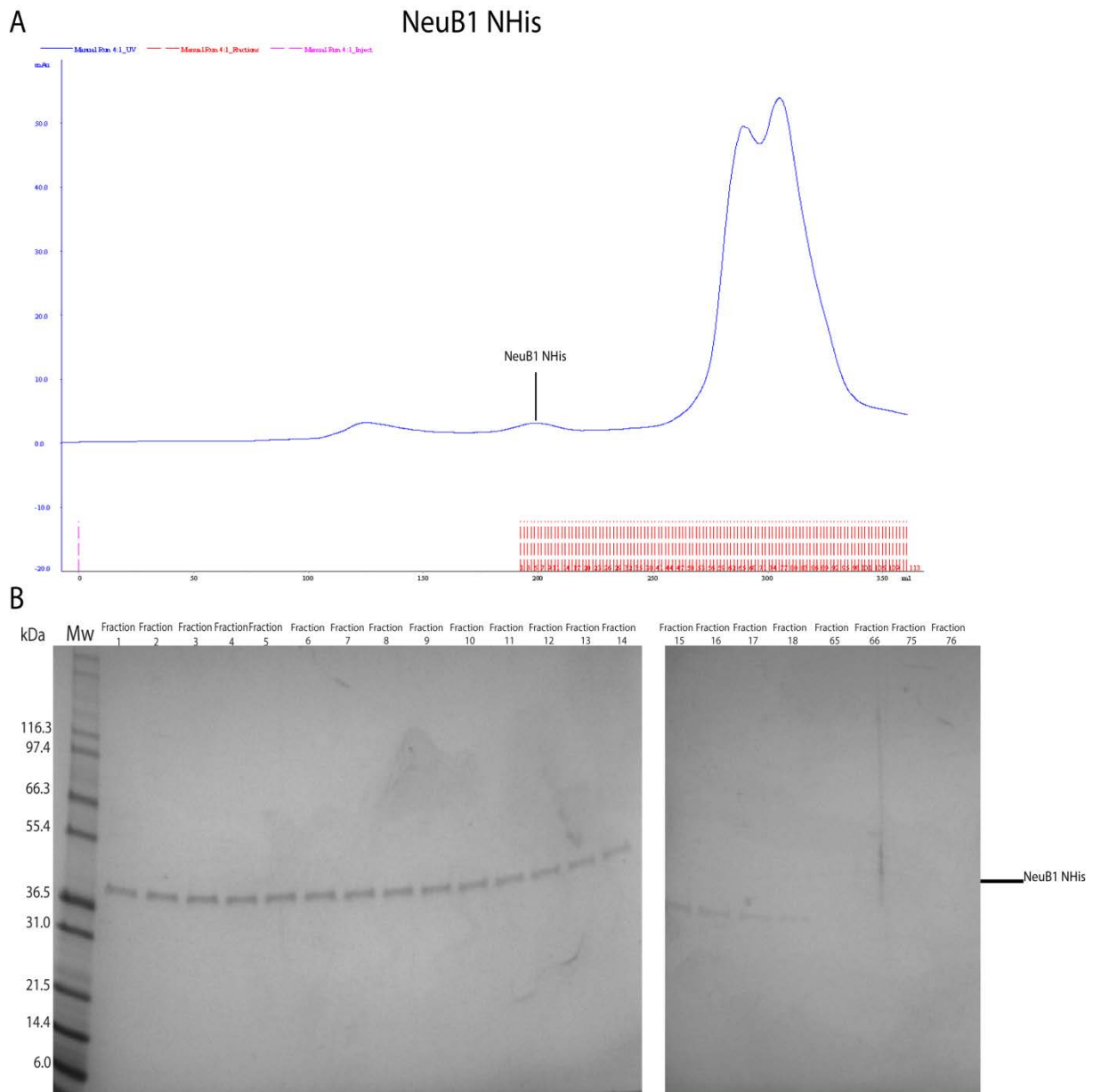


Figure 6.22: NeuB1 NHis final purification step using a Superdex 200 26/600 gel filtration column. A) shows the chromatogram from the purification, where the blue line is the absorbance at 280 nm and the red lines are fractions. The sample was loaded on the column and washed through with Gel Filtration Buffer, the eluted protein peak is indicated in the chromatogram. B) Fractions 1-18, 65, 66, 75 and 76 were analysed on SDS-PAGE. Bands corresponding to NeuB1 NHis are indicated in the figure.

6.7.2 Purification of CHis

The NeuB1 CHis was purified from 1 L culture in two steps. The first step was affinity chromatography on a HisTrap column as described for small scale purification, but using a 5 mL column. The column was equilibrate, the sample applied and washed with HisTrap Buffer A and 5% HisTrap Buffer B before eluting bound protein using 5-100% HisTrap Buffer B. Fractions of 1.5 mL were collected as gradient was begun. Fractions 10-22 were run on an SDS-PAGE. The chromatogram and gel is shown in figure 6.19.

Fractions 10-22 from the HisTrap purification was pooled giving a total volume of 19.5 mL and purified using gel filtration column Superdex 200 26/600. Selected fractions corresponding to the peaks was run on SDS-PAGE. Chromatogram and gel is shown in figure 6.19. The NeuB1 CHis was eluted from the column around 200 mL, corresponding to a molecular weight of around 75 kDa.

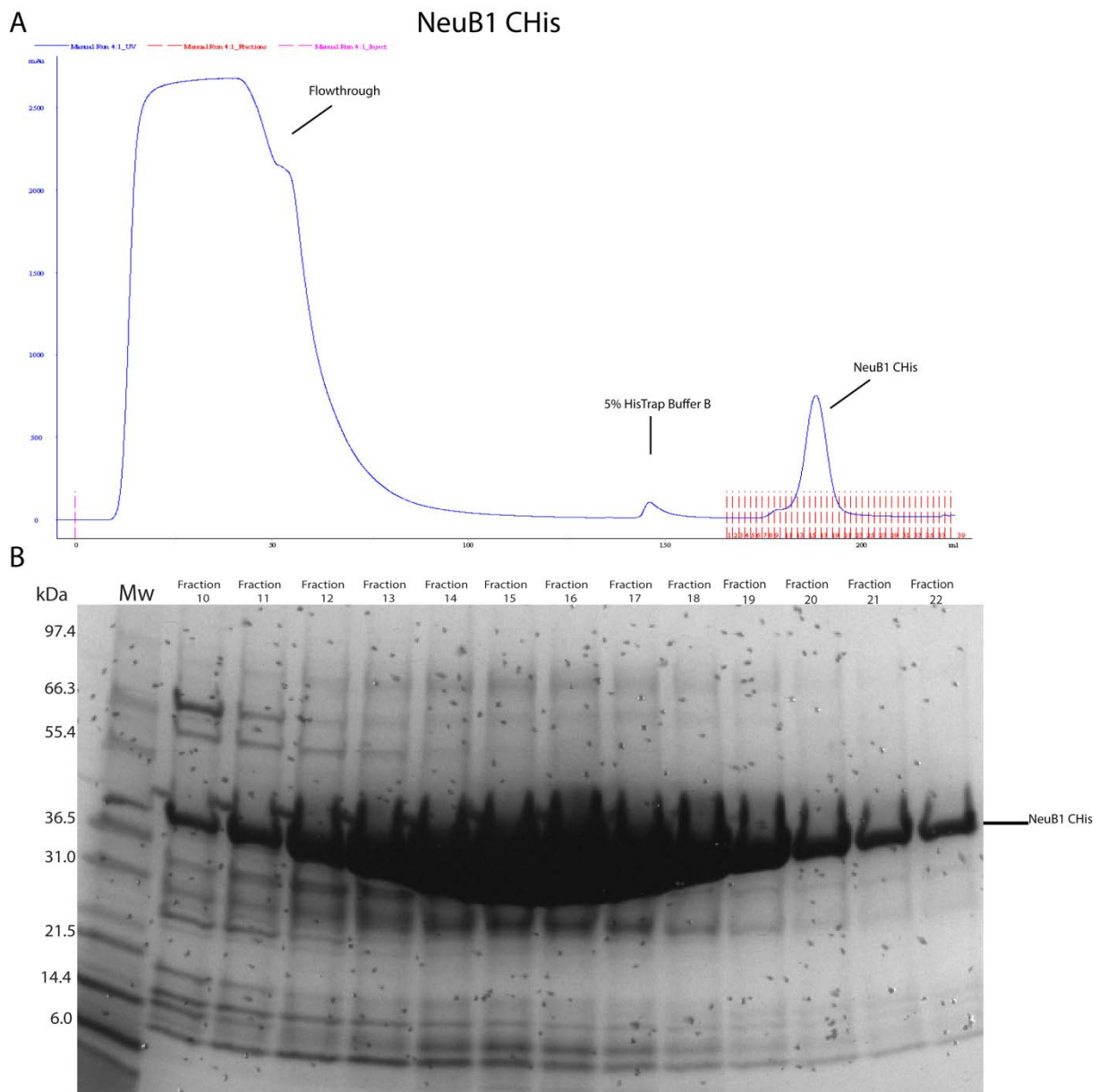


Figure 6.23 NeuB1 CHis was in the first step purified from using a HisTrap HP 5 mL column. **A)** shows the chromatogram from the purification where the blue line is the absorbance at 280 nm, the green line is the % concentration of HisTrap Buffer B and the red lines are fractions. The sample was loaded on the column and washed through with HisTrap Buffer A and 5% HisTrap Buffer B before eluting the bound protein with 5-100% HisTrap Buffer B. Fractions 10-22 from the purification were run on SDS-PAGE. Bands corresponding to NeuB1 CHis is indicated in the figure.

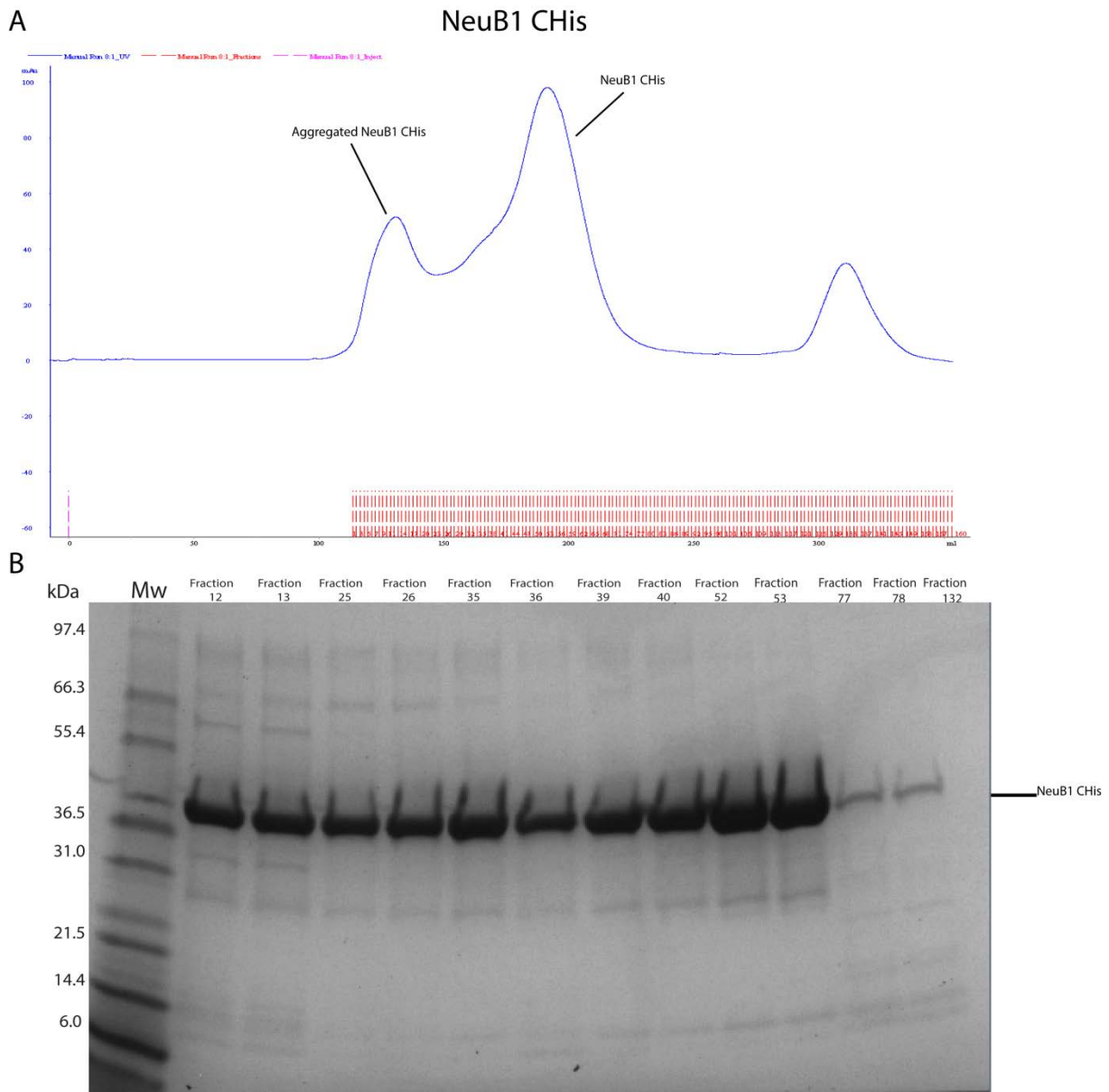


Figure 24: NeuB1 CHis was in the second step purified using a Superdex 200 26/600 gel filtration column. A) shows the chromatogram from the purification, where the blue line is the absorbance at 280 nm and the red lines are fractions. The sample was loaded on the column and washed through with Gel Filtration Buffer. The eluted protein peak is indicated in the chromatogram. B) Selected fractions were run on SDS-PAGE. Bands corresponding to NeuB1 NHis is indicated in the figure.

6.8 Purification table

The purification process of NeuB1 NHis and NeuB1 CHis have been investigated by making a purification table. In order to generate the table the volume loaded at the start of the purifications and after the final purification steps, in addition to protein concentration and enzyme activities measured from those samples are needed. The Bradford assay was used for measuring protein concentration. The unknown samples were prepared as undiluted and diluted. The assay was performed with three parallels with water as blank and absorbance was measured at 595 nm. The determined concentrations are presented in table 6.3 for NHis and 6.4 for CHis. Rawdata in Appendix II

To determine the activity of the samples, 200 μL of each sample was dialysed in Assay Buffer as described as preparation for TBA assay. The activity was tested with 10 mM ManNAc, 10 mM PEP, 120 mM Tris-HCl pH 8, 5 mM MnCl_2 and 20 μL of each sample and water to a final volume of 50 μL .. The measured absorbance as activity is presented in table 6.3 for NHis and 6.4 for CHis.

Table 6.12: To analyse the effectiveness of the purification of the NeuB1 NHis a purification table was made. NeuB1 NHis was purified in three steps, where the first two were HisTrap purification with intermediate TEV cleaving followed by gelfiltration. The total activity is the amount of units of protein in the sample, the total protein is the amount of protein in milligrams. The specific activity specifies the activity of target protein per milligram sample and increases with effective purification. The yield is the percentage of the activity and shows the amount of target protein. The purification fold is calculated based on the specific activity and an increase in fold between steps shows if the purification was worthwhile.

Step	Volume (mL)	Activity (U/mL)	Protein Concentration (mg/mL)	Total Activity (U)	Total Protein (mg)	Specific Activity (U/mg)	Yield (%)	Fold
Lysate	66,5	46,80	8,069	3112,20	536,61	5,80	100	1
HisTrap HP Column 5 mL	20	1,71	0,341	34,14	6,82	5,00	1	1
	TEV cleavage							
HisTrap HP Column 5 mL Superdex 26/200	20,5	1,19	0,047	24,33	0,958	25,41	0,8	4
	1,7	10,95	0,116	18,62	0,197	94,52	0,6	16

Table 6.13: To analyse the effectiveness of the purification of the NeuB1 CHis a purification table was made. CHis was purified in two steps, where the first was HisTrap purification followed by gelfiltration. The definitions are described for the previous purification table

Step	Volume (mL)	Activity (U/mL)	Protein Concentration (mg/mL)	Total Activity (U)	Total Protein (mg)	Specific Activity (U/mg)	Yield (%)	Fold
Lysate	34,5	149,43	11,499	5155,5	396,73	12,99	100	1
HisTrap HP Column 5 mL Superdex 200 26/600	19	116,43	2,831	2212,2	53,79	41,13	43	3
	83	26,63	0,406	2210,6	33,67	65,66	43	5

6.9 pH Optimum

The NeuB1 CHis was used for characterization studies. To determine the optimum pH for the enzyme, a sample was prepared in Assay Buffer and reaction set up using HEPES and Tris-HCl as buffers and as described in the methods section. The experiment was carried out with three parallels and blanks using Assay Buffer. The absorbance was measured at 549 nm and data was plotted using SigmaPlot. The resulting pH profile is shown in figure 6.21. The graph show a sharp increase in % relative activity at pH 6.5 and a maximum activity around pH 7.0 before decreasing slowly towards pH 10. Raw data in Appendix III.

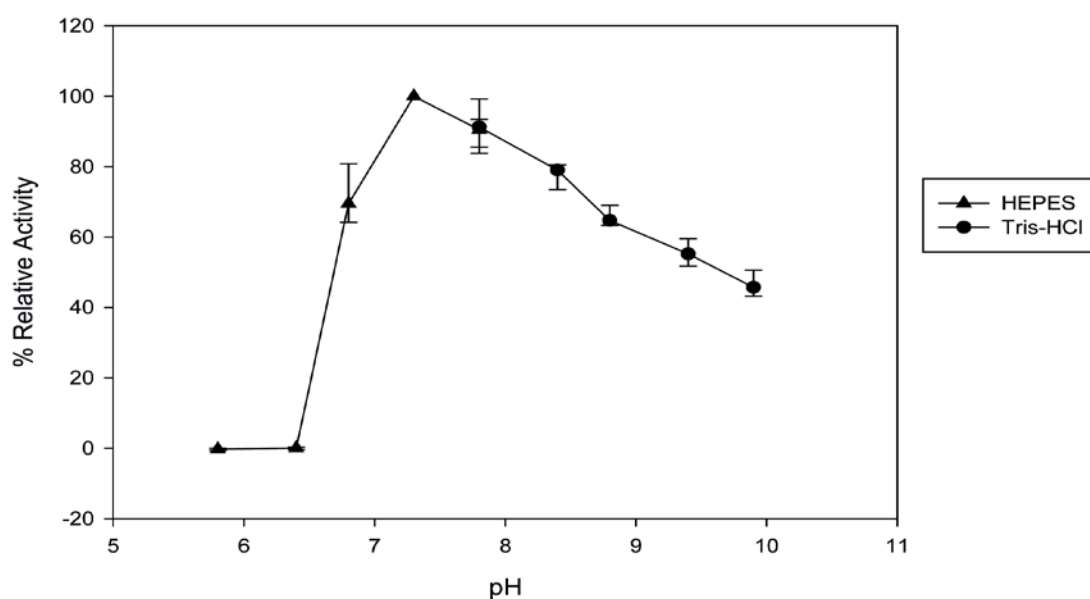


Figure 6.25: The pH optimum for NeuB1 CHis was determined using the buffers HEPES and Tris-HCl at varying pH. HEPES was used with a range from 6.0-8.0 while Tris-HCl was used between 8.0-10.0. The activity was measured using the TBA assay and plotted using SigmaPlot. The resulting graph show that there is no activity until pH reaches around 6.5 where it increases sharply to a maximum % relative activity at around pH 7.0. 50% relative activity at pH 10.0.

6.9 Temperature Optimum

The optimum temperature for the NeuB1 CHis activity was measured by carrying out the reaction at different set temperatures using a thermocycler from 5 to 55°C and as described in the methods. The absorbance was measured at 549 nm and data was plotted using SigmaPlot. The resulting temperature profile is shown in figure 6.22. The relative enzyme activity is

approximately 20% at 5°C and increasing to a maximum around 30°C. The activity decreases sharply and no activity is remaining at 55°C. Raw data in Appendix IV.

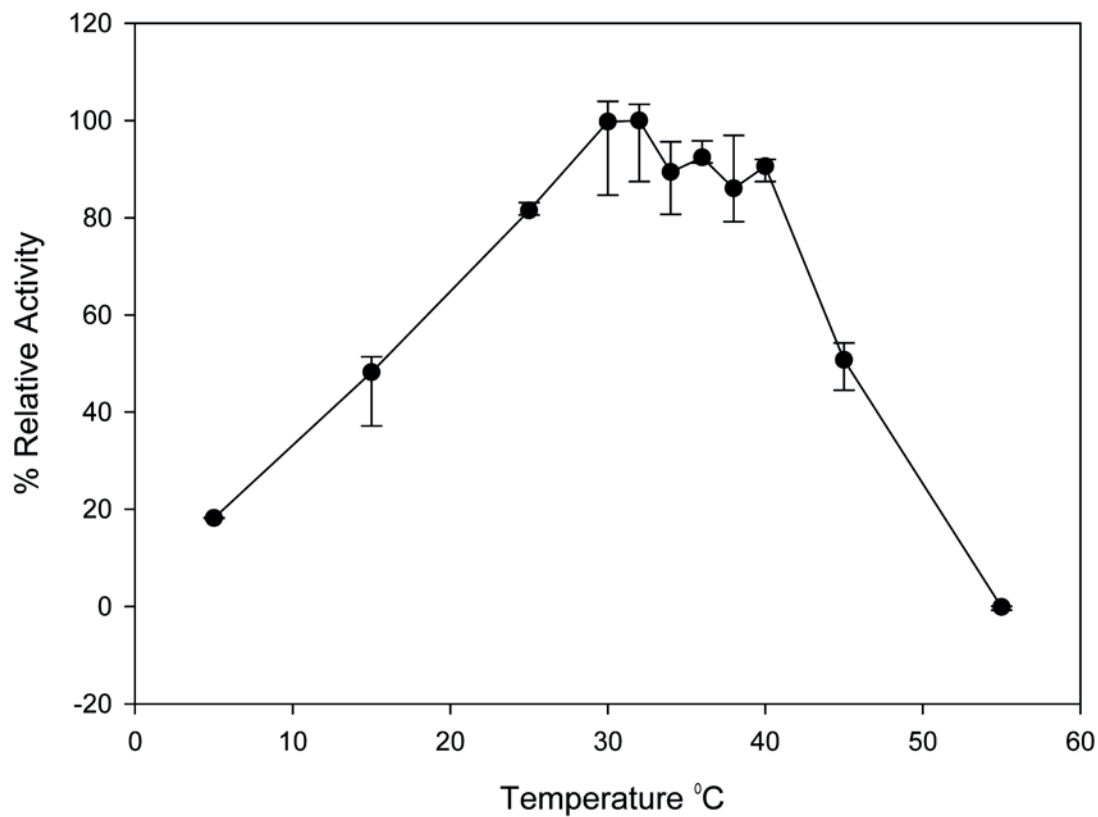


Figure 6.26: The optimum temperature for NeuB1 CHis was determined by carrying out the enzymatic reaction at different temperatures ranging from 5°C to 55°C. The activity was measured using the TBA assay and plotted using SigmaPlot. There is 20% relative activity at 5°C which increases to a maximum at around 30°C. From 40 to 55°C the activity decreases sharply and the enzyme is inactive at 55°C.

6.10 Metal Dependency

The enzymatic reaction of NeuB1 requires metal to function and to measure the dependency of metal three different metals at varying concentrations was used. The apoenzyme was prepared by dialysing with EDTA to remove metals followed by dialysis in Assay Buffer without metal present. The divalent metals cobalt, manganese and magnesium were used with a range from 0 to 7.0 mM metal concentration and reactions carried out as described in methods. The absorbance was measured at 549 nm and data plotted using SigmaPlot, figure 6.23. Without metal present there is no enzymatic activity as shown in figure 6.23, but with the addition of 0.1 mM there is a sharp increase to almost 100% relative activity for Co^{2+} , while for Mn^{2+} and Mg^{2+} the increase is slower. After 1.0 mM of Co^{2+} the activity decreases towards zero. There was observed a yellow colour in the tubes containing 3.0, 5.0 and 7.0 mM Co^{2+} . Raw data in Appendix V.

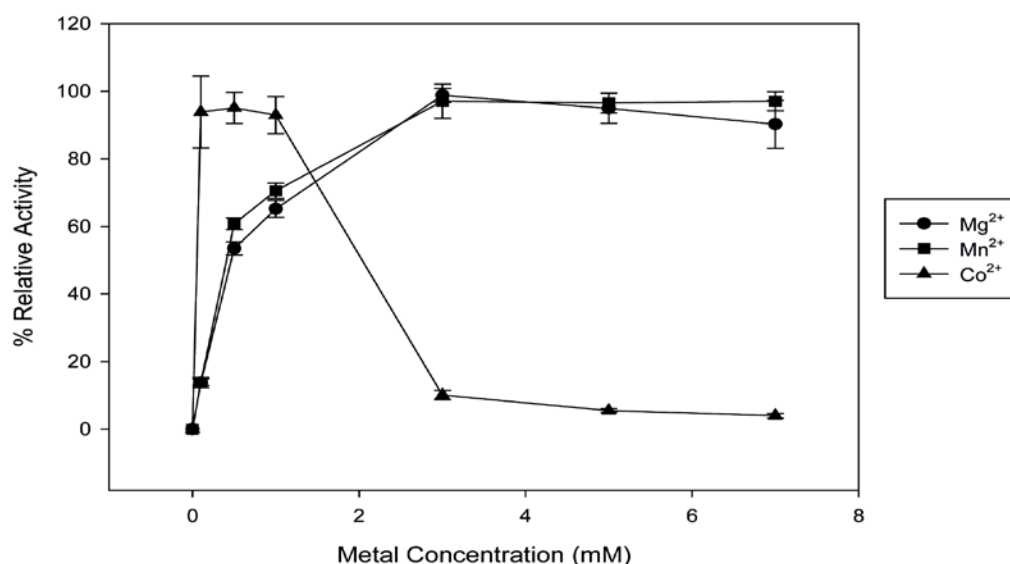


Figure 6.27: The metal dependency of NeuB1 CHis was investigated using three different divalent metals, Mn^{2+} , Mg^{2+} and Co^{2+} . The apoenzyme was prepared by dialysis in EDTA containing buffer and assayed with a range of metal concentrations from 0 to 7.0 mM. The activity was measured using the TBA assay and plotted using SigmaPlot. No activity is observed for samples without metal present, but with the increase to 0.1 mM the activity rises sharply especially for Co^{2+} which then decreases to minimum activity after 1 mM metal concentration.

6.11 Stability Assay

The stability of the protein at three different temperatures over time was measured by incubating NeuB1 CHis at the temperatures 25, 37 and 45°C for 2 hours, 1 hour and 30 minutes respectively. The residual activity was then measured using the TBA assay and compared to a sample incubated on ice as full activity. The data was plotted using SigmaPlot, figure 6.24. The axis representing % residual activity is presented as logarithmic. For the enzyme incubated at 25°C the stability decreases to around 65% after two hours, with incubation at 37°C the activity decreases to 20% after one hour and for incubation at 45°C the activity decreases to 4.5% after 30 minutes. Raw data in Appendix VI.

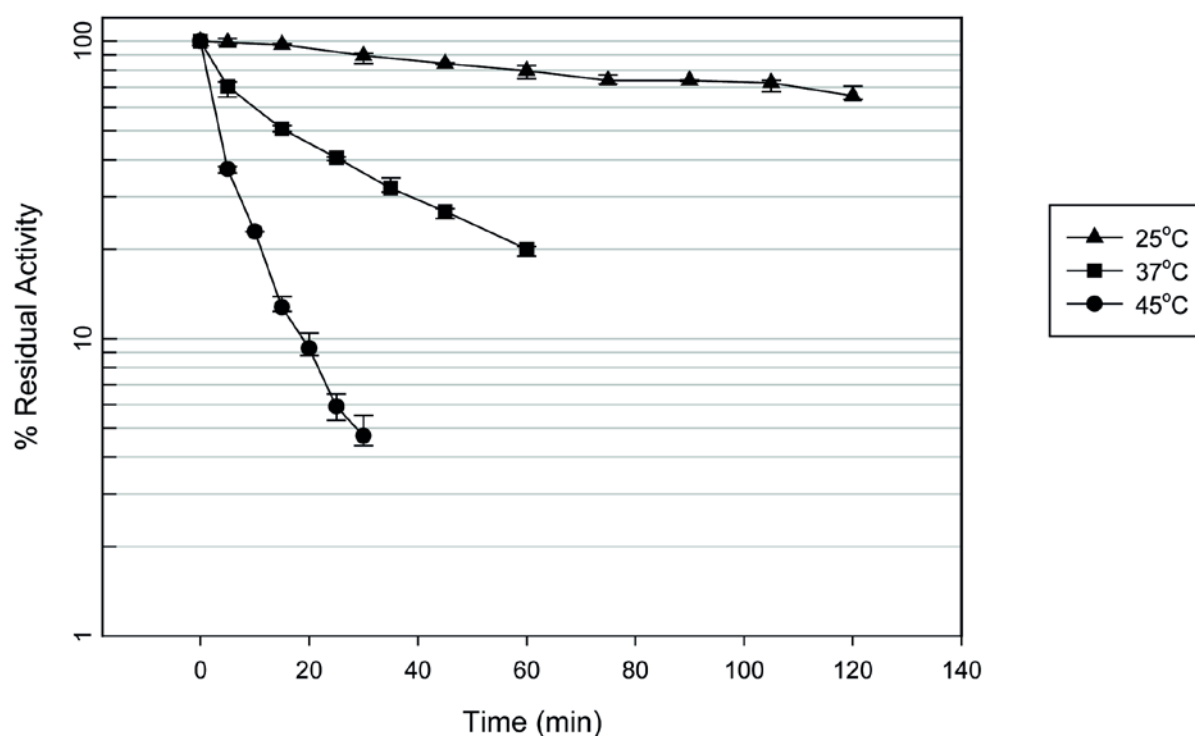


Figure 6.28: The stability of NeuB1 CHis at the temperatures 25, 37 and 45°C was investigated by incubating the protein at the specific temperature and taking out samples at specific timepoints. The residual activity was measured using the TBA assay and measuring absorbance at 549 nm. The values obtained were compared to a zero sample stored on ice and plotted using SigmaPlot. For the sample incubated at 25°C the residual activity was 65% after two hours incubation, while for the sample incubated at 37°C the residual activity after 1 hour was 20%. For incubation at 45°C the residual activity was 4.5% after 30 minutes.

6.12 Kinetics

The kinetics of NeuB1 CHis was carried out using the coupled enzymatic reaction described in methods in order to determine the K_m and V_{max} values of PEP and ManNAc.

6.13.1 Pilot Experiments

In order to determine if the PNP enzyme could be used at 25°C the PNP coupled enzyme reaction was carried out as described in section XXX with incubation at both temperatures 25°C and 37°C for 5 minutes. Absorbance was read at 360 nm. It was found that the absorbance reading and calculated V_{max} for both temperatures were similar and that 25°C could be used for kinetic experiments (data not shown).

To determine the amount of protein to use in the kinetic assay a range of NeuB1 CHis amounts was assayed using the PNP coupled enzyme reaction. The read absorbance plot for the different enzyme amounts is shown in figure 6.25. In order to estimate the V_{max} and K_m values data from the initial linear area of the graph is needed. The amounts 0.25 to 1.0 μg stays in linear area while from the amount of 2 μg and up the enzyme is saturated and the absorbance flattens out.

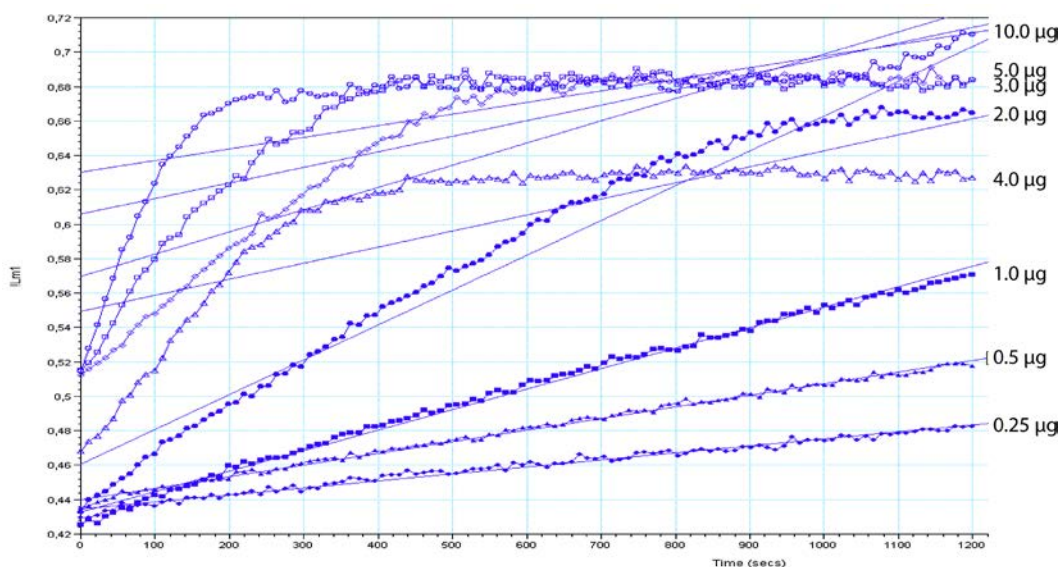


Figure 6.29: To determine the appropriate amount of protein to use in the kinetic assay an experiment with different amounts of NeuB1 CHis was performed. The amounts were in the range 0.25, 0.5, 1.0, 2.0, 3.0, 4.0, 5.0 and 10.0 μg . The experiment was carried out with the PNP coupled enzyme assay and measuring absorbance at 360 nm. The curve given by SoftMax Pro 5.2 shown with the NeuB1 CHis amounts corresponding to each curve.

6.13.2 ManNAc Kinetics

To determine the V_{\max} and K_m values for ManNAc the PNP coupled enzyme assay was used. The concentrations of ManNAc were varied from 0.1 to 60.0 mM and as the reaction performed as described in sectionXXX. The generated data was calculated in SigmaPlot Enzyme Kinetics Tool and Michaelis-Menten plot, figure 6.26, was made. The V_{\max} for ManNAc was determined to 10.0353 ± 1.1304 and K_m to 18.1254 ± 5.2537 . The R^2 of the plot was calculated to be 0.896. Raw data in Appendix VII.

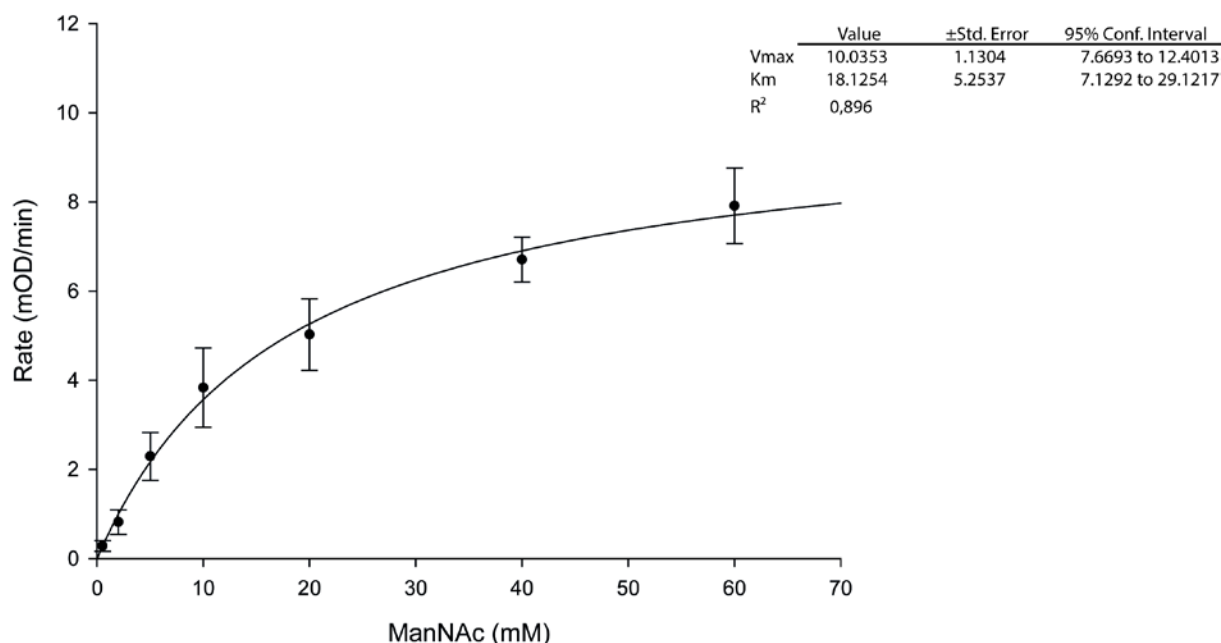


Figure 6.30: V_{\max} and K_m for ManNAc were found by using the PNP coupled enzyme assay measuring absorbance at 360 nm. Different concentrations of ManNAc, 0.1, 0.5, 2.0, 5.0, 10.0, 20.0, 40.0 and 60.0 mM, were used combined with 0.95 μ g of NeuB1 NHis. The reactions was carried out at 25°C. The generated data was used to make a Michaelis-Menten plot in SigmaPlot Enzyme Kinetics Tool and the V_{\max} was determined to 10.0353 ± 1.1304 and K_m to 18.1254 ± 5.2537 . The R^2 of the plot was calculated to be 0.896.

6.13.3 PEP Kinetics

To determine the V_{\max} and K_m values for PEP the PNP coupled enzyme assay was used. The concentrations of PEP was varied from 0.05 to 10.0 mM and the reaction was carried out as described in section XXX. The generated data was calculated in SigmaPlot Enzyme Kinetics Tool and Michaelis-Menten plot, figure 6.27, was made. ManNAc V_{\max} was determined to 10.8542 ± 0.6477 and K_m to 0.7646 ± 0.1674 . The R^2 of the plot was calculated to be 0.901. Raw data in Appendix VII.

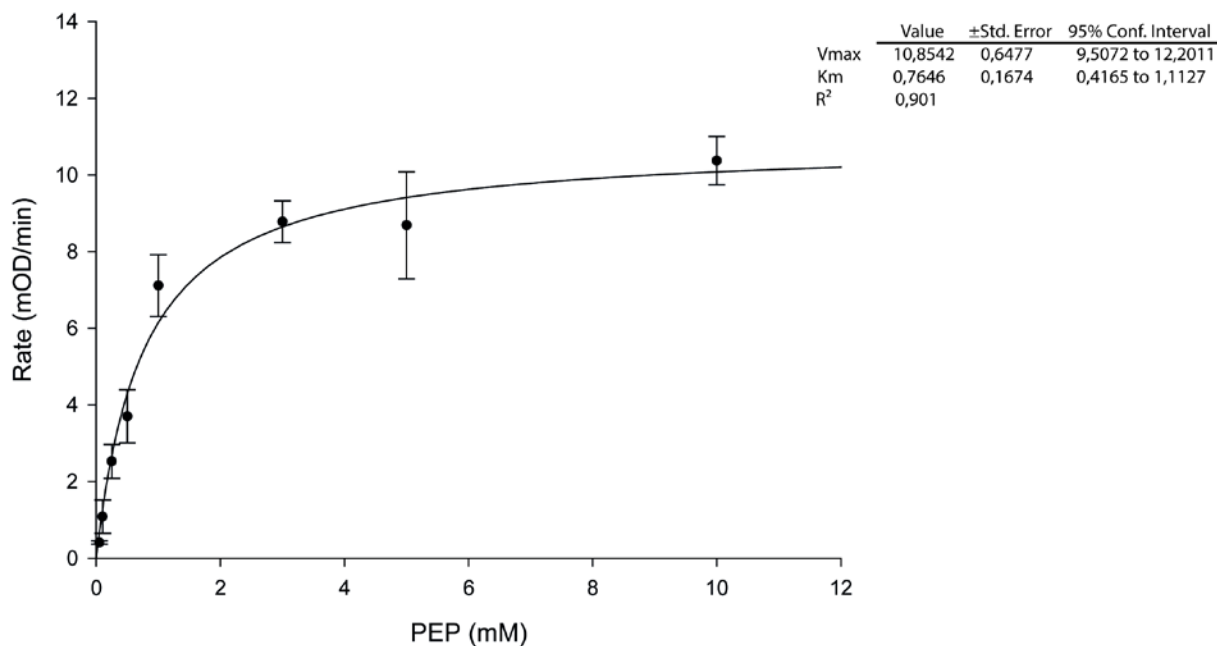


Figure 6.31: V_{max} and K_m for PEP was found by using the PNP coupled enzyme assay measuring absorbance at 360 nm. Different concentrations of PEP 0.05, 0.1, 0.25, 0.5, 1.0, 3.0, 5.0 and 10.0 mM, were used combined with 5 μ g of NeuB1 NHis. The reactions was carried out at 25°C. The generated data was used to make a Michaelis-Menten plot in SigmaPlot Enzyme Kinetics Tool and the V_{max} was determined to 10.8542 ± 0.6477 and K_m to 0.7646 ± 0.1674 . The R^2 of the plot was calculated to be 0.901.

6.13.4 Phosphate Standard Curve

In order to calculate the catalytic constant k_{cat} for the enzyme the measured OD for the PNP catalysed reaction needed to be converted to amount of neuraminic acid produced. Since one molecule of neuraminic acid corresponds to one molecule of 2-amino-6-mercapto-7-methylpurine formed, a standard curve was made with different concentrations of phosphate as substrate ranging from 1.75 μ M to 175 μ M. The standard curve was generated using SigmaPlot and linear regression, figure 6.28. The values from 1.75 to 17.5 μ M were omitted because of negative measured OD and one parallel from 105 μ M was omitted to fit the line. Raw data in Appendix VIII. The equation, equation 6.1 for the linear curve was determined to be;

$$y = 0.00275x - 0.06478 \quad 6.1$$

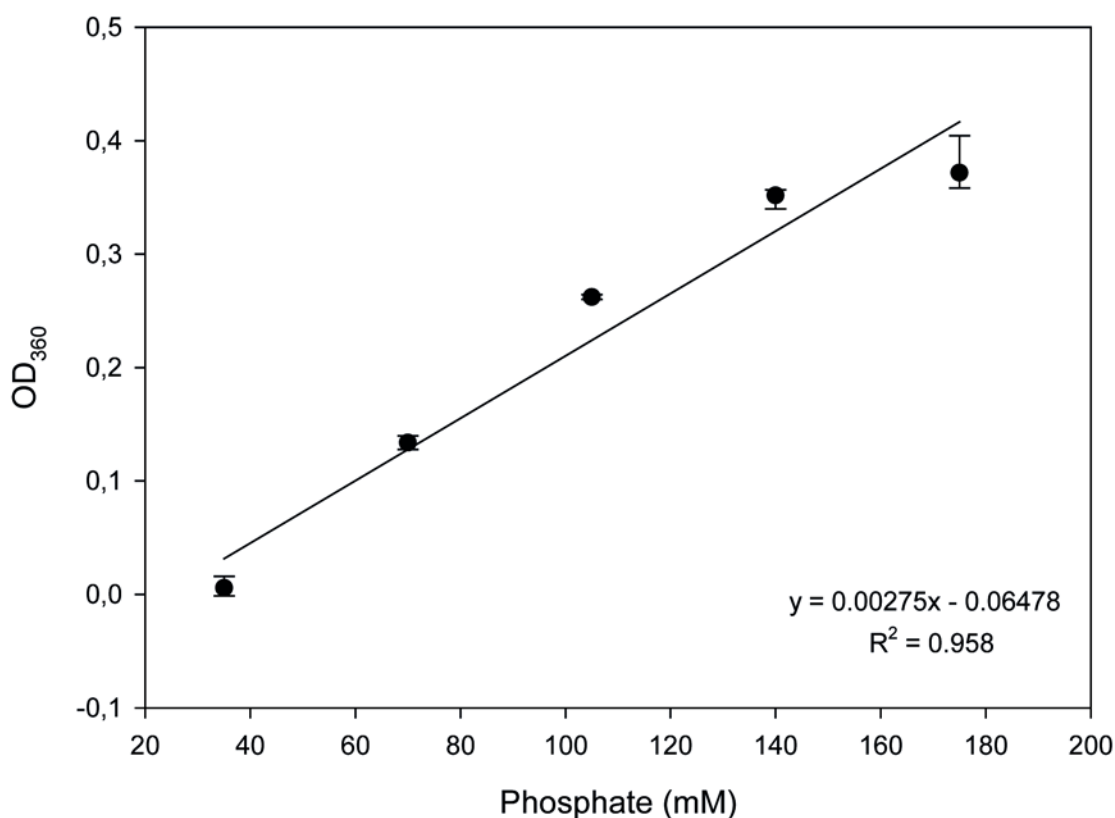


Figure 6.32: In order to calculate the k_{cat} of NeuB1 CHis the measured OD value needed to be converted to amount of neuraminic acid produced. Using different concentrations of phosphate as substrate for PNP the reaction was carried out at room temperature for 30 minutes and absorbance was measured at 360 nm. The OD values for each concentration was used to make a standard curve in SigmaPlot using linear regression giving the equation for the curve that is used in the conversion. The equation and R^2 is given in the figure

6.13.5 NeuB1 k_{cat}

The k_{cat} for the enzyme was calculated on the basis of the obtained V_{max} values from ManNAc and PEP. The V_{max} value which is given in mOD is converted to phosphate concentration given by the equation 6.1 and is divided by the enzyme concentration. This value is multiplied with the enzyme molecular weight giving k_{cat} . For ManNAc the k_{cat} was determined to 222.997 min^{-1} and for PEP determined to 225.438 min^{-1} . The calculations are shown in Appendix IX.

6.14 Crystallization

Crystallization conditions were found with the screen KCSG set up with robot in the well containing 20% PEG 3350 and 0.1 M sodium citrate pH 8.5 giving needles. The conditions

were tried optimized by screening around it. Addition of 10% glycerol at 4°C screens gave needles in more of wells. For screens in room temperature a PEG 3350 percentage of 20-35 gave small needles independent of sodium citrate concentration, while with the addition of glycerol, lower percentage of PEG, 14-18%, gave bigger needles at a sodium citrate concentration of 0.2 M. Streak seeding was performed on conditions 30% PEG 3350 and 0.1 M sodium citrate which gave a crystalline matter. The crystal was sent to the synchrotron in Berlin (Bessy). It was confirmed to be protein but no data could be collected.

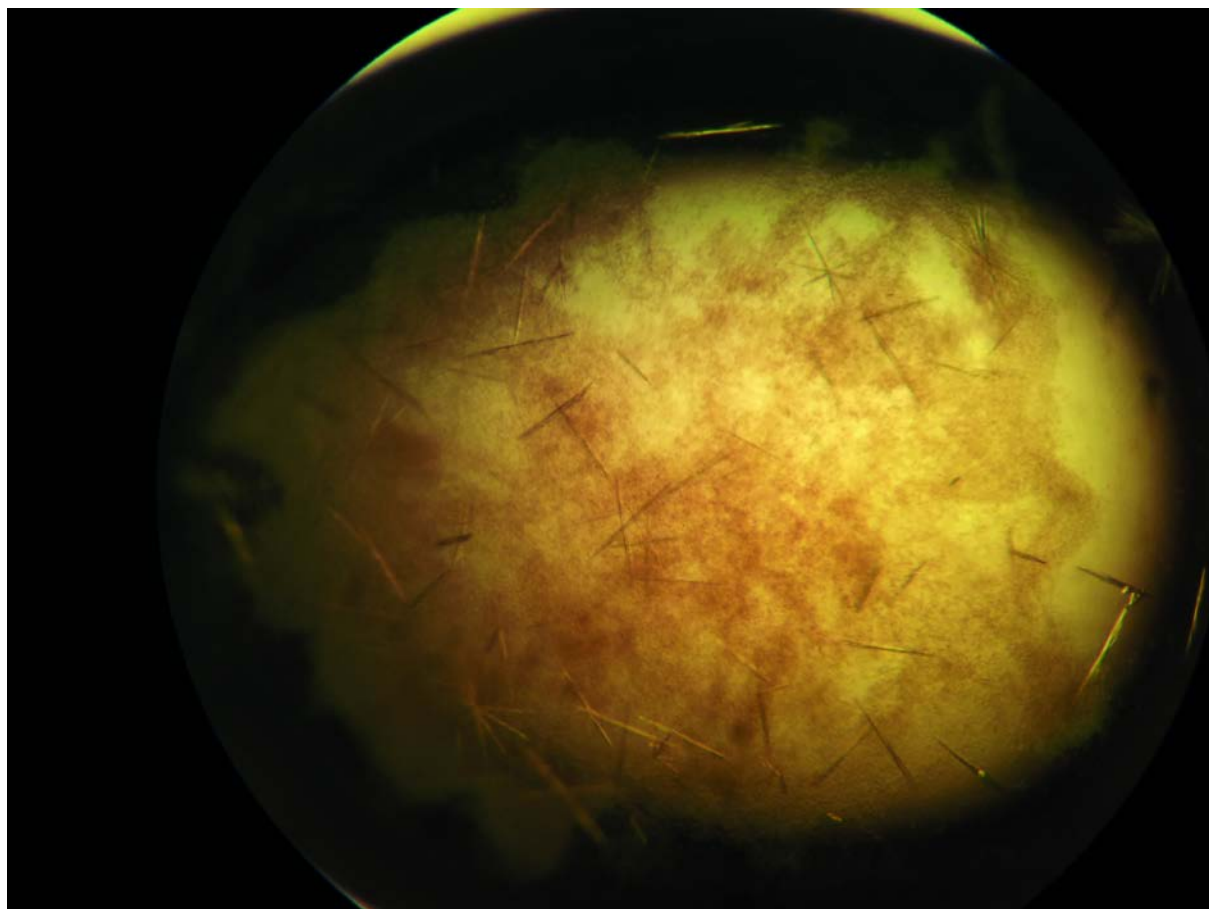


Figure 6.33: The NeuB1 protein was tried crystallized by screening around the found conditions PEG 3350 and sodium citrate. Needles were formed but they were not of good enough quality to collect data. Addition of glycerol and screening at 4°C improved the size of the needles. The needles in the figure were formed under the conditions 15% PEG 3350, 0.2 M sodium citrate and 10% glycerol at 4°C.

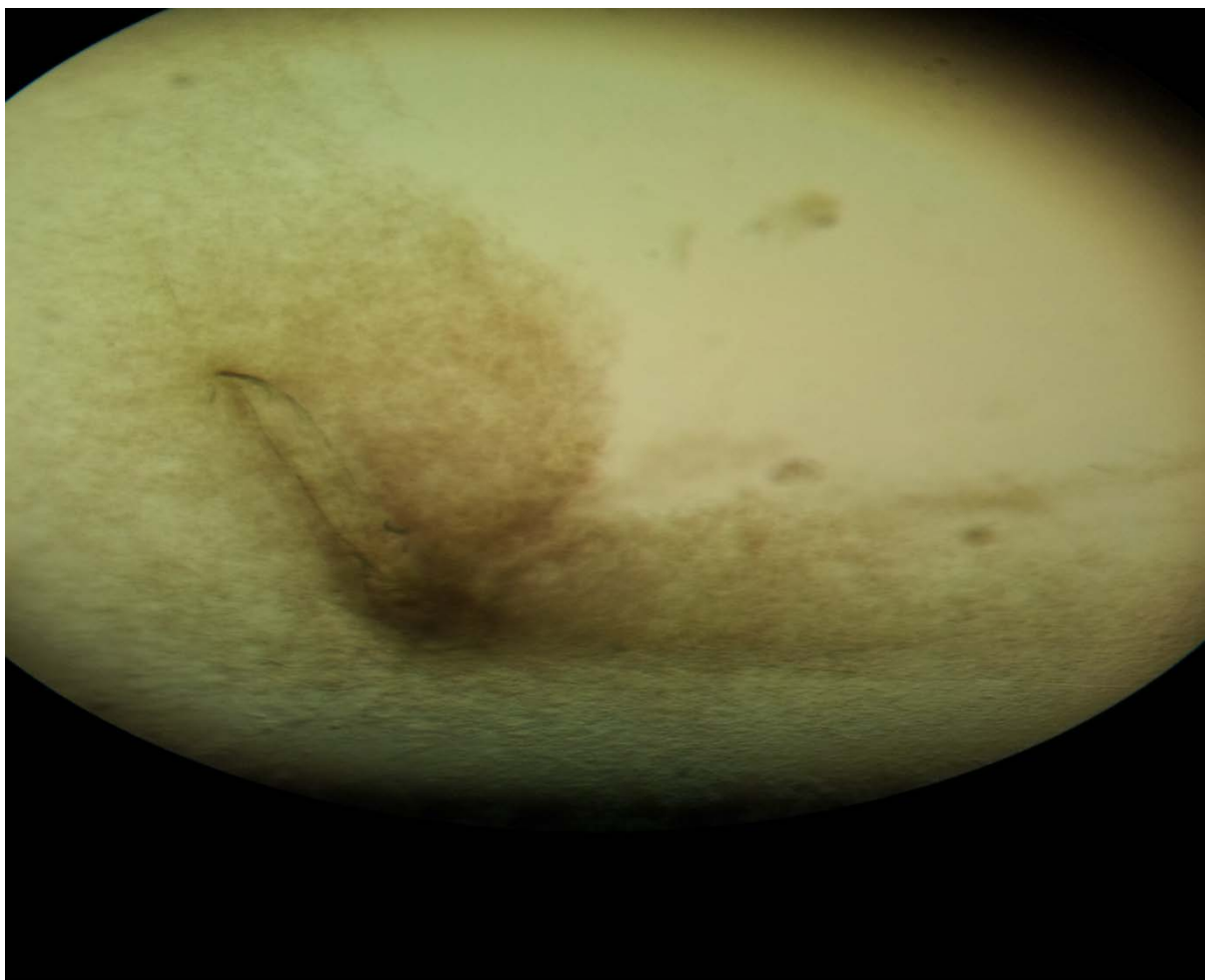


Figure 6.34: Using seed streaking a crystalline matter was formed under the conditions with 30% PEG 3350 and 0.1 M sodium citrate at room temperature. The crystal was mounted and brought to the synchrotron in Berlin (Bessy). The crystal was confirmed to be protein but diffracted too poorly to collect data.

6.15 Sialic acid Mass Spectrometry

Initial investigation of Sia expression in *M. viscosa* was performed by growing the bacteria under different growth conditions and releasing the Sia by mild acid hydrolysis followed labelling the free Sia with DMB. The samples were analysed by HPLC-MS/MS. Four samples in total were analysed as described in section XX, in addition to the standard NeuNAc and a standard panel containing a mixture of different Sia.

All the bacterial growth conditions were found to express Sia, but to various degrees. The amount of in the samples could be determined by HPLC-MS and by comparison to a standard curve (Appendix) generated with the known amounts of NeuNAc..

Table 6.14: The amount of NeuNAc expressed in *M. viscosa* under different growth conditions were determined by HPLC-MS. LB-bacterial sample from LB-plate; BA-bacterial sample from blood agar plate; BALB-bacteria from blood agar plate further grown in liquid LB; MB-bacteria from LB-plate further grown in liquid marine broth.

Sample	Amount of Neu5Ac (pmol)
LB	13.736
BA	33.936
BALB	422.928
MB	19.518

In addition to NeuNAc, a diacetylated neuraminic acid (Neu5,7Ac₂) was also expressed in addition to what might be Pse5,7Ac₂ (structures shown in figure 6.31), for the samples BA, BALB and MB. The MS and MS² spectra for BALB are shown in figure 6.32 and 6.33, as a representative. Data for BA, MB and LB is shown in Appendix X. The MS spectra for BALB shows the peak for NeuNAc at retention time 4.68 at m/z = 426.1481 – 426.1533 (A), Neu5,7Ac₂ at retention time 5.99 at m/z = 468.1585 – 468.1641 (B) and what corresponds to the mass for Pse5,7Ac₂ at retention time 4.81 at m/z = 451.1796 – 451.1850 (C). The peaks were further analysed with MS² where for NeuNAc and Neu5,7Ac₂ there were found the characteristic fragments m/z = 313, 295, 283 and 229 [98] (figure A and B respectively). The MS² spectra for Pse5,7Ac is also shown but no literature values for the fragmentation of pseudaminic acid is available to judge characteristic fragment ions. The results were compared to MS and MS² data obtained for the NeuNAc standard. The presence of Neu5,7Ac₂ could be confirmed by comparing to spectra obtained for the same mass from the standard panel, also containing Neu5,7Ac₂. The Neu5,9Ac₂ would give the same mass, but lack the fragment 295 [98]. No quantitative data can be obtained for Sia in a mixture.

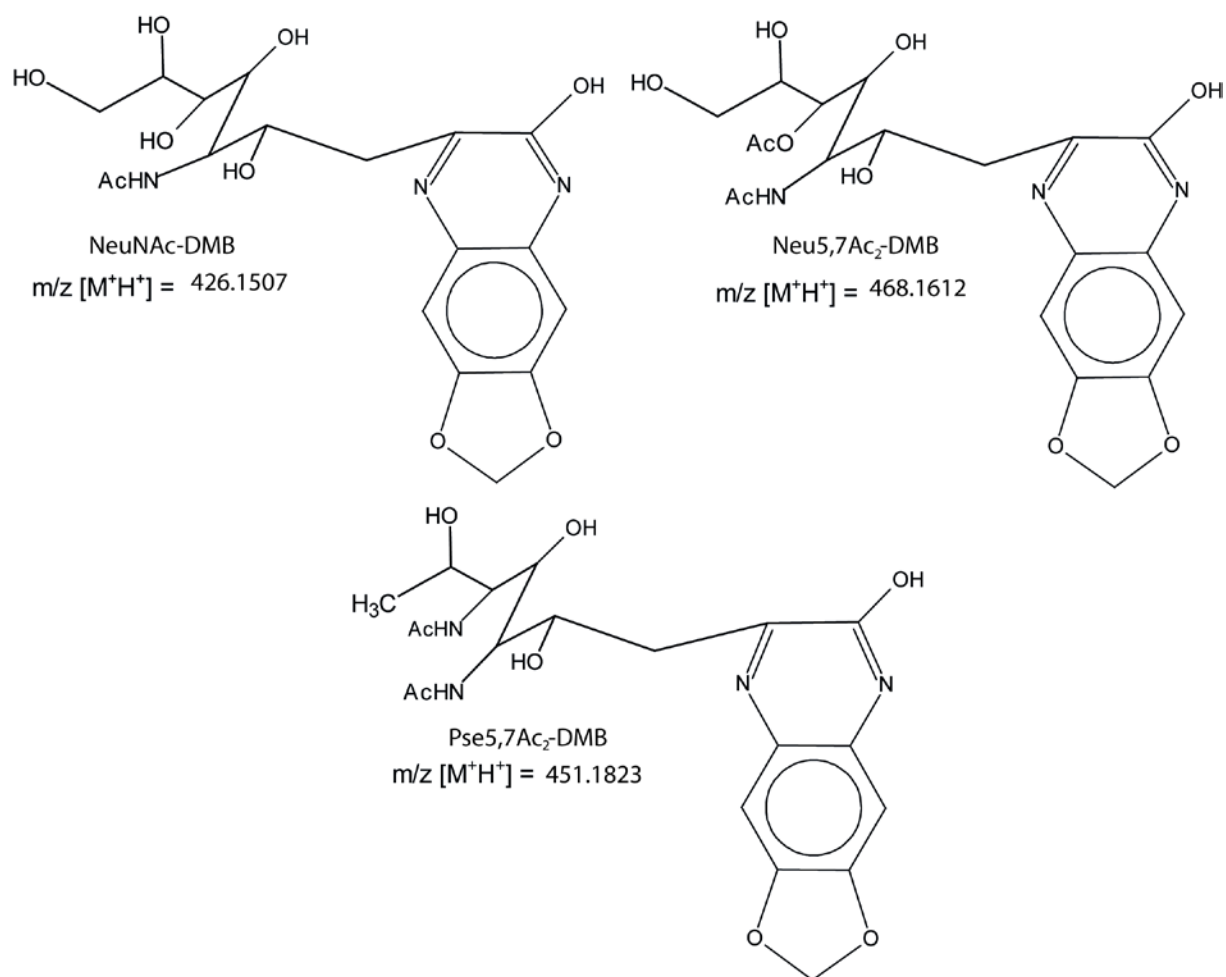


Figure 6.35: The DMB label is able to react with various forms of sialic acids as shown, where NeuNAc, diacetylated neuraminic acid (Neu5,7Ac₂) and what corresponds to the mass of pseudaminic acid (Pse5,7Ac₂) is found in the mass spectrometry analysis of sialic acid expression.

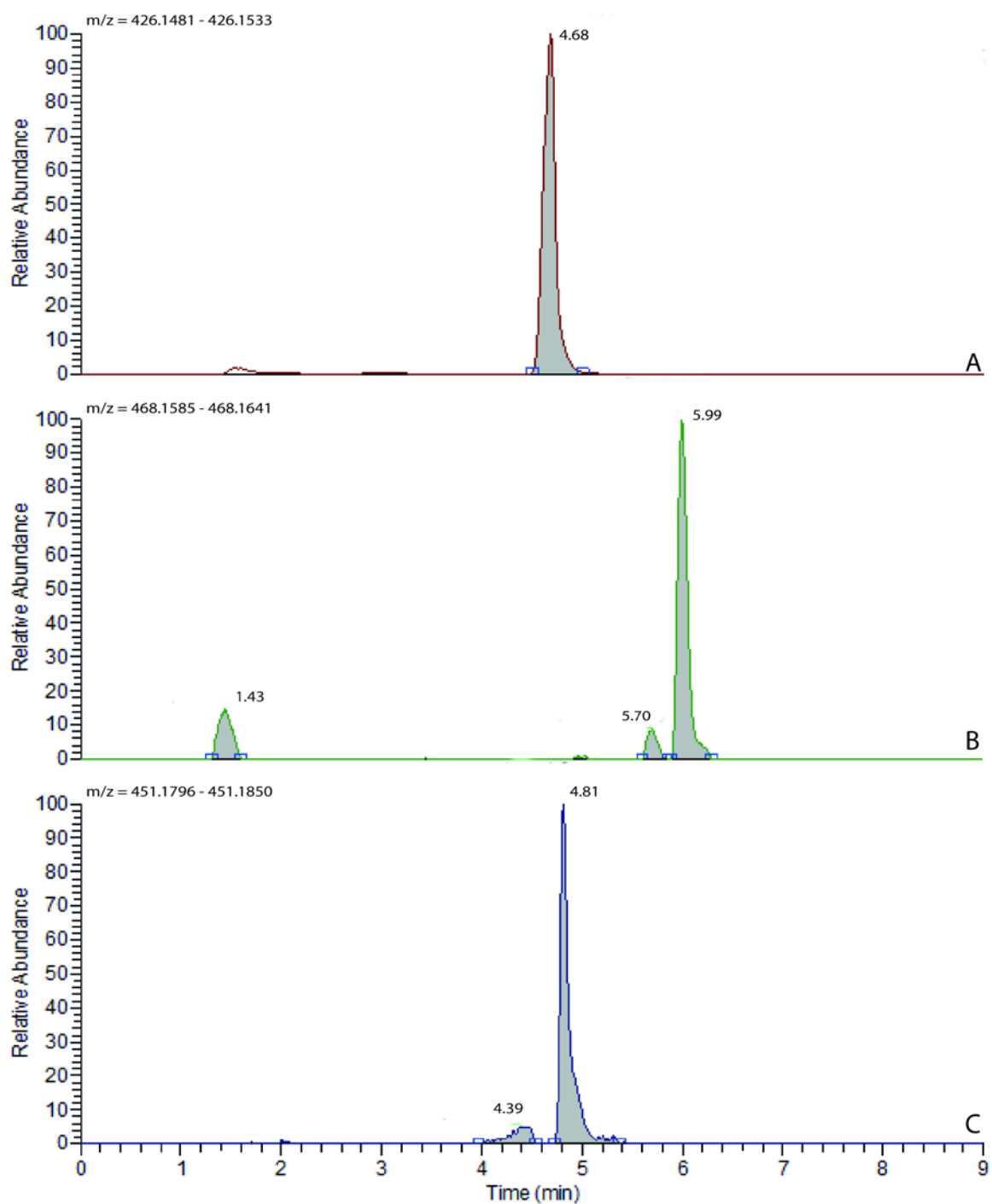


Figure 6.36: Peaks were located in the MS-spectra of BALB corresponding to the sialic acids Neu5Ac (A), with retention time 6.68, Neu5,7Ac (B), with retention time 5.99 and Pse5,7Ac (C) with retention time 4.81.

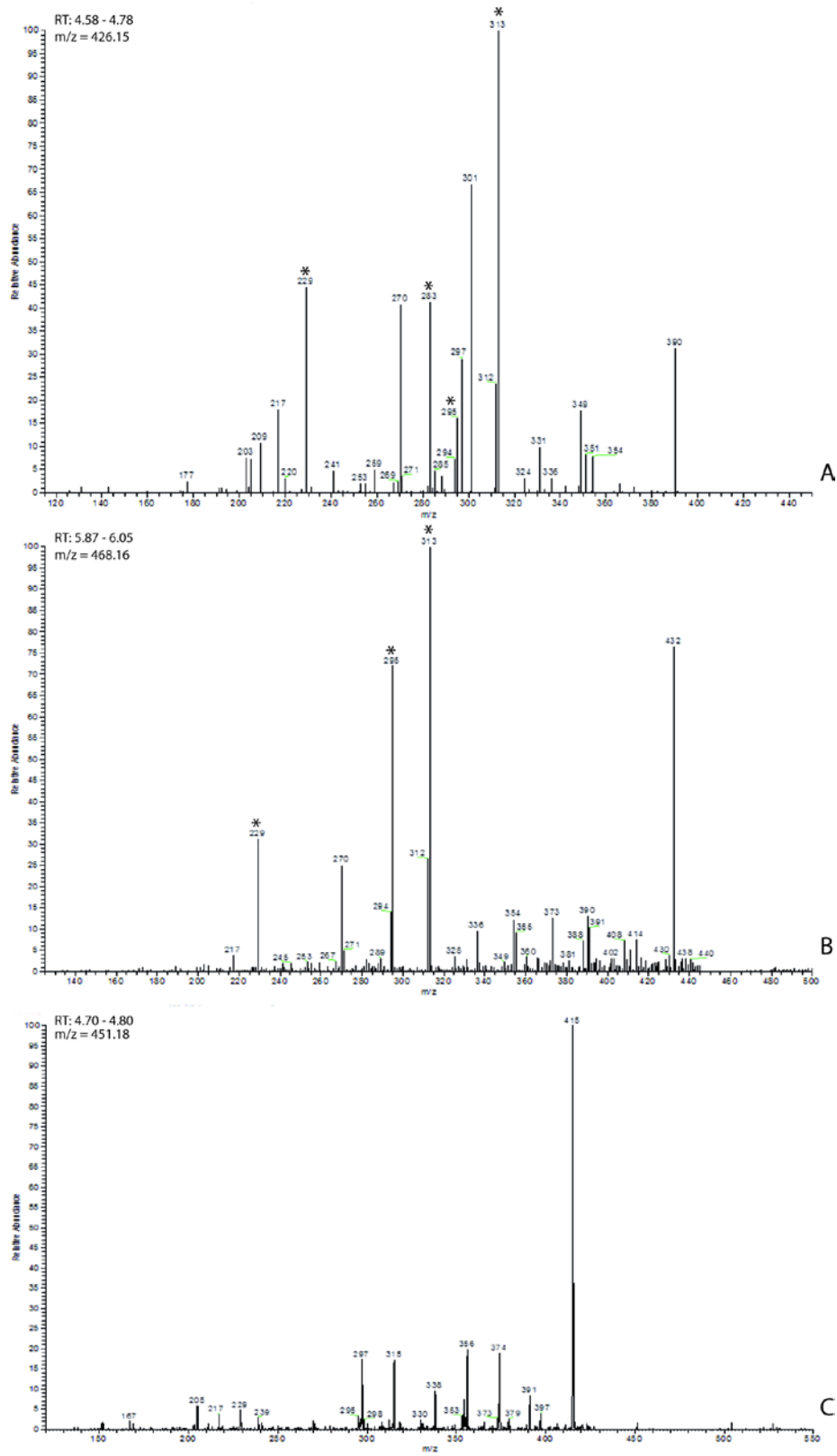


Figure 6.37: The MS/MS spectra for the three sialic acids, Neu5Ac (A), Neu5,7Ac (B) and Pse5,7Ac (C). The Neu5Ac and Neu5,7Ac show the characteristic fragment ions $m/z = 313, 295, 283$ and 229 which are marked with *, while for Pse5,7Ac no specific fragment ions are documented.

7. Discussion

7.1 Bioinformatic analysis of NeuB1

Analysis of the NeuB1 protein sequence and the constructs made was done with the ProtParam tool to find molecular weight, average extinction coefficient and pI, table 6.1. The first two values were used in the protein concentration determination with Nanodrop 2000c for use in the endpoint assays. The pI value is a theoretical value in this case where the protein carries no electrical charge. Knowledge of this helps to avoid pH regions when making buffers that could cause the protein to precipitate. Information regarding overall charge of the protein is also useful when choosing buffer system and purification strategy.

A multiple sequence alignment was created where NeuB1 from *Moritella viscosa* was compared to NeuB1 from other organisms in order to find conserved areas in the sequence and find the sequence identity compared to those. The aligned sequences along with the predicted and known secondary structures presented in figure 6.1 shows that the predicted secondary structure of mvNeuB1 fits well with the known *N. meningitides* secondary structures. Most of the residues involved in the secondary structures elements are either identical or preserved with the same physiochemical properties. The amino acids involved in ligand binding (Mn^{2+} , PEP and ManNAc) are known from the *N. meningitides* NeuB1 and are found to be conserved through the NeuB1 sequences from all the organisms. The sequence identity for *M. viscosa* table shown in table 6.2 reveals that the highest identity is between *M. viscosa* and *N. meningitides* (63%) while for the rest the identity is around 30%.

Based on the high sequence identity between NeuB1 from *M. viscosa* and *N. meningitides* the latter was used as template to make a homology model of the mvNeuB1 three dimensional structure. The model made (using SWISS-Model) gave the QMEAN Z-value of -0.93 which reflects the absolute quality of the model. The value is in this case low meaning that the template provided enough information to build an accurate model. The quality of the model was further examined through a Ramachandran plot to reveal amino acid conformations that normally is not found in the protein structures. The plot gave two residues outside the generously allowed area, Ser-9 and Asp-338. These are located in the area near the N-terminal and C-terminal end of the protein respectively and are substituted for Gly-10 and Gly-340 in the template sequence. Glycine is special in the case of conformations since its functional group is hydrogen it can adopt many more than the other amino acids. The substituted amino acids Ser-9 and Asp 338 have a polar and negatively charged functional groups respectively

giving a drastic change in the sequence compared, but this should not disqualify the model. The model was further analysed by colouring by B-factor in PyMol, (figure 6.3). This colouring shows how much of the structure the SWISS-Model was able to model based on the available information. Blue colour represent areas where the template information was sufficient to predict the structure while red are used on areas where the information was insufficient. Two red areas were found both are coil areas that could be flexible, making it difficult to predict a structure and interactions with other residues. Figures of the electrostatic surface potential maps are shown in figure 6.5 and 6.6. It is seen that the charged surface area is more or less identical between the mvNeuB1 model and the *N.meningitidis* NeuB1 structure. The conserved substrate binding residues and similar structure strongly point towards the catalytical mechanism between the two should be the same

7.2 Purification of NeuB1

The NeuB1 NHis and CHis proteins were tested for expression in small scale using two expression hosts *E.coli* Rosetta 2 (DE3) pLysS and *E.coli* BL21* pRare 2 pLysS. The expression was similar in both strains for each protein version and each was test purified to judge which samples to use for upscaling scale. The *E.coli* Rosetta 2 (DE3) pLysS expression strain was chosen for large scale expression and purification judged on the amount of expressed protein purified by HisTrap affinity chromatography. To compare the purification process of NeuB1 NHis and NeuB1 CHis a purification table was generated for both. In general the purification of NeuB1 NHis gives purer samples because of the additional HisTrap purification to remove the TEV-protease used to cleave the NeuB1 NHis His-tag. But higher amounts NeuB1 CHis are purified compared to the NeuB1 NHis. This is believed to be caused by instability in the NeuB1 NHis construct causing it to precipitate after the sonication process. Figure 7.1 shows the terminal ends of the *M.viscosa* homology model where the four terminal residues are coloured blue and the structure is shown with red β -sheets, turkish α -helices and purple coils. The template substrates ManNAc and PEP are shown in green, and manganese in yellow, were they were overlapped with the model to show the active site. The His-tag is not shown in the figure but by extension of the N-terminal the tag would come close to the active site and could give unfavourable interactions causing the protein to lose its folding and precipitate. But some of the proteins manage to fold correctly and can be purified, so the reason for the incorrect fold can be thought to appear already at the translation stage. Bacteria transcribe and translate at the same time since they don't have to transport the mRNA outside the nucleus, so the ribozymes can bind the mRNA directly. Since some of the

proteins are folded correctly the first initial foldings of the N-terminal that is translated first must decide if the protein is able to achieve the correct fold or not. The incorrect ones are then later precipitated as they are centrifuged after sonication. The C-terminal His-tag is located outside the structure where it cannot interact with critical residues and disturb the active site making expression of this version of the protein favourable. Because of the low yield of NeuB1 NHis the characterization, kinetics and crystallization were done with the NeuB1 CHis after confirming that both protein versions were active and had the same activity.

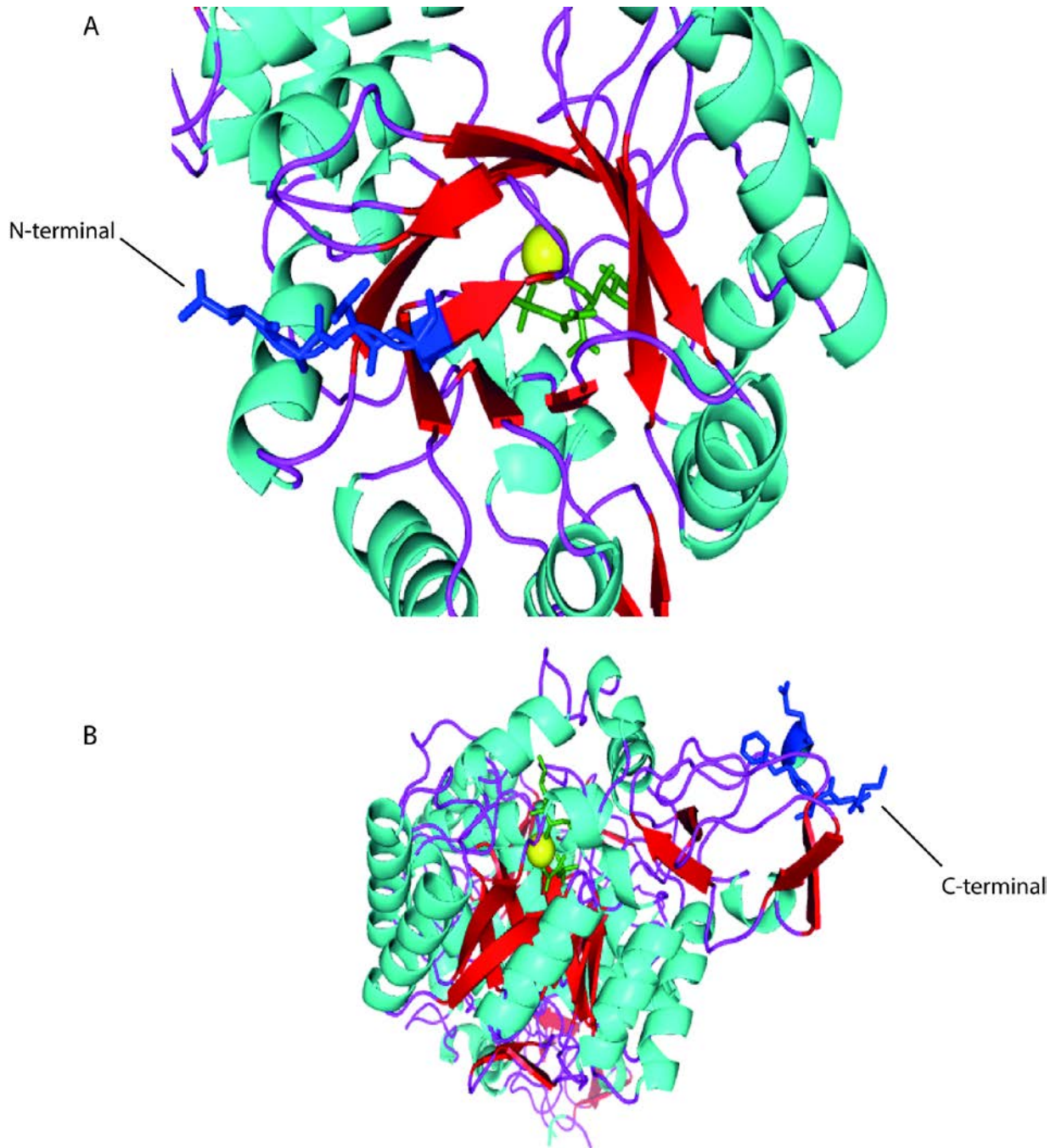


Figure 7.38: The NeuB1 NHis is thought to be destabilized by the presence of the His-tag in the N-terminal here illustrated using the NeuB1 homology model. α -helices are coloured with turquoise, β -sheets are coloured red and coils are coloured purple. The substrates PEP and ManNAc (green) in addition to manganese (yellow) were put in to show the active site. A) shows the location of the N-terminal end in the homology model with the first four residues coloured blue. B) shows the location of the C-terminal end where the last four residues are coloured blue.

7.3 NeuB1 Assay

To determine the activity of NeuB1 the thiobarbituric acid assay was used to measure the amount of neuraminic acid in the reaction samples. In order to perform the assay it was necessary to remove the glycerol from the purification buffers the protein was stored in. The exact mechanism for the influence of glycerol is not known but amounts as small as 1% are affecting the results. Another factor is the 2-mercaptoethanol used in the buffers, which can interfere with the oxidation step when adding sodium periodate, this has been observed when using low protein concentration samples, where higher volumes are needed in the assay to reach the wanted amount of enzyme.

7.3.1 pH optimum of NeuB1

The pH optimum of NeuB1 CHis was determined using the buffers HEPES and Tris-HCl. The pH optimum was found to be around pH 7.5 for the HEPES. An overlap should have been performed with Tris-HCl to see if this is the case for both or the buffers themselves some way could affect the optimum. It was observed that at pH 5.8 to 6.4 the enzyme is inactive before activity rises sharply towards the optimum and then slowly decreases towards pH 10. This might be due to the metal binding residues His-215 and His-236, figure 7.2. The imidazole of the histidine has a pKa of approximately 6.0 meaning that below this value the histidines will be protonated which will give a positive charge. In a protein the surrounding amino acid residues may affect this pKa value and either increase or decrease it. So if the histidines that bind to manganese are protonated at around pH 6.0 their positive charges may interfere with binding and stabilising the metal ion that is vital for the enzymatic process.

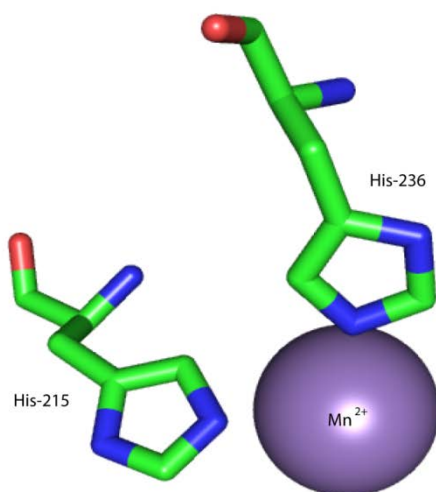


Figure 39: The activity of NeuB1 rises sharply around pH 6.5. This might be due to the metal binding histidines His-215 and His-236. When the pH is below 6.5 the imidazole rings become protonated and carries a positive charge which may influence the binding and coordination of the bound metal.

7.3.2 Temperature optimum of NeuB1

The temperature optimum of NeuB1 was determined by assaying the reaction at different temperatures, figure 6.20. The optimum temperature for the enzyme was found to be around 30°C, which represents a shift in optimum temperature compared to previously reported cases for NeuB1 in other organisms as *A. salmonicida* [88] and *E.coli K1* [99] where the optimum temperature was found to be 45°C. Comparing to those the activity at 5°C is also different as *M.viscosa* NeuB1 retain a higher activity, while for higher temperatures the activity drops from 40°C to 55°C where there is no activity. This seems also to be the case for *A.salmonicida* as the activity decreases rapidly after the optimum while for *E.coli* NeuB1 the decrease is slightly shifted towards higher temperatures. To try to define the optimum peak better it was tried to measure the activity at shorter intervals between 30 and 40°C, this is shown as fluctuations in the resulting graph, which might come from that the points being so close they are more sensitive to pipetting errors.

7.3.3 Metal Dependency of NeuB1

To test the dependency of and affinity to different metals, a metal titration was performed with the NeuB1 apoenzyme and the divalent cations Mn^{2+} , Mg^{2+} and Co^{2+} . The results presented in figure 6.21 shows that at low concentrations of metal cobalt binds stronger than

manganese and magnesium. As the metal concentration of manganese and magnesium increases the activity increases while for cobalt it decrease at around 3 mM. The reason for this sudden drop for cobalt is thought to be caused by the formation of cobalt hydroxide ($\text{Co}(\text{OH})_2$). The solubility of cobalt hydroxide is 0.0003 g/100 g of water [100] meaning that depending on the solubility constant and the concentrations of cobalt and hydroxide in the solution it is likely to precipitate, disturbing the pH of the solution and inactivating the enzyme. Magnesium is also likely to react with hydroxide in the solution and form magnesium hydroxide ($\text{Mg}(\text{OH})_2$) with a solubility of 0.0012 g/100 g of water [100]. Magnesium hydroxide is more soluble than cobalt giving that higher concentration of magnesium can be added before precipitation. A possible sign of precipitation could be the weak decline in activity at 7 mM of magnesium, but this could also be an effect of unspecific binding of magnesium to the protein. There is no other reports of titration studies for other characterized NeuB1 enzymes, but rather investigation of the effect of single concentration additions of metals. For *A. salmonicida* NeuB1 5 mM of the same metals were used and manganese gave the highest activity followed by cobalt and magnesium [88]. For *N.meningitides* 1 mM of metals were used where cobalt gave the highest activity followed by manganese and magnesium [101] Similiar results were reported for *S.agalactiae* for 1 mM metal added [102]. The identity of the metal used in the native protein is not known, but manganese is used in assays probably because it does not react with hydroxide.

7.3.4 Stability of NeuB1

It was originally planned to use Differential Scanning Calorimetry (DSC) to determine the melting point and stability of NeuB1. This was performed with several buffers with glycerol and manganese as additives to increase stability as the protein precipitated in the cell, but no signal was observed. The pressure and the cell itself were tested to see if it caused the precipitation but nothing was observed. In order to investigate protein stability at different temperatures, the protein was incubated at 25°C, 37°C and 45°C to see how activity was affected over time, figure 6.22. The protein is most stable temperature at 25°C with 70% residual activity after 2 hours, while for 37°C the residual activity is 20% after one hour. At 45°C the residual activity was down to 5% after 30 minutes. *M. viscosa* NeuB1 has 50% residual activity after 15 minutes at 37°C, and comparing this to *N. meningitides* NeuB1, where the residual activity was still 100% after incubation at 40°C, this shows that *M.viscosa* NeuB1 is probably more thermolabile than the *N. meningitides* NeuB1.

7.5 NeuB1 Kinetics

The kinetic assays of NeuB1 to determine the K_m and k_{cat} for PEP and ManNAc were performed using the PNP coupled assay. Other reported kinetic studies of NeuB1 homologues have been performed at 37°C. For *M. viscosa* NeuB1 it was, however performed at 25°C because of the instability of the enzyme at 37°C. Since kinetic data are collected over time the enzyme need to be stable and not lose activity as it is performed since this would influence the kinetic results. The optimal situation would be to perform the kinetics at an even lower temperature to ensure continuous stability but the activity of the coupled enzyme PNP needed to be taken into account so 25°C was used. The PNP was initially tested at both temperatures to test if the activity was influenced, but it was confirmed that it was not, figure 6.23. The results from the kinetics assays are shown in figure 6.24 and 6.25 for ManNAc and PEP respectively. The K_m value for ManNAc was determined to be 18.1254 ± 5.2537 mM and the k_{cat} was 222.997 min^{-1} . For PEP the K_m value was 0.7646 ± 0.1674 mM and the k_{cat} 225.438 min^{-1} . There are reported kinetic values for *N.meningitides* and *C. jejuni* NeuB1 versions with the use of different assays at 37°C, where K_m for ManNAc is 9.4 mM and for PEP is 0.25 mM and a k_{cat} of 0.9 s^{-1} for *N.meningitides* NeuB1 [47] and K_m of 17.6 mM for ManNAc, 7.4 mM for PEP and k_{cat} 19.9 min^{-1} for ManNAc and 19.0 min^{-1} for PEP [103] In order to compare with other NeuB1 it would be optimal to perform the kinetic assays under the same conditions and temperature to ensure comparability.

7.7 Is NeuB1 Cold Adapted?

The bacterium *M. viscosa* is a fish pathogen that causes winter ulcer in salmon during cold periods. The bacterium is psychrophilic meaning that its optimal metabolism state is at low temperatures. Taking into account that sialic acids may be involved in virulence mechanism of the bacteria it is not unreasonable to think that the enzymes responsible for their biosynthesis are cold. The *M. viscosa* NeuB1 has been characterized with regards to optimum temperature, stability and kinetics. There is clearly a shift in the temperature optimum that allows the enzyme to work at lower temperatures, and the stability is lower at higher temperatures than to the compared NeuB1. The kinetic values are not directly comparable but they could indicate that the enzyme has a higher kinetic activity at lower temperatures. To help confirm the hypothesis DSC was tried performed in order to determine the enthalpy so it could be compared to see if the value was lower than for other known NeuB1. Structural determination of NeuB1 would be useful to investigate interactions in the structure that can make the enzyme cold adapted.

7.8 Crystallization

The crystallizations of NeuB1 were performed using the NeuB1 CHis version and conditions that gave needle formation was found. The conditions were tried optimized in order to give bigger crystals that could be used in structure determination, but this has not succeeded yet. A possible solution that could help is to try to crystallize without the His-tag as it could introduce a flexible area in the structure that makes crystal formation difficult. Assuming the protein stacks in the crystal with the tag out to the sides, the growth would be one dimensional and could explain the needles that are formed.

7.9 Sialic acid MS

By analysing the expression of sialic acids in *M. viscosa* using HPLC-MSMS it was found that the bacteria expresses Neu5Ac, Neu5,7Ac₂ and what is possibly Pseudaminic acid Pse5,7Ac₂. Pse5,7Ac₂ will have exactly the same mass as Legionaminic acid (Leg5,7Ac₂) another sialic acid, but genes for flagellar expression is found in close vicinity to the genes for pseudaminic acid biosynthesis. Pseudaminic acid is used for glycosylation of flagellas in other bacteria, and therefore it is assumed that the mass of 451.0 corresponds to Pse5,7Ac₂. The bacteria that expressed the highest amounts of all these sialic acids were grown on a blood agar plate followed by LB media. Since the bacteria was grown on blood agar the sample could be contaminated with Sia from the blood, but similar bacterial amounts originally scraped from blood agar plate for BA and BALB samples, gave much higher amounts of Neu5Ac in the BALB sample. The possible Pse5,7Ac₂ found, cannot be a contamination from blood, as this is a sialic acid found only in bacteria. The signal from Neu5Ac was higher than for Neu5,7Ac₂. Expression of the genes for neuraminic acid synthesis in *M. viscosa* is resulting in the monoacetylated Neu5Ac. The production of diacetylated neuraminic acid, Neu5,7Ac₂, might be a result of acetylation of the produced Neu5Ac by the acetyltransferase found in the pathway. In *A. salmonicida*, an acetyltransferase called NeuD1, is thought to be involved in the first step of Neu biosynthesis, resulting in the diacetylated Neu5,7Ac₂ [88]. The acetyltransferase found in *M. viscosa* is not very similar to the acetyltransferase NeuD1 from *A. salmonicida*, in addition it lacks a nucleotidyl binding area found in the other, so it will not be able to act on the substrates for the first step in the pathway (UDP-*N*-acetylglucosamine). The production of diacetylated Neu is therefore suspected to occur using produced Neu5Ac as substrate

8. Conclusion

The *neuB1* gene coding for neuraminic acid synthase in *Moritella viscosa* was successfully cloned into two constructs NHis and CHis which coded for a TEV cleavable His-tag and a non-cleavable His-tag. The constructs were successfully expressed in two different expression strains and purified based on affinity chromatography. The activity was tested with the TBA assay and both NHis and CHis were found to be active. Both were expressed and purified in large scale and a purification table was made to analyse the process. The NHis construct was found to precipitate during purification preparations and only a low amount of the protein was obtained. CHis was found to give high amounts of protein. The NeuB1 enzyme was characterized in regards to pH, temperature, metals and stability. It was found that the optimum pH was 8.0. The optimum temperature was 30°C and cobalt was found to bind strongly at low concentrations. The stability of NeuB1 was assayed at the three temperatures 25°C, 37°C and 45°C and it was found the residual activity after 2 hours, 1 hour and 30 minutes was 70, 20 and 5% respectively. K_m and k_{cat} was found for ManNAc and PEP. K_m was 18.1254 ± 5.2537 and k_{cat} was 222.997 for ManNAc and K_m was 0.7646 ± 0.1674 and k_{cat} was 225.438 for PEP. Crystallization conditions were found for NeuB1 to be PEG 3350 and sodium citrate, no crystals were obtained. Using HPLC-MSMS to detect sialic acids in *Moritella viscosa* gave positive results for several compounds.

9. Future work

The next logical step with the work on neuraminic acid synthase is the crystallization and optimization in order to get good enough crystals to determine the structure. The conditions have been found but trials with cleaved His-tag should be performed in order to see if that improves the conditions. Experiments with DSC was also performed in order to determine the melting temperature of the protein. This was not successful yet, but with screening around buffer conditions and setting could help. It was seen that *Moritella viscosa* produce sialic acids, so doing functional studies with knock out genes would be a logical next step.

11. Litterature

1. Nelson, D.L., M.M. Cox, and A.L.P.o.b. Lehninger, *Lehninger principles of biochemistry*. 5th ed. ed. 2008, New York ; Basingstoke: W.H. Freeman.
2. Landsteiner, K. and P. Levine, *On a Specific Substance of the Cholera Vibrio*. *J Exp Med*, 1927. 46(2): p. 213-21.
3. Faillard, H., *The early history of sialic acids*. *Trends Biochem Sci*, 1989. 14(6): p. 237-41.
4. Angata, T. and A. Varki, *Chemical diversity in the sialic acids and related alpha-keto acids: an evolutionary perspective*. *Chem Rev*, 2002. 102(2): p. 439-69.
5. Varki, A. and R. Schauer, *Sialic Acids*, in *Essentials of Glycobiology*, A. Varki, et al., Editors. 2009: Cold Spring Harbor (NY).
6. Schauer, R., *Sialic acids: fascinating sugars in higher animals and man*. *Zoology*, 2004. 107(1): p. 49-64.
7. Kelm, S. and R. Schauer, *Sialic acids in molecular and cellular interactions*. *Int Rev Cytol*, 1997. 175: p. 137-240.
8. van Seeventer, P.B., et al., *Synthesis of two analogues of the Sda determinant. Replacement of the sialic acid residue by a sulfate or a carboxymethyl group*. *Carbohydr Res*, 1997. 299(3): p. 171-9.
9. Muller, E., et al., *Binding and phagocytosis of sialidase-treated rat erythrocytes by a mechanism independent of opsonins*. *Hoppe Seylers Z Physiol Chem*, 1983. 364(10): p. 1419-29.
10. Probstmeier, R., A. Bilz, and J. Schneider-Schaulies, *Expression of the neural cell adhesion molecule and polysialic acid during early mouse embryogenesis*. *J Neurosci Res*, 1994. 37(3): p. 324-35.
11. Stasche, R., et al., *A bifunctional enzyme catalyzes the first two steps in N-acetylneuraminic acid biosynthesis of rat liver. Molecular cloning and functional expression of UDP-N-acetyl-glucosamine 2-epimerase/N-acetylmannosamine kinase*. *J Biol Chem*, 1997. 272(39): p. 24319-24.
12. Wang, B., et al., *Dietary sialic acid supplementation improves learning and memory in piglets*. *Am J Clin Nutr*, 2007. 85(2): p. 561-9.
13. Nakata, D. and F.A. Troy, 2nd, *Degree of polymerization (DP) of polysialic acid (polySia) on neural cell adhesion molecules (N-CAMS): development and application of a new strategy to accurately determine the DP of polySia chains on N-CAMS*. *J Biol Chem*, 2005. 280(46): p. 38305-16.
14. Kiss, J.Z. and G. Rougon, *Cell biology of polysialic acid*. *Curr Opin Neurobiol*, 1997. 7(5): p. 640-6.
15. Rutishauser, U., *Polysialic acid at the cell surface: biophysics in service of cell interactions and tissue plasticity*. *J Cell Biochem*, 1998. 70(3): p. 304-12.
16. El Maarouf, A., A.K. Petridis, and U. Rutishauser, *Use of polysialic acid in repair of the central nervous system*. *Proc Natl Acad Sci U S A*, 2006. 103(45): p. 16989-94.
17. Dityatev, A., G. Dityateva, and M. Schachner, *Synaptic strength as a function of post- versus presynaptic expression of the neural cell adhesion molecule NCAM*. *Neuron*, 2000. 26(1): p. 207-17.
18. Angata, K. and M. Fukuda, *Polysialyltransferases: major players in polysialic acid synthesis on the neural cell adhesion molecule*. *Biochimie*, 2003. 85(1-2): p. 195-206.
19. Cremer, H., et al., *Inactivation of the N-CAM gene in mice results in size reduction of the olfactory bulb and deficits in spatial learning*. *Nature*, 1994. 367(6462): p. 455-9.
20. Savaki, H.E. and G.M. Levis, *Changes in rat brain gangliosides following active avoidance conditioning*. *Pharmacol Biochem Behav*, 1977. 7(1): p. 7-12.
21. Gottschalk, A., *Glycoproteins. Their composition, structure and function*. Rev. and expanded 2d. ed. B B A library,. 1972, Amsterdam, New York,: Elsevier Pub. Co.
22. Hirst, G.K., *Adsorption of Influenza Hemagglutinins and Virus by Red Blood Cells*. *J Exp Med*, 1942. 76(2): p. 195-209.
23. von Itzstein, M., W.Y. Wu, and B. Jin, *The synthesis of 2,3-didehydro-2,4-dideoxy-4-guanidiny-N-acetylneuraminic acid: a potent influenza virus sialidase inhibitor*. *Carbohydr Res*, 1994. 259(2): p. 301-5.
24. Prinz, C., et al., *Key importance of the Helicobacter pylori adherence factor blood group antigen binding adhesin during chronic gastric inflammation*. *Cancer Res*, 2001. 61(5): p. 1903-9.
25. Urashima, T., et al., *Oligosaccharides of milk and colostrum in non-human mammals*. *Glycoconj J*, 2001. 18(5): p. 357-71.
26. Vimr, E.R., et al., *Diversity of microbial sialic acid metabolism*. *Microbiol Mol Biol Rev*, 2004. 68(1): p. 132-53.
27. Corfield, T., *Bacterial sialidases--roles in pathogenicity and nutrition*. *Glycobiology*, 1992. 2(6): p. 509-21.
28. Bouchet, V., et al., *Host-derived sialic acid is incorporated into Haemophilus influenzae lipopolysaccharide and is a major virulence factor in experimental otitis media*. *Proc Natl Acad Sci U S A*, 2003. 100(15): p. 8898-903.
29. Shakhnovich, E.A., S.J. King, and J.N. Weiser, *Neuraminidase expressed by Streptococcus pneumoniae desialylates the lipopolysaccharide of Neisseria meningitidis and Haemophilus influenzae: a paradigm for interbacterial competition among pathogens of the human respiratory tract*. *Infect Immun*, 2002. 70(12): p. 7161-4.
30. Sohanpal, B.K., et al., *Integrated regulatory responses of fimB to N-acetylneuraminic (sialic) acid and GlcNAc in Escherichia coli K-12*. *Proc Natl Acad Sci U S A*, 2004. 101(46): p. 16322-7.

31. Sohanpal, B.K., et al., *Multiple co-regulatory elements and IHF are necessary for the control of fimB expression in response to sialic acid and N-acetylglucosamine in Escherichia coli K-12*. Mol Microbiol, 2007. 63(4): p. 1223-36.
32. Steenbergen, S.M., et al., *Separate pathways for O acetylation of polymeric and monomeric sialic acids and identification of sialyl O-acetyl esterase in Escherichia coli K1*. J Bacteriol, 2006. 188(17): p. 6195-206.
33. Vimr, E. and C. Lichtensteiger, *To sialylate, or not to sialylate: that is the question*. Trends Microbiol, 2002. 10(6): p. 254-7.
34. Roseman, S., et al., *Enzymatic Synthesis of Sialic Acid 9-Phosphates*. Proceedings of the National Academy of Sciences of the United States of America, 1961. 47(7): p. 958-&.
35. Ghosh, S. and S. Roseman, *Enzymatic Phosphorylation of N-Acetyl-D-Mannosamine*. Proceedings of the National Academy of Sciences of the United States of America, 1961. 47(7): p. 955-&.
36. Warren, L. and H. Felsenfeld, *The biosynthesis of sialic acids*. J Biol Chem, 1962. 237: p. 1421-31.
37. Warren, L. and H. Felsenfeld, *N-Acetylmannosamine-6-Phosphate and N-Acetylneuraminic Acid-9-Phosphate as Intermediates in Sialic Acid Biosynthesis*. Biochemical and Biophysical Research Communications, 1961. 5(3): p. 185-&.
38. Chou, W.K., et al., *Sialic acid biosynthesis: stereochemistry and mechanism of the reaction catalyzed by the mammalian UDP-N-acetylglucosamine 2-epimerase*. J Am Chem Soc, 2003. 125(9): p. 2455-61.
39. Hinderlich, S., et al., *A bifunctional enzyme catalyzes the first two steps in N-acetylneuraminic acid biosynthesis of rat liver. Purification and characterization of UDP-N-acetylglucosamine 2-epimerase/N-acetylmannosamine kinase*. J Biol Chem, 1997. 272(39): p. 24313-8.
40. Tanner, M.E., *Understanding nature's strategies for enzyme-catalyzed racemization and epimerization*. Acc Chem Res, 2002. 35(4): p. 237-46.
41. Campbell, R.E., et al., *The structure of UDP-N-acetylglucosamine 2-epimerase reveals homology to phosphoglycosyl transferases*. Biochemistry, 2000. 39(49): p. 14993-5001.
42. Lawrence, S.M., et al., *Cloning and expression of human genes involved in sialic acid metabolism*. Glycobiology, 2000. 10(10): p. 1116-1116.
43. Roggentin, P., et al., *The sialidase superfamily and its spread by horizontal gene transfer*. Mol Microbiol, 1993. 9(5): p. 915-21.
44. Traving, C. and R. Schauer, *Structure, function and metabolism of sialic acids*. Cell Mol Life Sci, 1998. 54(12): p. 1330-49.
45. Seeholzer, S.H., A. Jaworowski, and I.A. Rose, *Enolpyruvate: chemical determination as a pyruvate kinase intermediate*. Biochemistry, 1991. 30(3): p. 727-32.
46. Matte, A., et al., *Structure and mechanism of phosphoenolpyruvate carboxykinase*. J Biol Chem, 1997. 272(13): p. 8105-8.
47. Gunawan, J., et al., *Structural and mechanistic analysis of sialic acid synthase NeuB from Neisseria meningitidis in complex with Mn²⁺, phosphoenolpyruvate, and N-acetylmannosaminitol*. J Biol Chem, 2005. 280(5): p. 3555-63.
48. Margesin, R. and F. Schinner, *Biodegradation of diesel oil by cold-adapted microorganisms in presence of sodium dodecyl sulfate*. Chemosphere, 1999. 38(15): p. 3463-72.
49. Crawford, D.L. and D.A. Powers, *Evolutionary adaptation to different thermal environments via transcriptional regulation*. Mol Biol Evol, 1992. 9(5): p. 806-13.
50. Baldwin, J. and P.W. Hochachka, *Functional significance of isoenzymes in thermal acclimatization. Acetylcholinesterase from trout brain*. Biochem J, 1970. 116(5): p. 883-7.
51. Georlette, D., et al., *Some like it cold: biocatalysis at low temperatures*. FEMS Microbiol Rev, 2004. 28(1): p. 25-42.
52. Low, P.S., J.L. Bada, and G.N. Somero, *Temperature adaptation of enzymes: roles of the free energy, the enthalpy, and the entropy of activation*. Proc Natl Acad Sci U S A, 1973. 70(2): p. 430-2.
53. Lonhienne, T., C. Gerday, and G. Feller, *Psychrophilic enzymes: revisiting the thermodynamic parameters of activation may explain local flexibility*. Biochim Biophys Acta, 2000. 1543(1): p. 1-10.
54. Eyring, H. and A.E. Stearn, *The application of the theory of absolute reaction rates to proteins*. Chemical Reviews, 1939. 24(2): p. 253-270.
55. Siddiqui, K.S., R. Cavicchioli, and T. Thomas, *Thermodynamic activation properties of elongation factor 2 (EF-2) proteins from psychrotolerant and thermophilic Archaea*. Extremophiles, 2002. 6(2): p. 143-50.
56. Feller, G., *Molecular adaptations to cold in psychrophilic enzymes*. Cell Mol Life Sci, 2003. 60(4): p. 648-62.
57. Siddiqui, K.S. and R. Cavicchioli, *Cold-adapted enzymes*. Annu Rev Biochem, 2006. 75: p. 403-33.
58. Fields, P.A. and G.N. Somero, *Hot spots in cold adaptation: localized increases in conformational flexibility in lactate dehydrogenase A4 orthologs of Antarctic notothenioid fishes*. Proc Natl Acad Sci U S A, 1998. 95(19): p. 11476-81.
59. D'Amico, S., C. Gerday, and G. Feller, *Structural similarities and evolutionary relationships in chloride-dependent alpha-amylases*. Gene, 2000. 253(1): p. 95-105.
60. Smalas, A.O., et al., *Cold adapted enzymes*. Biotechnol Annu Rev, 2000. 6: p. 1-57.
61. Privalov, P.L. and S.J. Gill, *Stability of protein structure and hydrophobic interaction*. Adv Protein Chem, 1988. 39: p. 191-234.

62. Makhatadze, G.I. and P.L. Privalov, *Hydration effects in protein unfolding*. Biophys Chem, 1994. 51(2-3): p. 291-304; discussion 304-9.
63. Kumar, S., C.J. Tsai, and R. Nussinov, *Maximal stabilities of reversible two-state proteins*. Biochemistry, 2002. 41(17): p. 5359-74.
64. Kumar, S. and R. Nussinov, *Close-range electrostatic interactions in proteins*. Chembiochem, 2002. 3(7): p. 604-17.
65. Tsai, C.J., J.V. Maizel, Jr., and R. Nussinov, *The hydrophobic effect: a new insight from cold denaturation and a two-state water structure*. Crit Rev Biochem Mol Biol, 2002. 37(2): p. 55-69.
66. Leiros, H.K.S., N.P. Willassen, and A.O. Smalas, *Residue determinants and sequence analysis of cold-adapted trypsins*. Extremophiles, 1999. 3(3): p. 205-219.
67. Kumar, S. and R. Nussinov, *Different roles of electrostatics in heat and in cold: Adaptation by citrate synthase*. Chembiochem, 2004. 5(3): p. 280-290.
68. Lunder, T., et al., *Winter Ulcer in the Atlantic Salmon Salmo-Salar - Pathological and Bacteriological Investigations and Transmission Experiments*. Diseases of Aquatic Organisms, 1995. 23(1): p. 39-49.
69. Greger, E. and T. Goodrich, *Vaccine development for winter ulcer disease, Vibrio viscosus, in Atlantic salmon, Salmo salar L*. Journal of Fish Diseases, 1999. 22(3): p. 193-199.
70. Benediktsdottir, E., et al., *Characterization of Vibrio viscosus and Vibrio wodanis isolated at different geographical locations: a proposal for reclassification of Vibrio viscosus as Moritella viscosa comb. nov.* International Journal of Systematic and Evolutionary Microbiology, 2000. 50: p. 479-488.
71. Smith, P.A., et al., *Routes of entry of Piscirickettsia salmonis in rainbow trout Oncorhynchus mykiss*. Diseases of Aquatic Organisms, 1999. 37(3): p. 165-172.
72. Ringo, E., et al., *Damaging effect of the fish pathogen Aeromonas salmonicida ssp salmonicida on intestinal enterocytes of Atlantic salmon (Salmo salar L.)*. Cell and Tissue Research, 2004. 318(2): p. 305-312.
73. Ringo, E., et al., *Bacterial translocation and pathogenesis in the digestive tract of larvae and fry*. Aquaculture, 2007. 268(1-4): p. 251-264.
74. Ling, S.H., et al., *Green fluorescent protein-tagged Edwardsiella tarda reveals portal of entry in fish*. FEMS Microbiol Lett, 2001. 194(2): p. 239-43.
75. Coyne, R., et al., *Attempt to validate breakpoint MIC values estimated from pharmacokinetic data obtained during oxolinic acid therapy of winter ulcer disease in Atlantic salmon (Salmo salar)*. Aquaculture, 2004. 238(1-4): p. 51-66.
76. Coyne, R., et al., *Winter ulcer disease of post-smolt Atlantic salmon: An unsuitable case for treatment?* Aquaculture, 2006. 253(1-4): p. 171-178.
77. Bjellqvist, B., et al., *The focusing positions of polypeptides in immobilized pH gradients can be predicted from their amino acid sequences*. Electrophoresis, 1993. 14(10): p. 1023-31.
78. Bjellqvist, B., et al., *Reference points for comparisons of two-dimensional maps of proteins from different human cell types defined in a pH scale where isoelectric points correlate with polypeptide compositions*. Electrophoresis, 1994. 15(3-4): p. 529-39.
79. Notredame, C., D.G. Higgins, and J. Heringa, *T-Coffee: A novel method for fast and accurate multiple sequence alignment*. J Mol Biol, 2000. 302(1): p. 205-17.
80. Jones, D.T., *Protein secondary structure prediction based on position-specific scoring matrices*. J Mol Biol, 1999. 292(2): p. 195-202.
81. Guex, N. and M.C. Peitsch, *SWISS-MODEL and the Swiss-PdbViewer: an environment for comparative protein modeling*. Electrophoresis, 1997. 18(15): p. 2714-23.
82. Schwede, T., et al., *SWISS-MODEL: An automated protein homology-modeling server*. Nucleic Acids Res, 2003. 31(13): p. 3381-5.
83. Kiefer, F., et al., *The SWISS-MODEL Repository and associated resources*. Nucleic Acids Res, 2009. 37(Database issue): p. D387-92.
84. Schrödinger, L., *The AxPyMol Molecular Graphics for PowerPoint, Version 1.1*, 2010: Unpublished.
85. Schrödinger, L., *The JyMOL Molecular Graphics System, Version 1.0*, 2010: Unpublished.
86. Schrödinger, L., *The PyMOL Molecular Graphics System, Version 1.5.0.4*
2010: Unpublished.
87. Gopalakrishnan, K., et al., *Ramachandran plot on the web (2.0)*. Protein Pept Lett, 2007. 14(7): p. 669-71.
88. Gurung, M.K., et al., *Characterization of the sialic acid synthase from Aliivibrio salmonicida suggests a novel pathway for bacterial synthesis of 7-O-acetylated sialic acids*. Glycobiology, 2013.
89. Mullis, K., et al., *Specific enzymatic amplification of DNA in vitro: the polymerase chain reaction*. Cold Spring Harb Symp Quant Biol, 1986. 51 Pt 1: p. 263-73.
90. Kleppe, K., et al., *Studies on polynucleotides. XCVI. Repair replications of short synthetic DNA's as catalyzed by DNA polymerases*. J Mol Biol, 1971. 56(2): p. 341-61.
91. Chien, A., D.B. Edgar, and J.M. Trela, *Deoxyribonucleic acid polymerase from the extreme thermophile Thermus aquaticus*. J Bacteriol, 1976. 127(3): p. 1550-7.
92. Saiki, R.K., et al., *Primer-directed enzymatic amplification of DNA with a thermostable DNA polymerase*. Science, 1988. 239(4839): p. 487-91.

93. Esposito, D., L.A. Garvey, and C.S. Chakiath, *Gateway cloning for protein expression*. Methods Mol Biol, 2009. 498: p. 31-54.
94. Romero, E.L., et al., *Sialic acid measurement by a modified Aminoff method: a time-saving reduction in 2-thiobarbituric acid concentration*. J Biochem Biophys Methods, 1997. 35(2): p. 129-34.
95. Warren, L., *The thiobarbituric acid assay of sialic acids*. J Biol Chem, 1959. 234(8): p. 1971-5.
96. Aminoff, D., *Methods for the quantitative estimation of N-acetylneuraminic acid and their application to hydrolysates of sialomucoids*. Biochem J, 1961. 81: p. 384-92.
97. Paerels, G.B. and J. Schut, *The mechanism of the periodate-thiobarbituric acid reaction of sialic acids*. Biochem J, 1965. 96(3): p. 787-92.
98. Klein, A., et al., *New sialic acids from biological sources identified by a comprehensive and sensitive approach: liquid chromatography-electrospray ionization-mass spectrometry (LC-ESI-MS) of SIA quinoxalinones*. Glycobiology, 1997. 7(3): p. 421-32.
99. Vann, W.F., et al., *Purification and characterization of the Escherichia coli K1 neuB gene product N-acetylneuraminic acid synthetase*. Glycobiology, 1997. 7(5): p. 697-701.
100. Aylward, G.H. and T.J.V. Findlay, *SI chemical data*. 5th ed. ed. 2002, Milton, Qld. ; [Chichester]: Wiley.
101. Hao, J., et al., *Cloning, expression, and characterization of sialic acid synthases*. Biochemical and biophysical research communications, 2005. 338(3): p. 1507-14.
102. Suryanti, V., A. Nelson, and A. Berry, *Cloning, over-expression, purification, and characterisation of N-acetylneuraminic acid synthase from Streptococcus agalactiae*. Protein Expr Purif, 2003. 27(2): p. 346-56.
103. Sundaram, A.K., et al., *Characterization of N-acetylneuraminic acid synthase isoenzyme 1 from Campylobacter jejuni*. Biochem J, 2004. 383(Pt 1): p. 83-9.

Appendix I

Moritella viscosa NeuB1 DNA sequence

ATGACTAATCCGGTATTTGAAATCTCAGGCCGTAAAGTAGGCTTAGACTATGCCC
CTCTTGTTATTGCTGAAATTGGTATTAACCATGAAGGATCTTTAAAAACAGCATTT
GAAATGGTTGATGCTGCAATTGAAGGTGGTGCAGAGATAATTAAACATCAAATC
ATGTTATTGAAGATGAGATGAGTAGTGAAGCTAAAAAAGTTATCCCAGGTAATGC
AGATGTATCAATTTATGAAATCATGGATCGTTGTTCTTTAAATGAAGAAGATGAA
ATAAAATTAAGAAATATATCGAATCTAAAGGTGCTATTTTTATTAGTACGCCAT
TTTCAAGAGCCGCTGCTTTACGTTTAGAAAGAATGGGTGTATCAGCTTATAAAAT
TGGTTCAGGTGAATGTAATAACTATCCGTTATTAGATCTAATTGCGAGTTACGGT
AAACCTGTAATTTTAAGCACTGGTATGAATGATATCCCTTCTATCAGAAAATCAG
TTGAAATATTCAGAAAGTATAAGACACCTCTTTGTTTATTACATACGACAAATTTG
TACCCAACACCAGACCATTTAATTCGCATTGGTGCTATGGAAGAAATGCAACGTG
AATTTTCAGATGTAGTTGTTGGTTTATCAGATCATAGTATTGATAATTTAGCCTGT
CTAGGTGCTGTAGCAGCTGGTGCGTCAGTGTTAGAACGTCATTTTACAGATAATA
AAGCTCGCTCTGGTCCTGATATTTGTTGTTCAATGGATGGTGCTGAATGTGCTGAG
TTAATCTCACAATCAAACGCATGGCACAAATGCGTGGTGGTTCAAAGGGAGCTG
TTAAAGAAGAGCAAGTTACAATTGATTTTCGCTTATGCAAGCGTTGTGACAATTA
AGAAATCAAAGCCGGTGAGGCATTTACGAAAGATAACCTTTGGGTAAAACGTCC
CGGTACGGGTGACTTTTTAGCGGATGATTATGAAATGCTATTAGGTAAAAAAGCG
AGTCAAAATATCGACTTTGATGTGCAGCTTAAAAAAGAGTTTATAAAATAA

Moritella viscosa NeuB1 protein sequence

MTNPVFEISGRKVGLDYAPLVIAEIGINHEGSLKTAFEMVDAAIEGGAIEIKHQTHVIE
DEMSSEAKKVIPGNADVSIYEIMDRCSLNEEDEIKLKKYIESKGAIFISTPFSRAAALRL
ERMGVSAAYKIGSGECNNYPLLDLIASYGKPVILSTGMNDIPSIRKSVEIFRKYKTPLCL
LHTTNLYPTPDHLIRIGAMEEMQREFSDVVVGLSDHSIDNLA CLGAVAAGASVLERH
FTDNKARSGPDICCSMDGAECAELISQSKRMAQMRGGSKGAVKEEQVTIDFAYASV
VTIKEIKAGEAFTKDNLWVKRPGTGDFLADDDYEMLLGKKASQNIDFDVQLKKEFIK

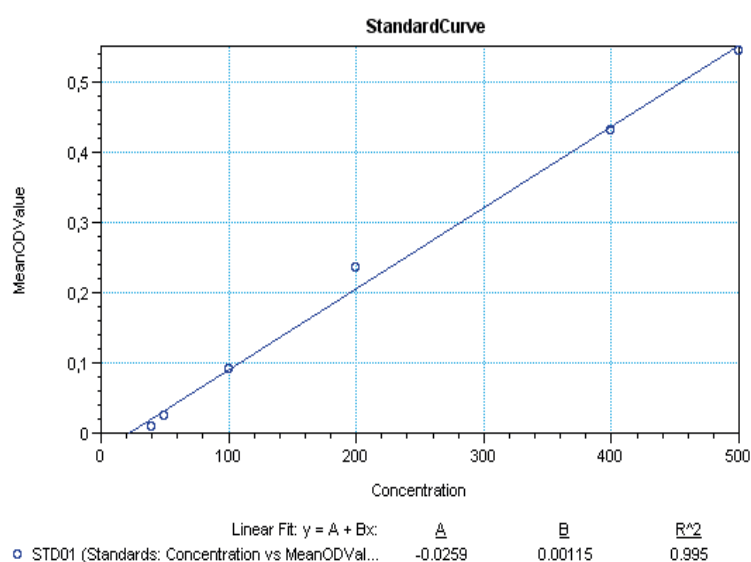
Appendix II

Raw data NeuB1 NHis Purification table

Measured absorbance from TBA assay and the corrected values. Total activity is gotten by dividing the measured absorbance on the volume used in the assay 25 μ L

Sample	Parallells (OD)			Mean value	Corrected for blank	Acitivity (U/mL)
	1	2	3			
Blank	0,114	0,114	0,119	0,116		
Lysate	1,282	1,338	1,237	1,286	1,170	46,80
1st HisTrap	0,163	0,165	0,147	0,158	0,043	1,707
2nd HisTrap	0,142	0,151	0,143	0,145	0,030	1,187
Superdex 200 26/600	0,402	0,377	0,389	0,389	0,274	10,95

The Bradford Standard Curve is shown for determination of protein concentrations



The raw values for the purification table, the determined protein concentration and measured volume for each purification

Sample	Concentration (mg/mL)	Volume (mL)
Lysate	8,069	66,5
1st HisTrap	0,341	20
2nd HisTrap	0,047	20,5
Superdex 200 26/600	0,116	1,7

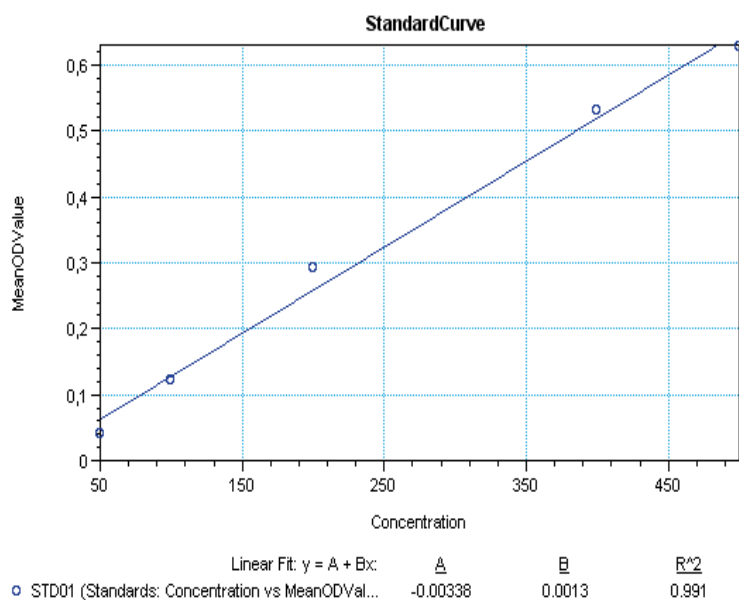
Raw data NeuB1 CHis Purification table

Measured absorbance from TBA assay and the corrected values. Total activity is gotten by dividing the measured absorbance on the volume used in the assay 25 µL

Samples	Parallels				Dilution Factor 4		
	1	2	3	Blank	1	2	3
Lysate	3,216	3,153	3,217	0,114	0,78	0,772	0,782
HisTrap	2,505	2,655	2,074	0,125	0,558	0,624	0,602
Superdex 200 26/600	0,624	0,686	0,658	0,131			
				0,123			

Corrected DF			Corrected Blank			Average	Actvitiy (U/mL)
1	2	3	1	2	3		
3,12	3,088	3,128	2,997	2,965	3,005	2,989	150,23
2,232	2,496	2,408	2,109	2,373	2,285	2,329	114,23
			0,501	0,563	0,535	0,533	26,73

The Bradford Standard Curve is shown for determination of protein concentrations



The raw values for the purification table, the determined protein concentration and measured volume for each purification

Sample	Protein Concentration (mg/mL)	Volume (mL)
Lysate	11,499	34,5
HisTrap	2,831	19
Superdex 200 26/600	0,406	83

Appendix III

Raw data pH optimum

Raw Data for pH Optimum for NeuB1 (5 µg, RT)

pH	Absorbance Parallels				Samples measured with Dilution Factor 4			Samples measured with Dilution Factor 10			Corrected (Df)			Corrected Blank		
	1	2	3	B	1	2	3	1	2	3	1	2	3	1	2	3
5,8	0,164	0,146	0,133	0,162							0,164	0,146	0,133	0,002	-0,016	-0,029
6,4	0,168	0,143	0,181	0,166							0,168	0,143	0,181	0,002	0,023	0,015
6,8	3,319	3,486	3,323	0,153	0,899	1,211	0,961	0,37	0,487	0,377	3,700	4,870	3,770	3,547	4,717	3,617
7,3	3,495	3,522	3,516	0,151	1,452	1,544	1,626	0,552	0,591	0,377	5,520	5,910	3,770	5,369	5,759	3,619
7,8	3,47	3,481	3,485	0,138	1,369	1,364	1,426	0,5	0,513	0,534	5,000	5,130	5,340	4,862	4,992	5,202
7,8	3,485	3,52	3,509	0,148	1,325	1,341	1,277	0,505	0,493	0,491	5,050	4,930	4,910	4,902	4,782	4,762
8,4	3,453	3,469	3,453	0,157	1,138	1,241	1,177	0,44	0,436	0,427	4,400	4,360	4,270	4,243	4,203	4,113
8,8	3,286	3,377	3,354	0,147	0,901	0,969	0,941				3,604	3,876	3,764	3,457	3,729	3,617
9,4	3,208	3,127	3,014	0,141	0,837	0,831	0,711				3,348	3,324	2,844	3,207	3,183	2,703
9,9	2,899	2,751	2,594	0,162	0,727	0,699	0,612				2,908	2,796	2,448	2,746	2,634	2,286

Appendix IV

Raw data Temperature optimum

Raw Data NeuB1 Temperature Optimum (5 µg, pH 8)													
Temperature C	Absorbance Parallels				Samples measured with a Dilution factor 10			Df Corrected			Blank Corrected		
	1	2	3	Blank	1	2	3	1	2	3	1	2	3
5	0,779	0,771	0,811	0,085				0,779	0,771	0,811	0,694	0,686	0,726
15	2,111	1,925	1,602	0,009	0,193	0,191	0,153	1,903	1,901	1,503	1,804	1,802	1,404
25	3,124	3,023	3,105	0,094	0,327	0,312	0,335	3,207	3,102	3,305	3,1076	3,0026	3,2056
30	3,176	3,007	3,172	0,095	0,39	0,321	0,409	3,903	3,201	4,009	3,805	3,115	3,9095
32	3,084	3,044	3,038	0,105	0,392	0,385	0,355	3,902	3,805	3,505	3,815	3,745	3,445
34	2,979	2,903	2,949	0,098	0,372	0,31	0,367	3,702	3,103	3,607	3,622	3,002	3,5072
36	2,901	2,881	2,862	0,101	0,377	0,356	0,378	3,707	3,506	3,708	3,607	3,406	3,608
38	2,832	2,818	2,786	0,098	0,338	0,376	0,331	3,308	3,706	3,301	3,282	3,662	3,212
40	2,774	2,756	2,735	0,095	0,355	0,336	0,375	3,505	3,306	3,705	3,455	3,265	3,6055
45	2,205	1,873	2,082	0,092	0,213	0,174	0,212	2,103	1,704	2,102	2,038	1,648	2,028
55	0,066	0,092	0,092	0,096				0,066	0,092	0,092	0,003	0,004	0,004

Appendix V

Raw data Metal Titration

Metal Concentration (mM)	Absorbance for each Metal											
	Mn				Mg				Co			
	1	2	3	Blank	1	2	3	Blank	1	2	3	Blank
0,1	0,482	0,507	0,431	0,133	0,436	0,393	0,378	0,103	2,624	2,466	2,155	0,112
0,5	1,347	1,308	1,304	0,138	1,161	1,186	1,109	0,115	2,559	2,453	2,474	0,095
1	1,709	1,731	0,696	0,147	1,455	1,525	1,466	0,137	2,465	2,457	2,371	0,125
3	2,432	2,401	2,349	0,109	1,71	1,809	1,741	0,145	0,349	0,342	0,293	0,107
5	2,32	2,242	2,22	0,135	1,684	1,645	1,604	0,116	0,24	0,243	0,234	0,119
7	2,127	2,071	2,091	0,129	1,676	1,629	1,573	0,121	0,191	0,201	0,185	0,105

Metal Concentration (mM)	Samples measured with Dilution Factor 10								
	Mn			Mg			Co		
	1	2	3	1	2	3	1	2	3
0,1							0,254	0,215	0,183
0,5	0,145	0,142	0,149	0,131	0,133	0,133	0,203	0,202	0,202
1	0,175	0,108	0,168	0,152	0,155	0,161	0,223	0,201	0,213
3	0,257	0,258	0,257	0,202	0,211	0,195			
5	0,266	0,241	0,237	0,215	0,198	0,188			
7	0,221	0,241	0,246	0,203	0,206	0,205			

Corrected for Df								
Mn			Mg			Co		
1	2	3	1	2	3	1	2	3
0,482	0,5 07	0,4 31	0,4 36	0,3 93	0,3 78	2,5 4	2,1 5	1,8 3
1,45	1,4 2	1,4 9	1,3 1	1,3 3	1,3 3	2,3	2,0 2	2,2
1,75	1,8	1,6 8	1,5 2	1,5 5	1,6 1	2,2 3	2,1	2,1 3
2,57	2,5 8	2,5 7	2,1 2	2,1 1	1,9 5	0,3 49	0,3 42	0,2 93
2,66	2,4 1	2,3 7	2,1 5	1,9 8	1,8 8	0,2 4	0,2 43	0,2 34
2,21	2,4 1	2,4 6	2,0 3	2,0 6	2,0 5	0,1 91	0,2 01	0,1 85

Metal Concentration (mM)	Corrected for Blank								
	Mn			Mg			Co		
	1	2	3	1	2	3	1	2	3
0,1	0,4 82	0,5 07	0,4 31	0,3 06	0,2 63	0,2 48	2,4 28	2,0 38	1,7 18
0,5	1,4 50	1,4 20	1,4 90	1,1 95	1,2 15	1,2 15	2,2 05	1,9 25	2,1 05
1	1,7 50	1,8 00	1,6 80	1,3 83	1,4 13	1,4 73	2,1 05	1,9 75	2,0 05
3	2,5 70	2,5 80	2,5 70	1,8 55	1,9 65	1,8 05	0,2 42	0,2 35	0,1 86
5	2,6 60	2,4 10	2,3 70	2,0 34	1,8 64	1,7 64	0,1 21	0,1 24	0,1 15
7	2,2 10	2,4 10	2,4 60	1,9 09	1,9 39	1,9 29	0,0 86	0,0 96	0,0 8

Average Blank		
Mn	Mg	Co
1,8 75	1,6 33	0,1 11

Appendix VI

Raw data Stability assay

25°C

Zero	1	2	3
	1,14 2	1,14 2	1,17 2
Df 2	0,56 6	0,55 1	0,56 4
Corrected DF	1,13 2	1,10 2	1,12 8
Corrected Blank	1,01 6	0,98 6	1,01 2
Average Reference sample	1,005	0	100
Blank	0,11 9	0,11 6	0,11 2
Average Blank	0,116		

Time (min)	Absorbance for 25°C Parallels			Samples with Dilution Factor 2			Corrected DF			Corrected Blank			Relative Activity %		
	1	2	3	1	2	3	1	2	3	1	2	3	1	2	3
5	1,17 7	1,09 1	1,10 3	0,57 3	0,55 6	0,54 8	1, 14 6	1, 11 2	1, 09 6	1, 03 0	0, 99 6	0, 98 0	93 4	92 1	86 6
15	1,11 4	1,10 5	1,08 1	0,54 7	0,54 8	0,55 2	1, 09 4	1, 09 6	1, 10 4	0, 97 8	0, 98 0	0, 98 8	92 1	92 8	82 2
30	1,03 7	1,03 4	1,01 4	0,50 8	0,50 8	0,47 8	1, 01 6	1, 01 6	0, 95 6	0, 90 0	0, 90 0	0, 84 0	85 4	80 3	75 7
45	0,96 2	0,96 5	0,95 4							0, 84 6	0, 84 9	0, 83 8	0 0	0 0	71 1
60	0,91 6	0,86 4	0,94 4							0, 80 0	0, 74 8	0, 82 8	0 0	0 0	67 3
75	0,85 8	0,89 3	0,84 3							0, 74 2	0, 77 7	0, 72 7	0 0	0 0	62 4
90	0,86	0,85 8	0,85 2							0, 74 4	0, 74 2	0, 73 6	0 0	0 0	62 5
105	0,79	0,84 5	0,84 5							0, 67 4	0, 72 9	0, 72 9	0 0	0 0	56 7
120	0,83 2	0,77 4	0,76 9							0, 71 6	0, 65 8	0, 65 3	0 0	0 0	60 2

Appendix VII

Raw data ManNAc kinetics

Kinetic data for varying concentrations of ManNAc (Protein concentration 0,95 µg, T = 25 °C)

Parallel I	1			2			3			Blank			Corrected with Specific Blank			
	Concen- tration (mM)	Vmax (mOD /min)	R 2	Poi- nts	Vmax (mOD /min)	R 2	Poi- nts	Vmax (mOD /min)	R 2	Poi- nts	Vmax (mOD /min)	R 2	Poi- nts	Paral- lell	1	2
0,1	0,703	0,931	0-12	0,593	0,93	0-18	0,682	0,95	0-180	0,923	0,94	0-18	0,1	-	-	-
0,5	1,223	0,958	0-90	0,814	0,96	0-18	1,052	0,96	500-180	0,748	0,93	30-18	0,1	0,22	0,33	0,241
2	1,454	0,971	20-12	1,331	0,98	25-18	2,203	0,98	400-180	0,845	0,98	30-18	0,5	0,475	0,066	0,304
5	2,881	0,992	10-12	2,462	0,99	60-18	4,232	0,98	100-180	0,9	0,98	10-18	2	0,609	0,486	1,358
10	4,451	0,996	15-12	3,574	0,99	90-18	6,568	0,99	10-460	1,031	0,99	50-18	5	1,981	1,562	3,332
20	5,347	0,998	10-12	4,669	0,99	90-18	7,351	0,99	90-180	0,766	0,99	30-18	10	3,42	2,543	5,537
40	7,112	0,999	9-12	6,974	0,99	90-15	8,544	0,99	90-140	0,834	0,99	20-18	20	4,581	3,903	6,585
60	7,733	0,999	9-12	8,15	0,99	100-13	10,456	0,99	90-100	0,866	0,99	30-18	40	6,278	6,14	7,71
													60	6,867	7,284	9,59

Raw data PEP kinetics

Kinetic data for varying concentrations of PEP (Protein concentration 0,95 µg, T = 25 °C)

Parallel	1			2			3			Blank		
Concentration (mM)	Vmax (mOD/min)	R	Points									
0,05	2,699	0,99	25 0-12 00	2,616	0,92	12 0-12 00	1,865	0,98	20 0-18 00	2,248	0,92	10 0-10 00
0,1	3,807	0,99	20 0-10 00	3,263	0,91	20 0-10 00	2,316	0,98	23 0-1 0,1	2,043	0,91	50-90 0
0,25	5,282	0,99	60-50 0	4,082	0,92	42 0-90 0	3,858	0,91	90-79 0	1,879	0,91	10 0-18 00
0,5	4,556	0,99	26 0-90 0	6,879	0,98	40 0-50 0	5,207	0,99	10 0-90 0	1,845	0,98	10 0-18 00
1	9,167	0,99	10-71 0	9,922	0,99	10 0-65 0	7,213	0,99	10 0-80 0	1,65	0,99	10 0-18 00
3	8,443	0,99	50-40 0	10,322	0,98	40 0-10 00	9,483	0,99	10 0-90 0	0,632	0,97	0-10 00
5	7,277	0,99	50 0-18 00	11,917	0,97	10 0-69 0	8,438	0,99	10 0-90 0	0,519	0,95	0-10 00
10	11,812	0,99	10 0-10 00	11,881	0,96	17 0-86 0	13,735	0,99	0-60 0	2,101	0,94	10 0-10 00

Corrected with Specific Blank			
Parallel	1	2	3
Concentration (mM)	Vmax (mOD/min)	Vmax (mOD/min)	Vmax (mOD/min)
0,05	0,451	0,368	- 0,383
0,1	1,764	1,22	0,273
0,25	3,403	2,203	1,979
0,5	2,711	5,034	3,362
1	7,517	8,272	5,563
3	7,811	9,69	8,851
5	6,758	11,398	7,919
10	9,711	9,78	11,634

Appendix VIII

Raw data phosphate standard curve

Phosphate Standard Curve for Kinetics				
	Parallels			
Concentration	1	2	3	Blank
175	0,88	0,837	0,844	0,475
140	0,827	0,824	0,811	0,465
105	0,736	0,914	0,733	0,477
70	0,606	0,6	0,612	0,472
35	0,478	0,472	0,489	
17,5	0,427	0,415	0,419	
10,5	0,407	0,403	0,405	
3,5	0,388	0,379	0,443	
1,75	0,435	0,443	0,432	

Appendix IX

Kcat calculations

The determined for ManNAc; $V_{\max} = 10.0353 \text{ mOD/min}$

Formula for conversion to μM

$$y = 0.00275x - 0.06478$$

where y is the measured OD and x is the concentration in μM

converting the V_{\max} to OD/min gives

$$V_{\max} = 0.0100353 \text{ OD/min}$$

Substituting this for y in the formula gives that

$$x = \frac{0.0100353 + 0.06478}{0.00272}$$

$$x = 27.2056 \mu\text{M/min}$$

This is converted to $\mu\text{mol} \cdot \text{mL}^{-1} / \text{min}$ which gives the value

$$0.02721 \mu\text{mol} \cdot \text{mL}^{-1} / \text{min}$$

This is divided on the enzyme concentration in the assay in mg/mL to give

$$5.72749 \mu\text{mol} \cdot \text{min}^{-1} / \text{mg}$$

The kcat is now achieved by multiplying the gotten value with the molecular weight of the protein, in this case the NeuB1 CHis given in mg/ μmol

$$5.72749 \frac{\mu\text{mol}}{\text{min}} * 38.9345 \frac{\text{mg}}{\mu\text{mol}} = 222.99 \text{ min}^{-1}$$

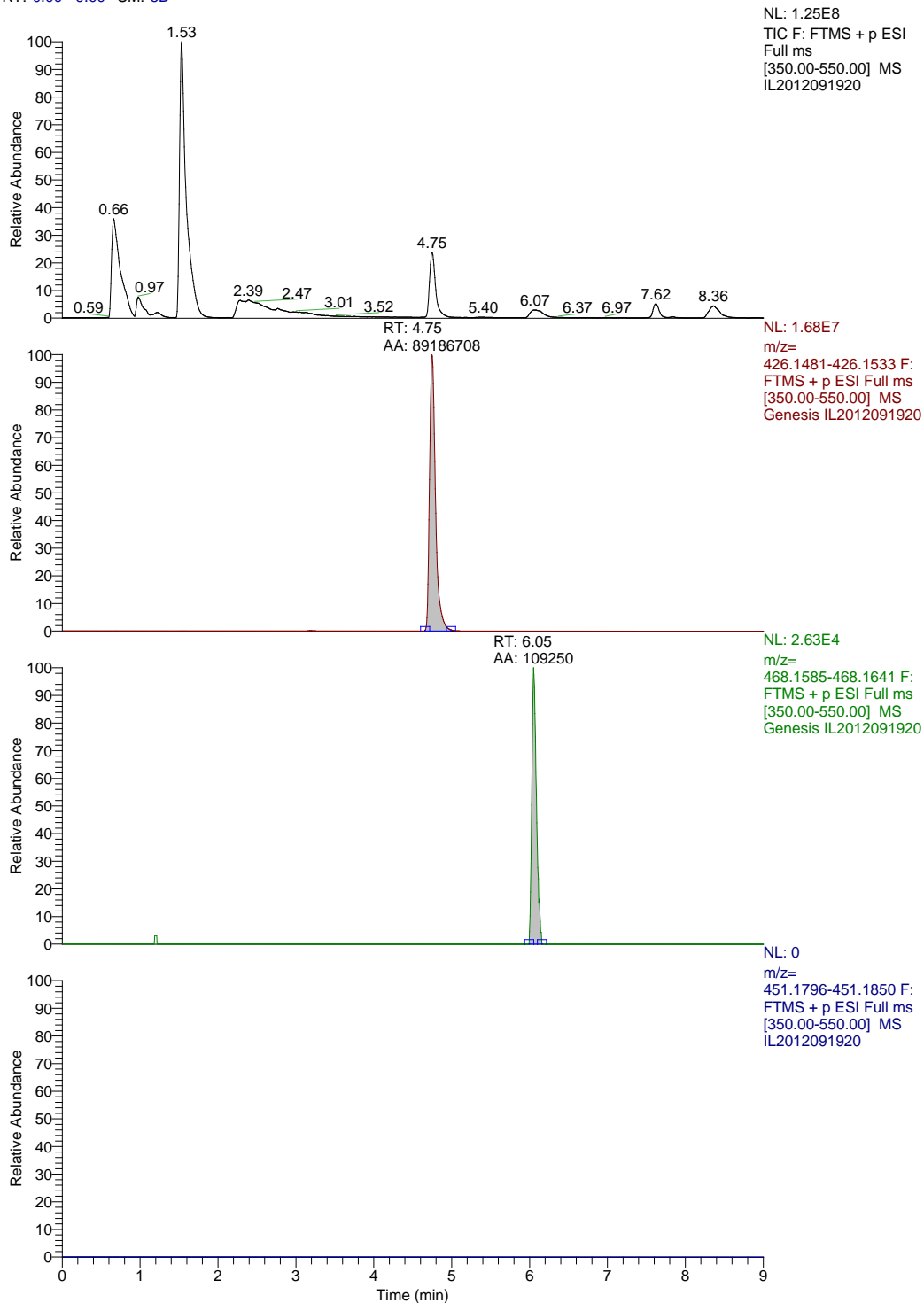
The same procedure is done for the V_{\max} value of PEP

Appendix X

HPLC-MS and MS² spectra

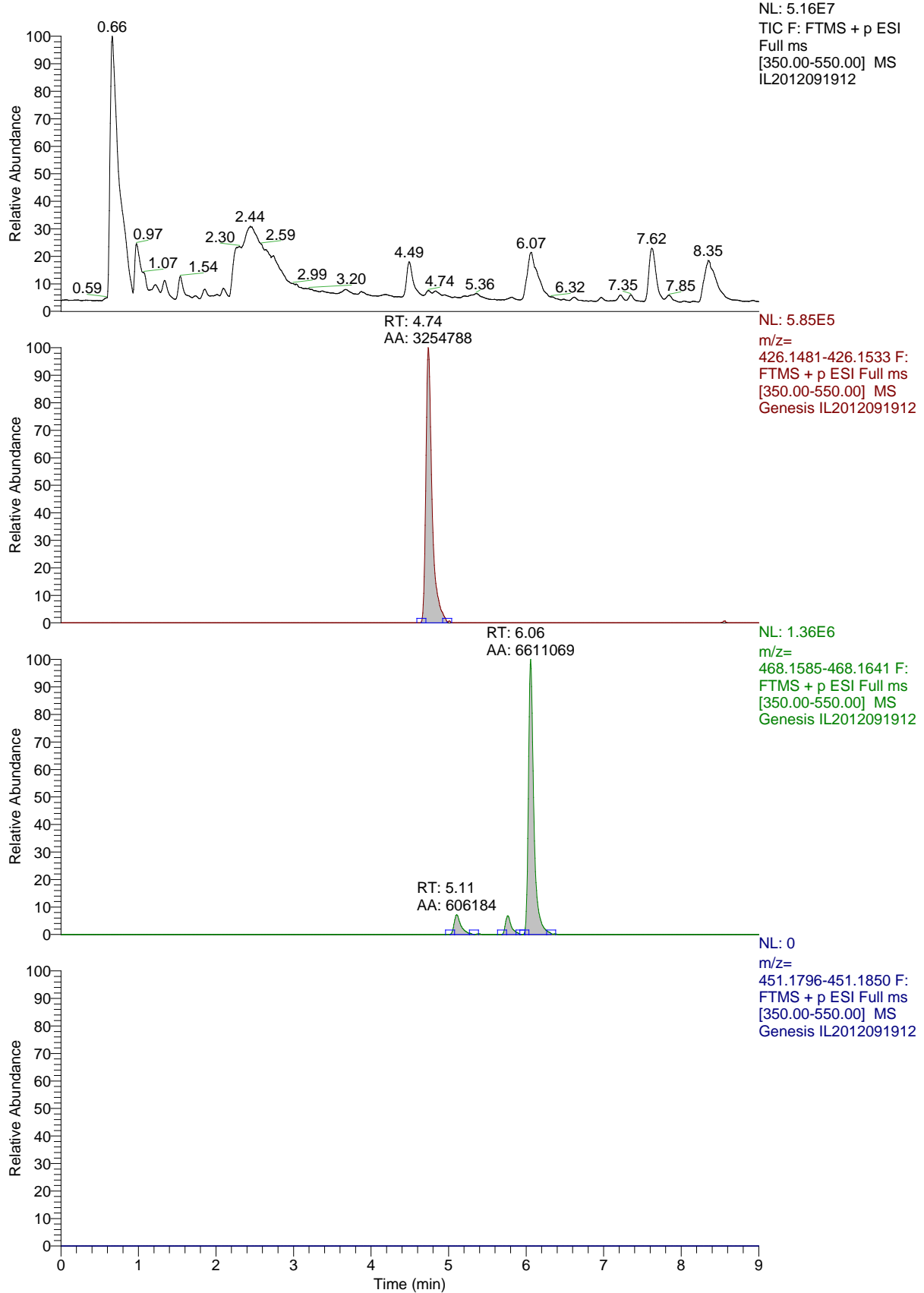
HPLC-MS Standard panel NeuNAc

RT: 0.00 - 9.00 SM: 5B



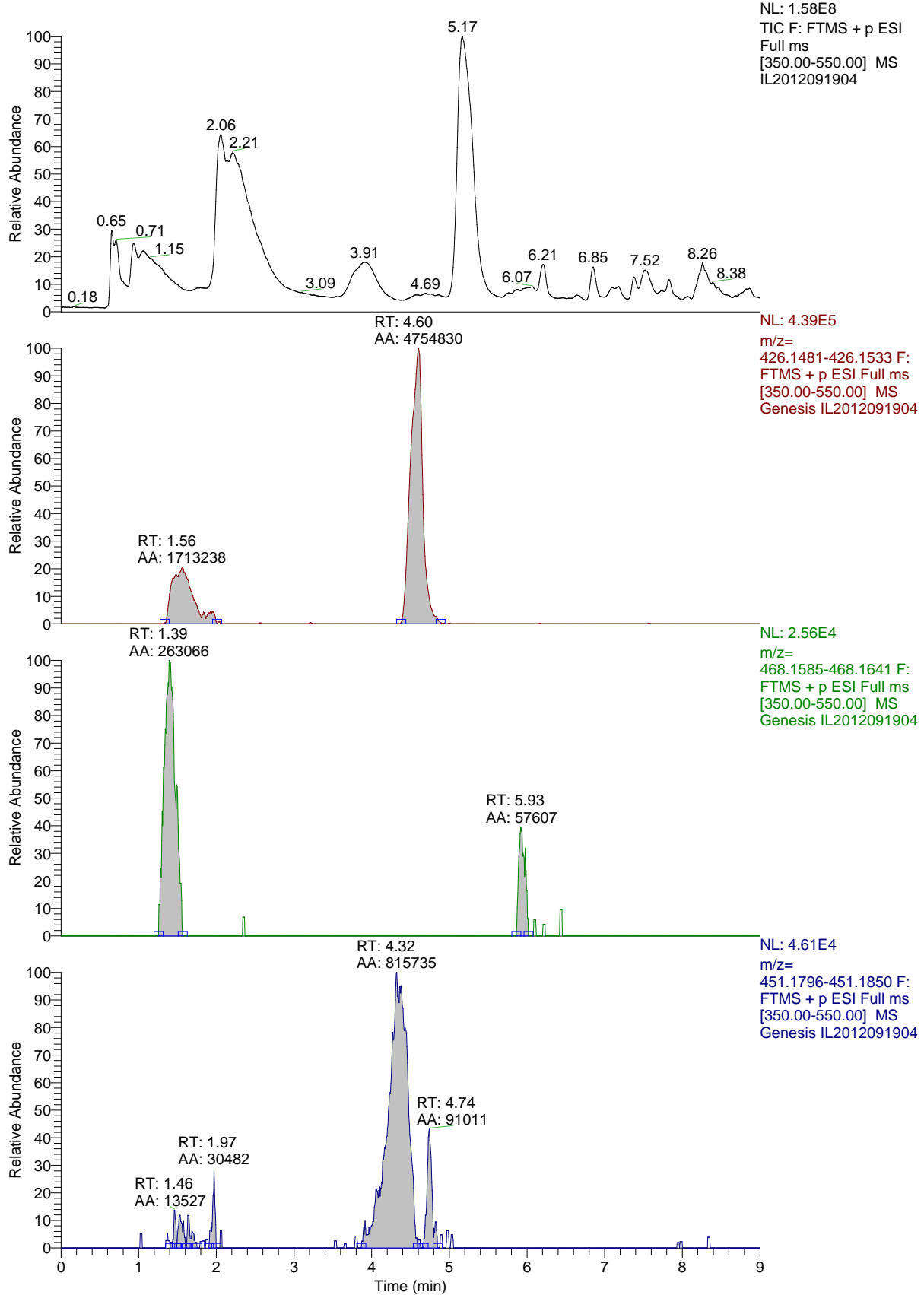
HPLC-MS Standard panel Sia mixture

RT: 0.00 - 9.00 SM: 5B



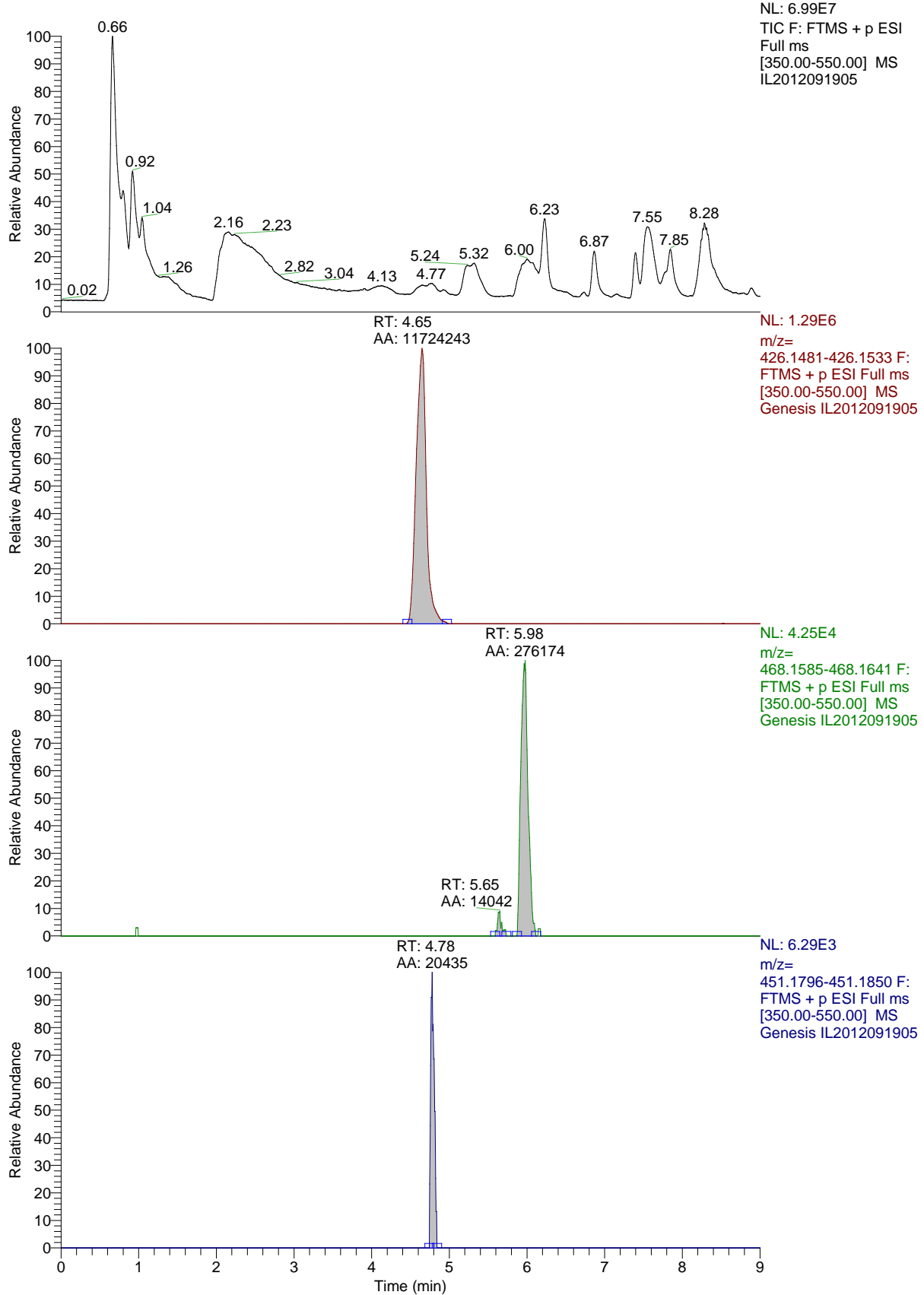
HPLC-MS LB-sample

RT: 0.00 - 9.00 SM: 5B



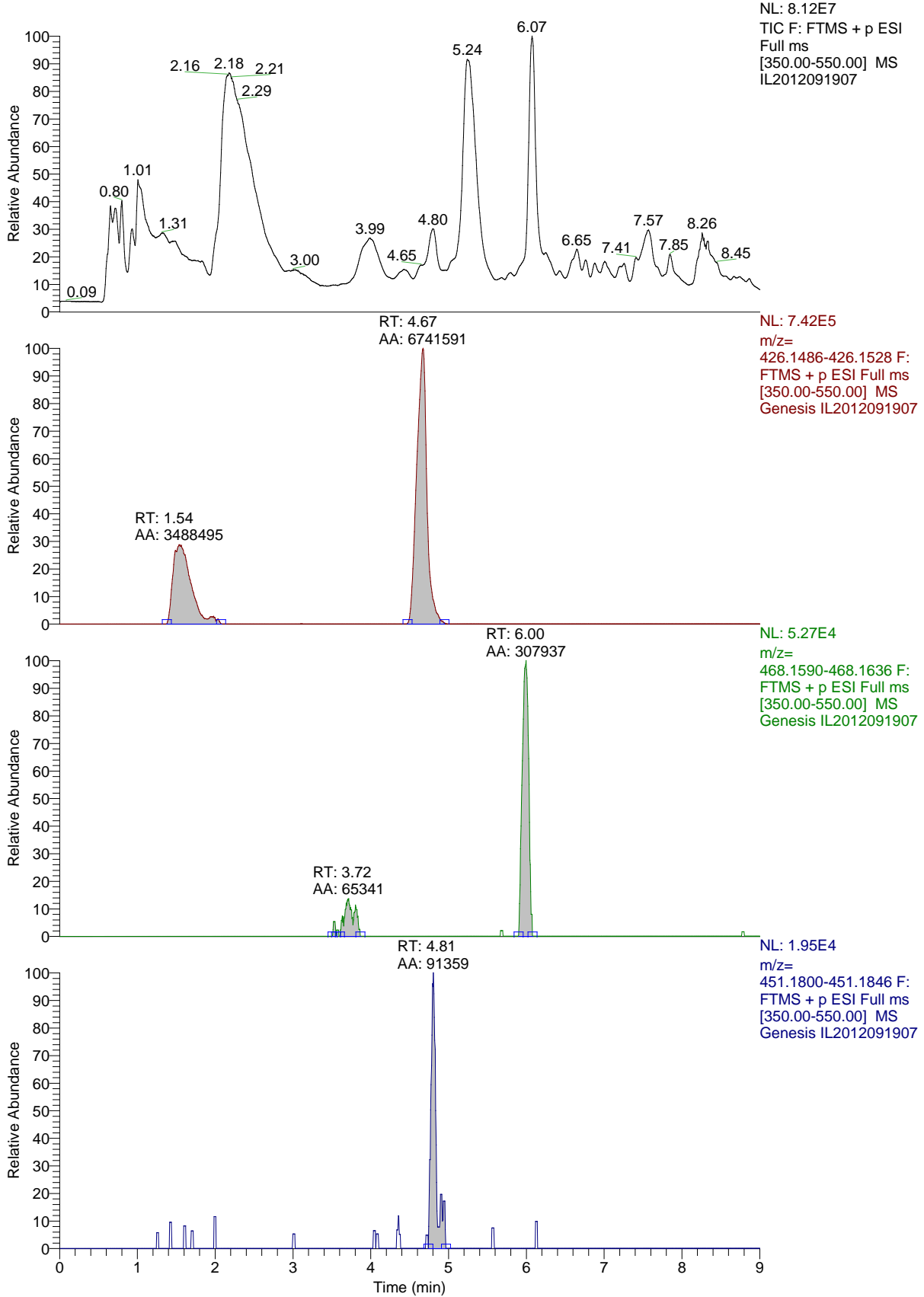
HPLC-MS BA-sample

RT: 0.00 - 9.00 SM: 5B



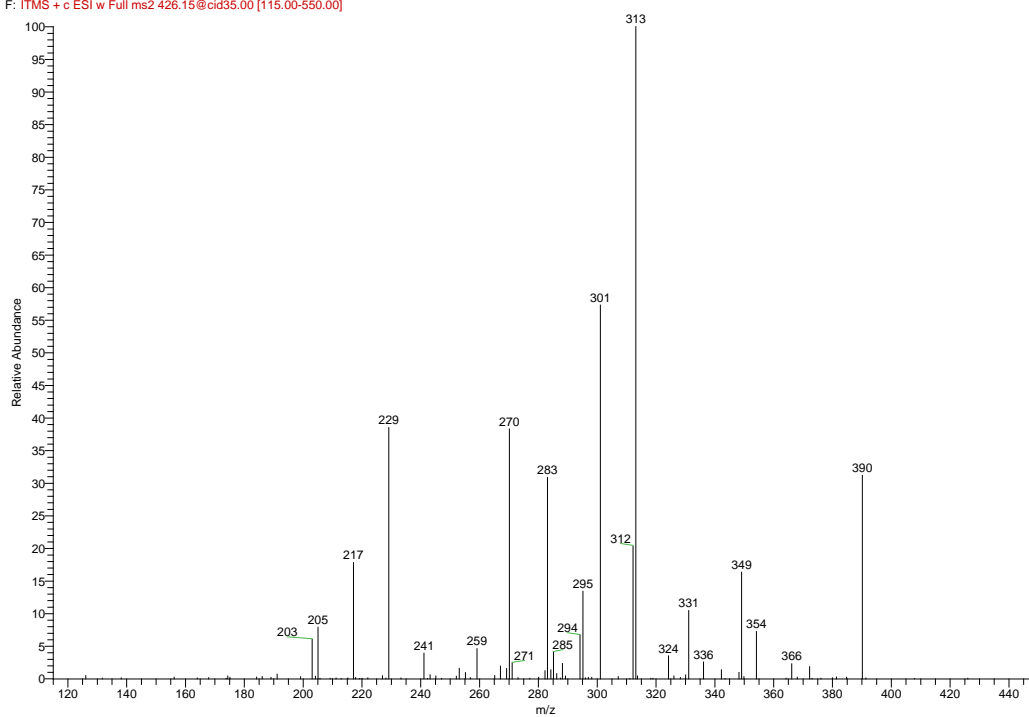
HPLC-MS MB-sample

RT: 0.00 - 9.00 SM: 5B



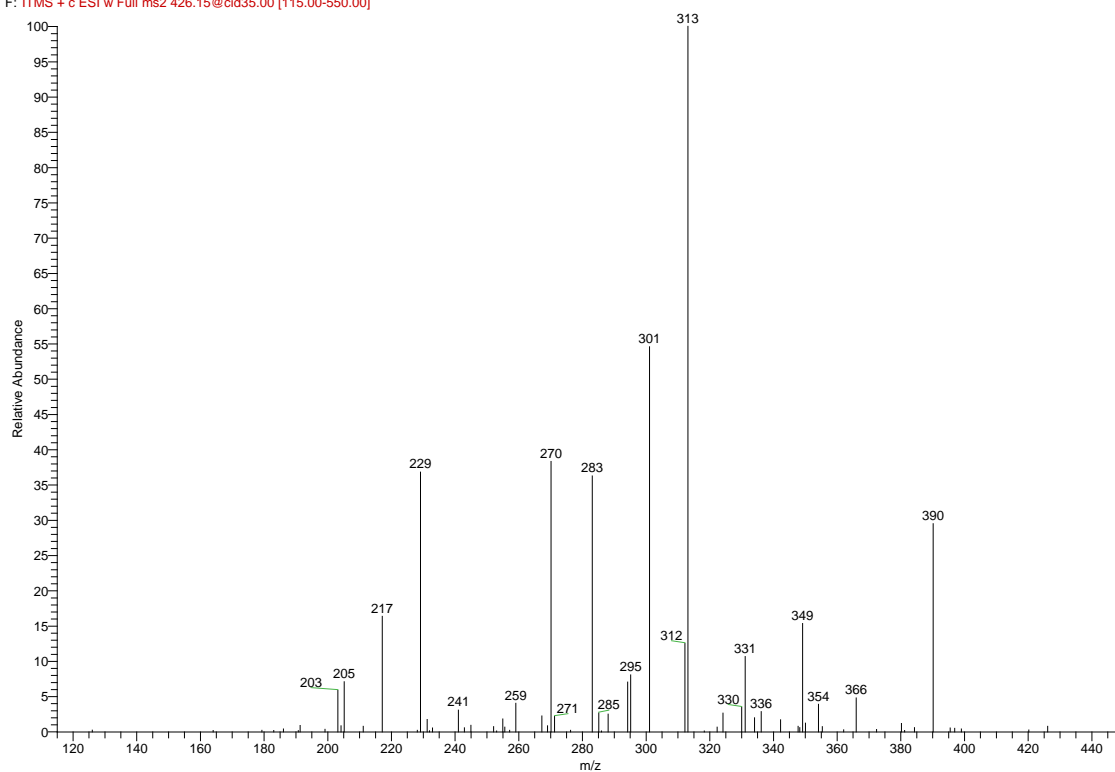
MS² Standard panel NeuNAC

IL201209190_MS2_18 #1215-1268 RT: 4.59-4.77 AV: 13 NL: 2.29E3
F: ITMS + c ESI w Full ms2 426.15@cid35.00 [115.00-550.00]



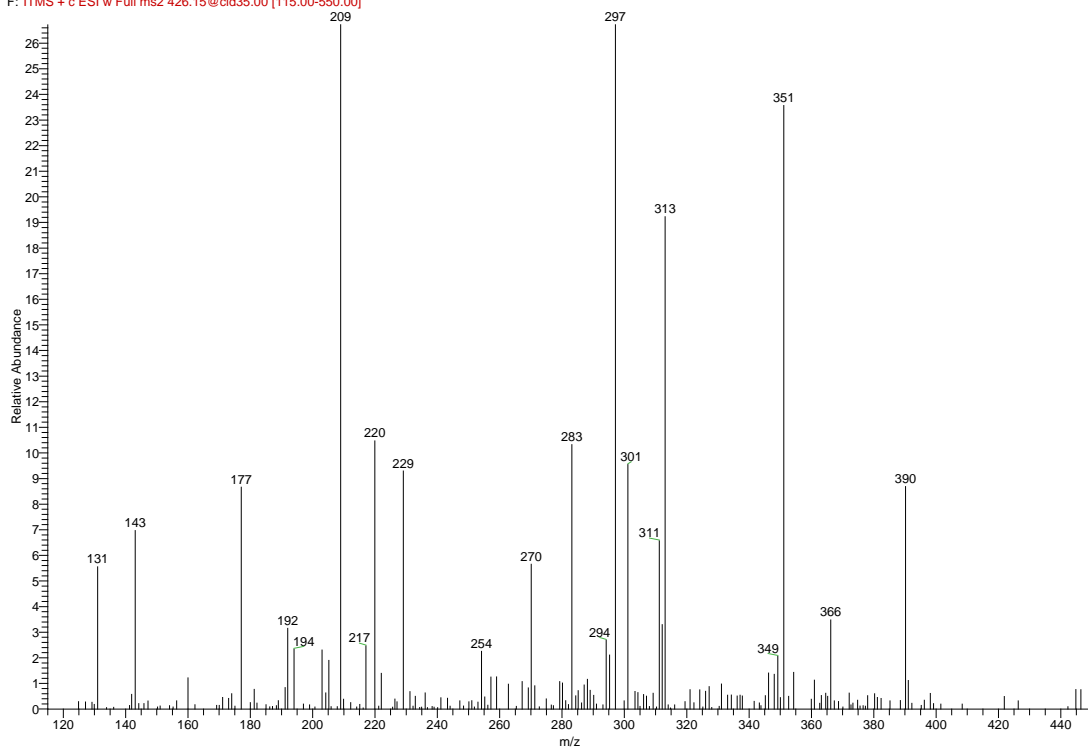
MS² Standard panel Sia mixture

IL201209190_MS2_13 #1215-1268 RT: 4.59-4.77 AV: 13 NL: 6.13E2
F: ITMS + c ESI w Full ms2 426.15@cid35.00 [115.00-550.00]



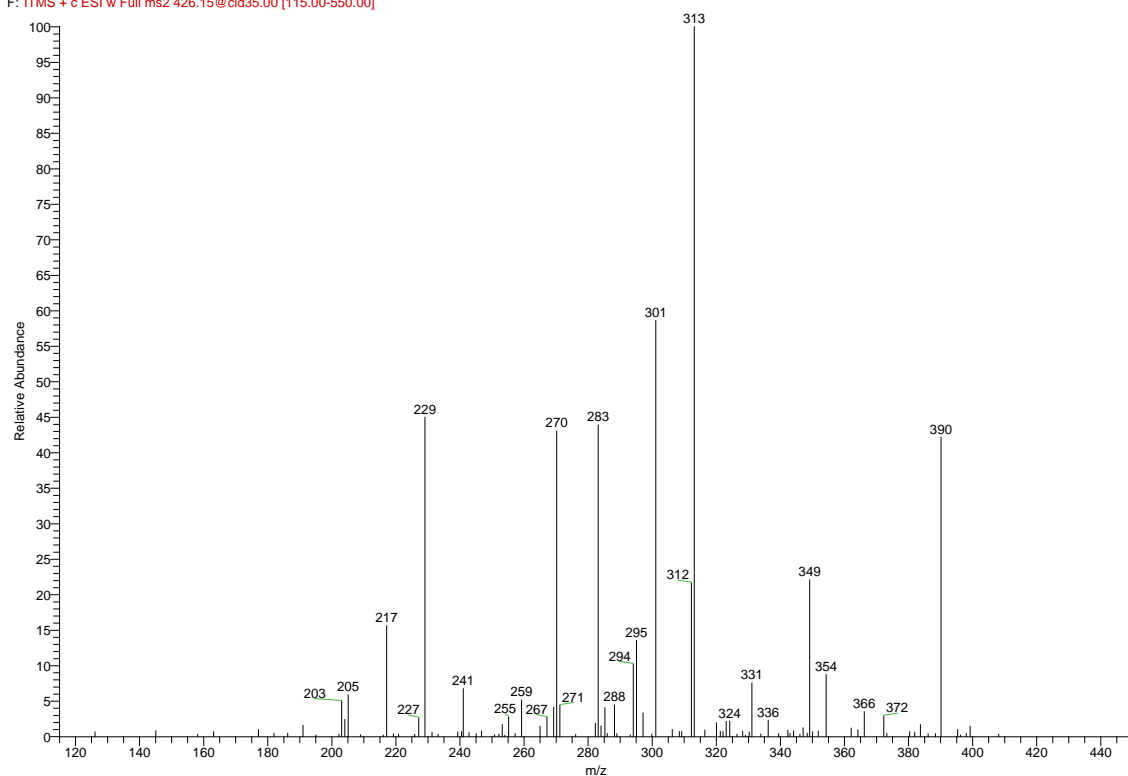
MS² LB-sample

IL201209190_MS2_04 #1214-1267 RT: 4.58-4.78 AV: 14 NL: 1.42E3
F: ITMS + c ESI w Full ms2 426.15@cid35.00 [115.00-550.00]



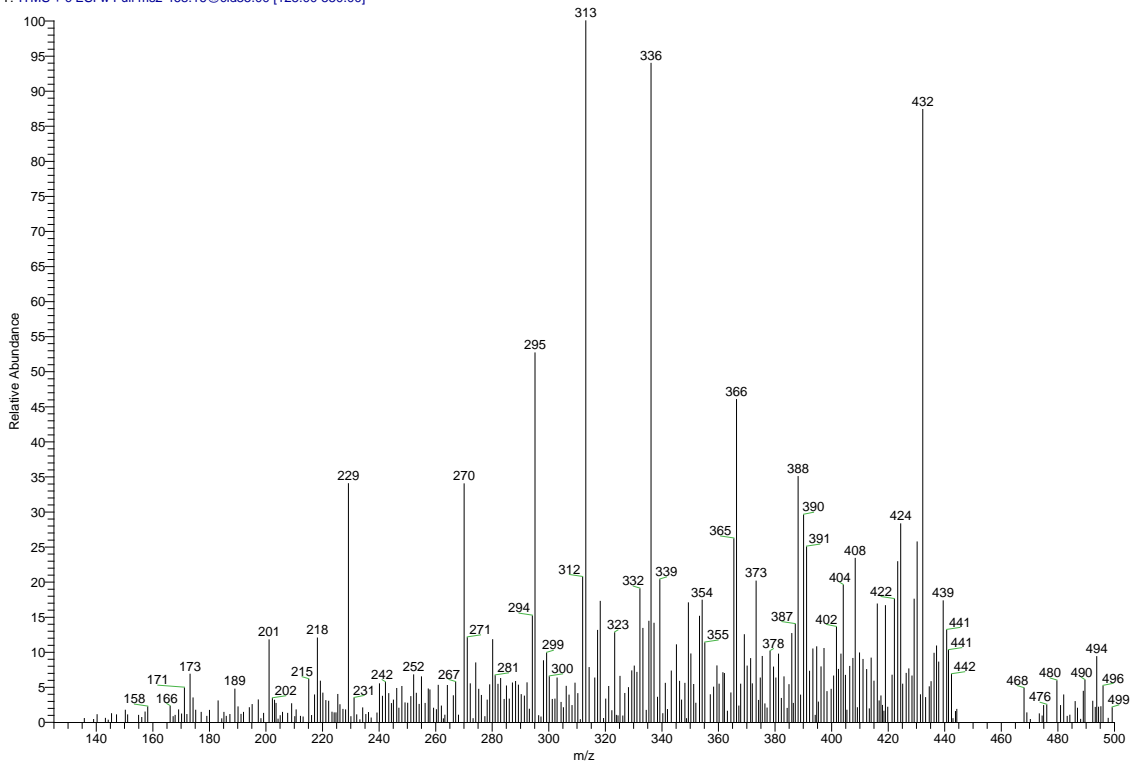
MS² BA-sample

IL201209190_MS2_05 #1215-1268 RT: 4.59-4.77 AV: 13 NL: 4.81E2
F: ITMS + c ESI w Full ms2 426.15@cid35.00 [115.00-550.00]

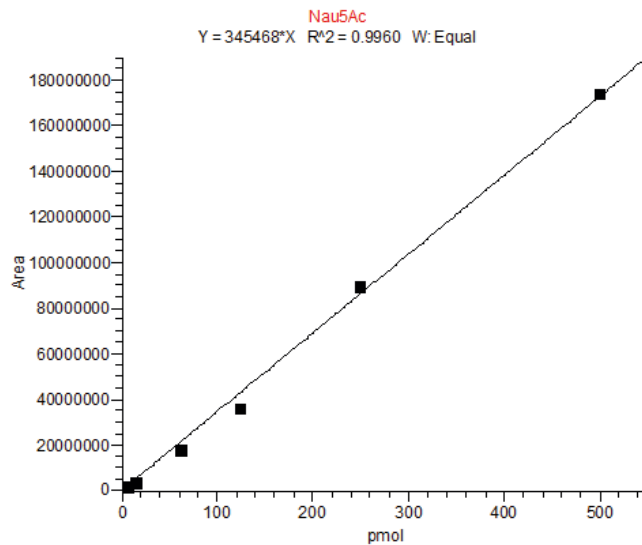


MS² MB-sample

IL201209190_MS2_468_07 #1733-1772 RT: 5.88-6.01 AV: 40 NL: 8.14E1
 T: ITMS + c ESI w Full ms2 468.16@cid35.00 [125.00-550.00]



Standardkurve Nau5Ac



Component Name	Curve Index	Weighting Index	Origin Index	Equation	Specified Amount	Calculated Amount	%Diff	Units	I
Nau5Ac	Linear	Equal	Force	$Y = 345468 * X \quad R^2 = 0.9960$					
IL2012091914	Std Bracket Sam; Std 1	Method Settings	NF		3.906	NF	NF	pmol	1
IL2012091915	Std Bracket Sam; Std 2	Method Settings	1599251		7.813	4.629	-41%	pmol	4
IL2012091916	Std Bracket Sam; Std 3	Method Settings	2877953		15.625	8.331	-47%	pmol	4
IL2012091918	Std Bracket Sam; Std 5	Method Settings	17215784		82.500	49.833	-20%	pmol	4
IL2012091919	Std Bracket Sam; Std 6	Method Settings	35809070		125.000	103.854	-17%	pmol	4
IL2012091920	Std Bracket Sam; Std 7	Method Settings	89172518		250.000	258.121	3%	pmol	4
IL2012091921	Std Bracket Sam; Std 8	Method Settings	173817588		500.000	503.137	1%	pmol	4
IL2012091901	Unknown Sample Blank H2O	Method Settings	NF		NA	NF	NF	pmol	1
IL2012091902	Unknown Sample Blank	Method Settings	NF		NA	NF	NF	pmol	1
IL2012091903	Unknown Sample 1	Method Settings	1718564		NA	4.975	NA	pmol	4
IL2012091904	Unknown Sample 2	Method Settings	4745374		NA	13.738	NA	pmol	4
IL2012091905	Unknown Sample 3	Method Settings	11723889		NA	33.938	NA	pmol	4
IL2012091908	Unknown Sample 4	Method Settings	148107890		NA	422.928	NA	pmol	4
IL2012091907	Unknown Sample 5	Method Settings	6742773		NA	19.518	NA	pmol	4

